19

JOURNAL OF APPLIED PHYSICS

AUG 12 1940

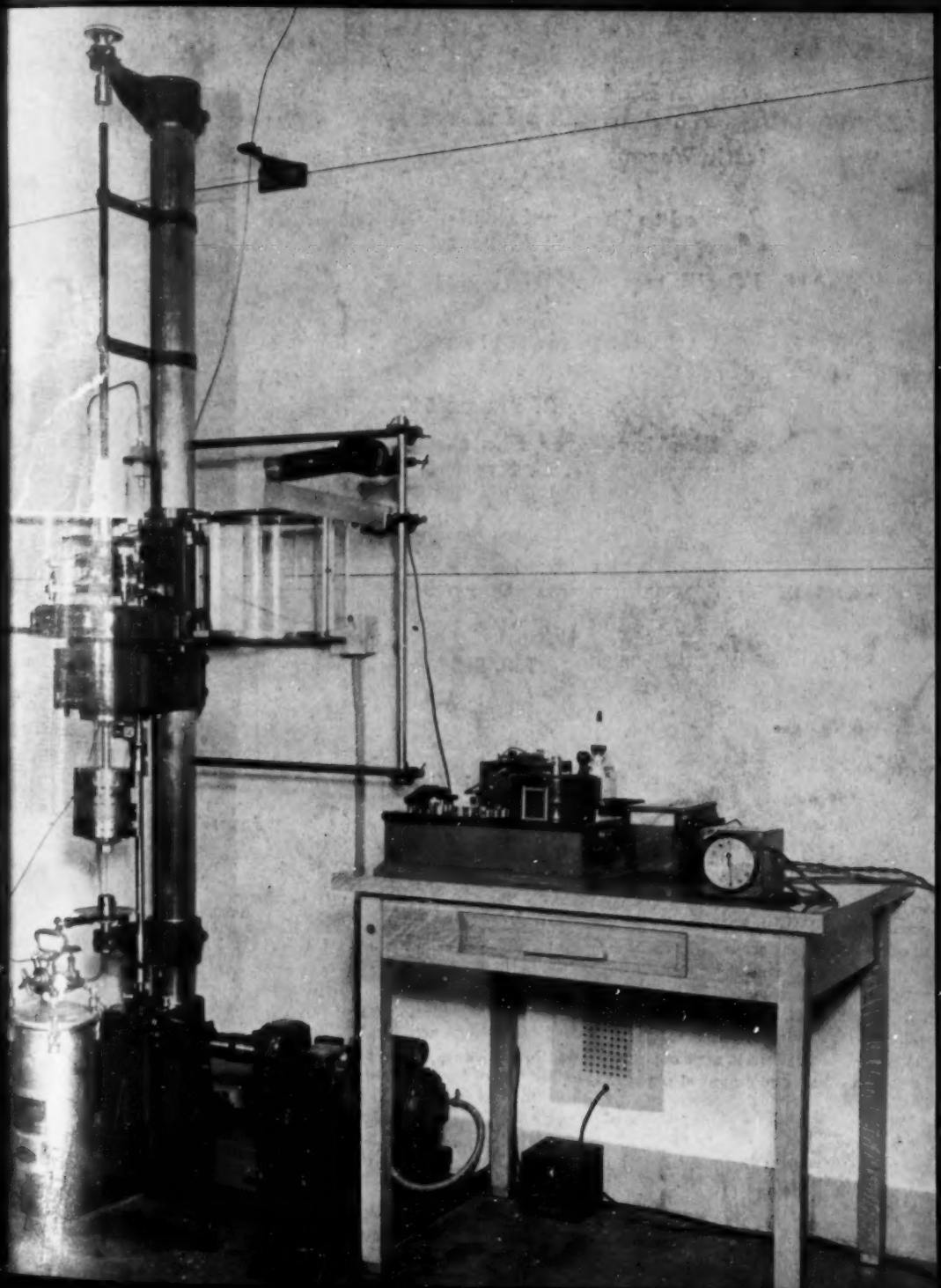

AUGUST
1940
Vol. 11 No. 8

Reorganization of Co-
Relation of Building
Education. See p. 541

JOURNAL OF APPLIED
PHYSICS

AUGUST, 1940 Vol. 11, No. 8

In This Issue

Page

National Defense and the Physicist. II. 509

Graphical Method for Selecting Suitable Targets for Precision Determination of Cubic Lattice Constants and for Solving Cubic Powder Patterns LOUIS A. CARAPELLA 510

Initial Stage of Plastic Deformation in Lead Under Compression W. JAMES LYONS 514

Influence of Initial Stress on Elastic Waves MAURICE A. BIOT 522

Equations of Finite Differences Applied to Torsional Oscillations of Crankshafts MAURICE A. BIOT 530

Theory of Frequency Controlled Oscillators SAMUEL SABAROFF 538

Studies in Lubrication. VIII. Lubrication of Plane Sliders F. MORGAN, M. MUSKAT AND D. W. REED 541

Rectilinear Electron Flow in Beams J. R. PIERCE 548

Temperature Measurement with Blocking-Layer Photo-Cells B. M. LARSEN AND W. E. SHENK 555

Letters to the Editor

Polonium Alloy for Spark Plug Electrodes ROBLEY D. EVANS 561

Answer to Communication by R. D. Evans J. H. DILLON 562

In Every Issue

Here and There 560, 563, 564

Contributors to This Issue 563

Recent Booklets 565

Innovations in Instruments 566

Index to Advertisers vi

BOARD OF EDITORS

ELMER HUTCHISSON, *Editor*

Associate Editors

F. BITTER
W. E. FORSYTHE
L. A. JONES
B. E. WARREN
J. B. WHITEHEAD

Publication of the
American Institute of Physics

ADMINISTRATIVE STAFF

HENRY A. BARTON, *Director*

MADELINE M. MITCHELL, *Publications Manager*

JOHN T. TATE, *Adviser on Publications*

GOVERNING BOARD

PAUL E. KLOPSTEG, *Chairman*
GEORGE B. PEGRAM, *Secretary*
KARL T. COMPTON
WHEELER P. DAVEY
FLOYD A. FIRESTONE
HARVEY FLETCHER
R. C. GIBBS
ARTHUR C. HARDY
GEORGE R. HARRISON
A. STUART HUNTER
H. R. LILLIE
FREDERIC PALMER, JR.
GEORGE B. PEGRAM
W. B. RAYTON
JOHN T. TATE
WALLACE WATERFALL

THE JOURNAL OF APPLIED PHYSICS, published monthly at Prince and Lemon Sts., Lancaster, Pa., is devoted to physics in its role as the science basic to other natural sciences and to the arts and industries. Previous to 1937 this publication was known as PHYSICS. It aims to be of service not only in physical laboratories, but also in the laboratories of industrial, chemical, geological, geophysical, meteorological, radio, and similar concerns. THE JOURNAL OF APPLIED PHYSICS publishes editorials, news of physicists and reviews, as well as technical papers of applied physics.

Manuscripts should be submitted to Elmer Hutchisson, Editor, University of Pittsburgh, Pittsburgh, Pennsylvania.

SUBSCRIPTION PRICE

	U. S., POSS. AND CANADA	FOREIGN
To members of scientific societies	$5.00	$5.70
To all others	7.00	7.70

Single copies are $.70 each.

Changes of address and proofs should be addressed to the Publications Manager.

Subscriptions and orders for back numbers should be addressed to Prince and Lemon Streets, Lancaster, Pa. or to the American Institute of Physics, 175 Fifth Avenue, New York, N. Y.

Advertising rates supplied on request. Orders, advertising copy and cuts should be sent to the American Institute of Physics.

Entered as second class matter at the Post Office at Lancaster, Pennsylvania, under the Act of March 3, 1897. Accepted for mailing at the special rate of postage provided for in the Act of February 28, 1925, authorized May 2, 1932.

Copyright 1940, by the American Institute of Physics.

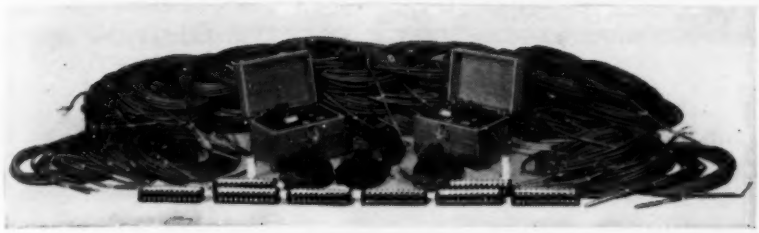

Forty-two Leeds & Northrup Resistance Thermometers, two L&N Wheatstone Bridges and various accessories are now located at various points in the Antarctic. Information about sub-surface conditions is made available by this equipment.

Antarctic Snow Is Measured At 160 Foot Depth

L&N Bridges Used To Study Temperature

Apparatus which the Antarctic Expedition is using to determine the temperature of snow and ice at various depths was made by Leeds & Northrup and calibrated at the National Bureau of Standards.

The expedition is installing electrical resistance thermometers in the snow at the surface and at various depths down to 160 feet, to measure the temperatures and to study the way in which they are influenced by air temperatures. In addition, measurements will be carried out at different stations to determine the influence of local topography on subsurface temperatures.

The Bureau of Standards supplied the expedition with the equipment, which consists of forty-two electrical resistance thermometers and two Wheatstone bridges, including such accessories as switches and extra galvanometers. The instruments are graduated from plus 50 degrees to minus 94 degrees Fahrenheit.

Thermometers are located in holes about two inches in diameter. Specially designed drills had to be constructed to make these holes. Where it is not possible to drill holes to the full depths with the limited manpower available, an electric heating device is used.

New Catalog Describes Type K Potentiometers

Interesting application pictures, a circuit diagram, and detailed closeups make this new catalog of Type K Potentiometers useful and easy to understand.

Devoted principally to the modernized, triple range Type K-2, this publication describes its convenient controls, covered switches, improved standardizing circuit and other features. A 24-page book, it gives information about assemblies for typical measurements and lists a complete line of accessories. Included are the L&N Thermionic Amplifier (for use in measuring potential in high-resistance circuits), galvanometers, reading devices, shunts, volt boxes, etc. Galvanometer damping is discussed, and a short description of the potentiometer principle is included. See Catalog E50B(3).

"Thermal-Free" Materials Improve Pinch-Type Switch

Materials which have no significant thermal effect make the newly redesigned Pinch-Type Switch suitable for the most precise thermocouple measurements. Now made with blades of beryllium-copper and with all other conducting parts of solid copper, they have shown under test that they develop

even less thermal emf than all-copper switches.

Pinch-Type Switches are useful where convenience and time are factors. Even when not fastened down, require only one hand to operate.

Bakelite base and handle make for light but rigid construction. The hollow base makes possible internal connections forming a reversing switch. This 3294 Pinch-Type Double-Pole, Double-Throw Switch sells for $3.00. Lots of 20 or more receive a discount of 10%. See Catalog EU2 for more complete details.

LEEDS & NORTHRUP COMPANY, 4978 STENTON AVE., PHILA., PA.
LEEDS & NORTHRUP
Measuring Instruments : Telemeters : Automatic Controls : Heat-Treating Furnaces

A New A. C. S. Monograph

PHENOMENA AT THE TEMPERATURE OF LIQUID HELIUM

by E. F. Burton, H. Grayson Smith and J. O. Wilhelm,
Dept. of Physics, University of Toronto

The first book on this intriguing subject!

IT IS of the greatest importance for both physicists and chemists to be familiar with the peculiar action of matter at excessively low temperatures. An understanding of the modern phases of low-temperature research requires discussion of the means of the producing low temperatures and of measuring both the temperature and the properties of the substance involved, as well as a general presentation of experimental results already obtained. This fundamental material is given in the early chapters.

The essence of the book is found in the latter half where are presented the results of the impact of curious low-temperature phenomena on modern theories of matter, the nature of superconductivity, the behavior of specific heats and magnetic properties of matter and the freakish antics of liquid helium below 2° K. Particular attention has been given to the definition and measurement of temperature, and to the intriguing problems of the approach to the absolute zero.

The experimental work discussed in this timely book was performed at the McLennan Laboratory in Toronto, one of the best equipped physical laboratories in the world! The authors are pioneers in low-temperature research, and their work will be of the greatest interest to chemists, physicists, engineers and metallurgists.

CONTENTS—Historical Introduction. The Liquefaction of Gases. The Measurement of Temperature. The Physical Properties of Liquid and Solid Helium. Superconductivity. Specific Heats at Low Temperatures. Magnetic Properties. Temperatures Below 1° K. Electrical and Thermal Conductivities. The Nature of the Superconducting State. The Transformation in Liquid Helium and the Nature of Helium II. Appendixes. Author Index. Subject Index.

384 Pages **Illustrated** **Price $6.00**

REINHOLD PUBLISHING CORP., 330 West 42nd Street, New York, U.S.A.

QUARTZ SPECTROGRAPH

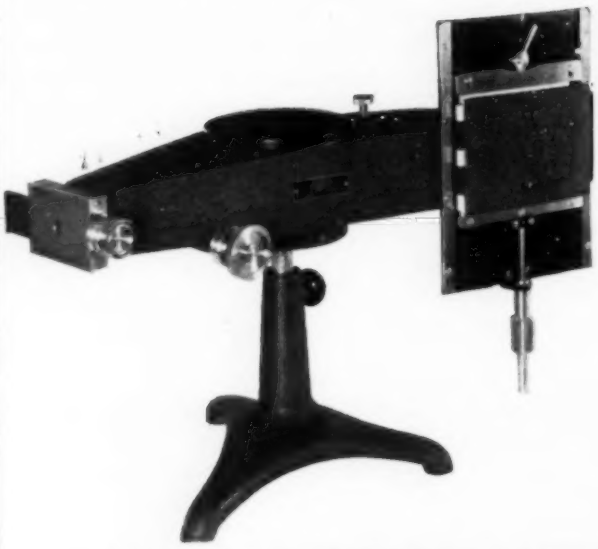

OUTSTANDING Features of the new "GAERTNER" Quartz Spectrograph L 250-93—

1. Range 185 to 800 mμ
2. Usable with 3¼" x 4¼" size plates or films
3. Accurate wavelength scale
4. Excellent definition over entire range
5. Rugged construction
6. Permanent accuracy

Descriptive Bulletin No. 149-04 on request

THE GAERTNER SCIENTIFIC CORPORATION

1212 Wrightwood Ave. **CHICAGO, U.S.A.**

HARVARD COLLEGE
AUG 12 1940
LIBRARY

Journal of Applied
Physics

Volume 11 August, 1940 Number 8

National Defense and the Physicist, II*

BEFORE attempting to suggest ways and means by which those special talents which physicists possess may be useful in national defense, it seems desirable to inquire into the fundamental purposes of defense. The ultimate goal is the protection of life, liberty of thought and action and of property. For defense purposes, the four principal weapons are: (1) Force of arms; (2) economic control by the development of internal sources of supply of raw materials and the perfection of efficient methods of manufacturing and agriculture; (3) propaganda to obtain national unity of purpose and international desire for peace; and (4) competent intelligence-service to obtain complete information regarding warlike preparations of any other nation. Formerly a fifth, that of setting up defensive alliances with other countries, would have been included, but experience has shown lately that such alliances often fail when needed most.

Undoubtedly the services of the physicist will be found useful in the expansion and improvement of all these weapons of defense. For this discussion we will limit ourselves to the part he may play in the development of a strong force of arms. Unfortunately, our remarks must be very superficial. A profound discussion would require both an extensive analysis of military methods and of each special field of physics. In spite of this difficulty, a brief survey may be useful since it may induce others to go into the subject more deeply.

Defense by force of arms divides itself rather naturally into three phases: (a) Detection of an advancing enemy at a great distance so as to prevent surprise attacks and to allow an advance guard to be properly prepared; (b) breaking up of the enemy's attack by the advance guard before he can do much damage; (c) adequate protection in case the advance guard fails to ward off the attack. Each phase presents problems which are almost uniquely in the bailiwick of the physicist.

The first phase involves the perfection of fog-penetrating searchlights, of detectors depending upon both acoustic and electromagnetic radiations, and of necessary signal alarms to warn of the approach particularly of airplanes, gliders, and submarines. The second phase requires extensive developments in aerodynamics and ballistics to improve attack-resisting airplanes and long range antiaircraft guns. Protection from the attack itself requires improvements in armor plate, bomb-proof shelters, and in methods of resistance against poisonous gases and flaming projectiles. Here the physicist's services enter directly into long range programs to improve materials and types of construction.

The variety of problems for the physicist is endless. Enough have been suggested to show the great need for further study and analysis if we are to prepare intelligently for a strong national defense.

* The first of these notes on national defense appeared in the July issue of the *Journal of Applied Physics*. In it the opportunity of the physicist to aid in a general training program was stressed.

A Graphical Method for Selecting Suitable Targets for Precision Determination of Cubic Lattice Constants and for Solving Cubic Powder Patterns

LOUIS A. CARAPELLA
Laboratory of Physical Metallurgy, Harvard University, Cambridge, Massachusetts
(Received February 5, 1940)

Graphical charts from which the angles of diffraction lines may be obtained as a function of lattice constant and radiation have been prepared for cubic powder patterns. The charts are especially useful in predicting positions of back-reflection lines in order that suitable targets for precision determinations of lattice constants may be chosen. Moreover, cubic powder patterns may be quickly indexed, beta-lines identified, and lattice constants read to better than one percent. No calculations are necessary after the angles of diffraction have been measured.

INTRODUCTION

PRECISION methods of determining lattice constants are based on the fact that the accuracy is greater the nearer the measured diffraction lines approach back-reflection. For extrapolation methods,[1–3] which aim to increase the accuracy by extrapolating to complete back-reflection; i.e., $\theta = 90°$ (θ = Bragg angle of diffraction), a minimum of two back-reflection lines (with $\theta > 60°$) is essential for cubic crystals, while a larger number is desirable for higher accuracy. Jette and Foote[4] recommend that for one of the lines at least, θ should be greater than 72°. To meet these conditions, it is necessary to select a target suitable to the (approximately known) lattice constant. Often this cannot be done with a single radiation and an alloy target must be used.[4]

Calculations of the approximate positions of back-reflection lines for an estimated or roughly determined lattice constant for each of the half-dozen common target materials is obviously laborious; yet the positions must be known if the best choice is to be made. In the appended charts, these line positions may be quickly read for the $K\alpha$ and $K\beta$ radiations of the usual target materials. The most favorable radiation or combination of radiations may then be quickly and easily selected.

The charts may further be used for indexing of lines, or for predicting their positions in cubic powder patterns. Beta-lines may also be identified without calculation. Lattice constants to better than one percent are read directly off the charts. These charts yield more information and require less preliminary calculation than the charts of Pauli,[5] Schiebold,[6] or Eulitz,[7] which also deal with cubic powder patterns and are reproduced in the *International Tables*.[8]

CONSTRUCTION AND USE OF THE CHARTS

For a cubic crystal, it can easily be shown from the Bragg equation, $\lambda = 2d \sin\theta$, and a consideration of the space geometry of the lattice, that:

$$\frac{2\sin\theta}{(h^2+k^2+l^2)^{\frac{1}{2}}} = \frac{\lambda}{a_0} \tag{1}$$

where λ is the wave-length, a_0 the lattice constant, θ the diffraction angle, and hkl, the Miller indices of the diffracting planes. We may then set each side of this equation equal to a parameter, χ; thus:

$$\chi = 2\sin\theta/(h^2+k^2+l^2)^{\frac{1}{2}}, \tag{2a}$$

$$\chi = \lambda/a_0. \tag{2b}$$

In the charts, χ is plotted as the ordinate, first against θ for various sets of indices hkl, and then against a_0 for the common characteristic radiations* as shown in Figs. 1, 2 and 3. Fig. 3 is

[1] A. E. van Arkel, Zeits. f. Krist. **67**, 235 (1928).
[2] A. J. Bradley and A. H. Jay, Proc. Phys. Soc. London, **44**, 563 (1932).
[3] M. U. Cohen, Rev. Sci. Inst. **6**, 68, 1935; **7**, 155 (1936); Zeits. f. Krist. **94**, 288, 306 (1936).
[4] E. R. Jette and F. Foote, J. Chem. Phys. **3**, 605 (1935).
[5] O. Pauli, Zeits. f. Krist. **56**, 591 (1921).
[6] E. Schiebold, Zeits. f. Physik **28**, 355 (1924).
[7] W. Eulitz, Zeits. f. Physik **64**, 452 (1930).
[8] *Internationale Tabellen zur Bestimmung von Kristallstrukturen* (G. Borntraeger, Berlin, 1935), Vol. 2, p. 665.
* The average wave-lengths of the $K\alpha$ doublets were used.

essentially an enlargement and continuation of Fig. 2 for back-reflection lines of higher order.

Since both sets of curves are plotted to a common χ-scale, the values of χ obtained from one set of curves apply as well to the other set. Thus, if a_0 is given, the value of χ may be found from the curve of the radiation in question (its numerical value is unimportant; hence the ordinate is not numbered). The horizontal line representing this value of χ intersects the curves of the various planes at their angles of diffraction, so that the positions of the diffraction lines may be read directly. Of course, it must be remembered that certain lines will vanish according to the Bravais lattice of the crystal. From the number and distribution of possible back-reflection lines (beyond $\theta = 60°$), the best radiation or combination of radiations for precision determi-

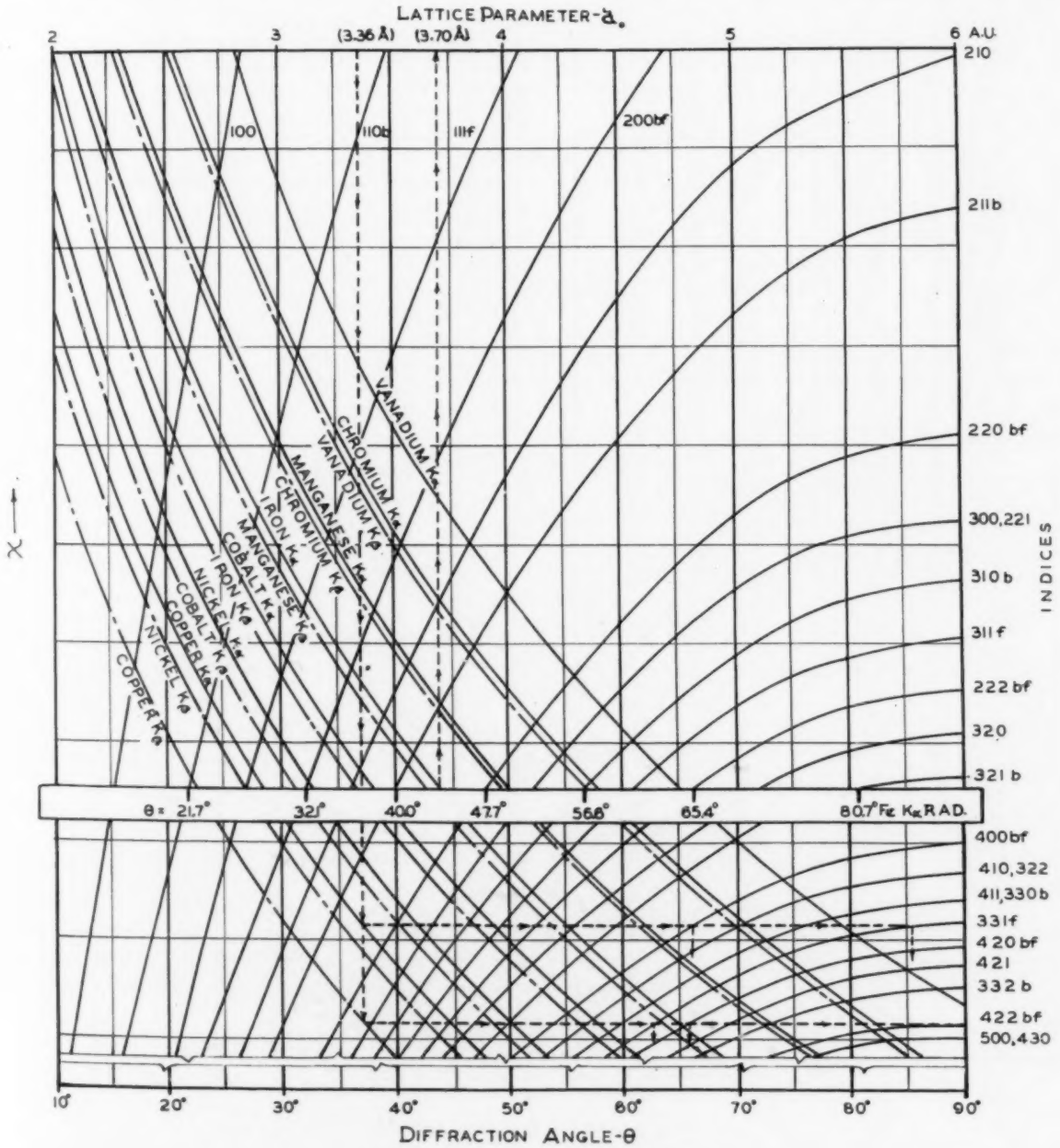

FIG. 1. b=b.c.c. lines, f=f.c.c. lines.

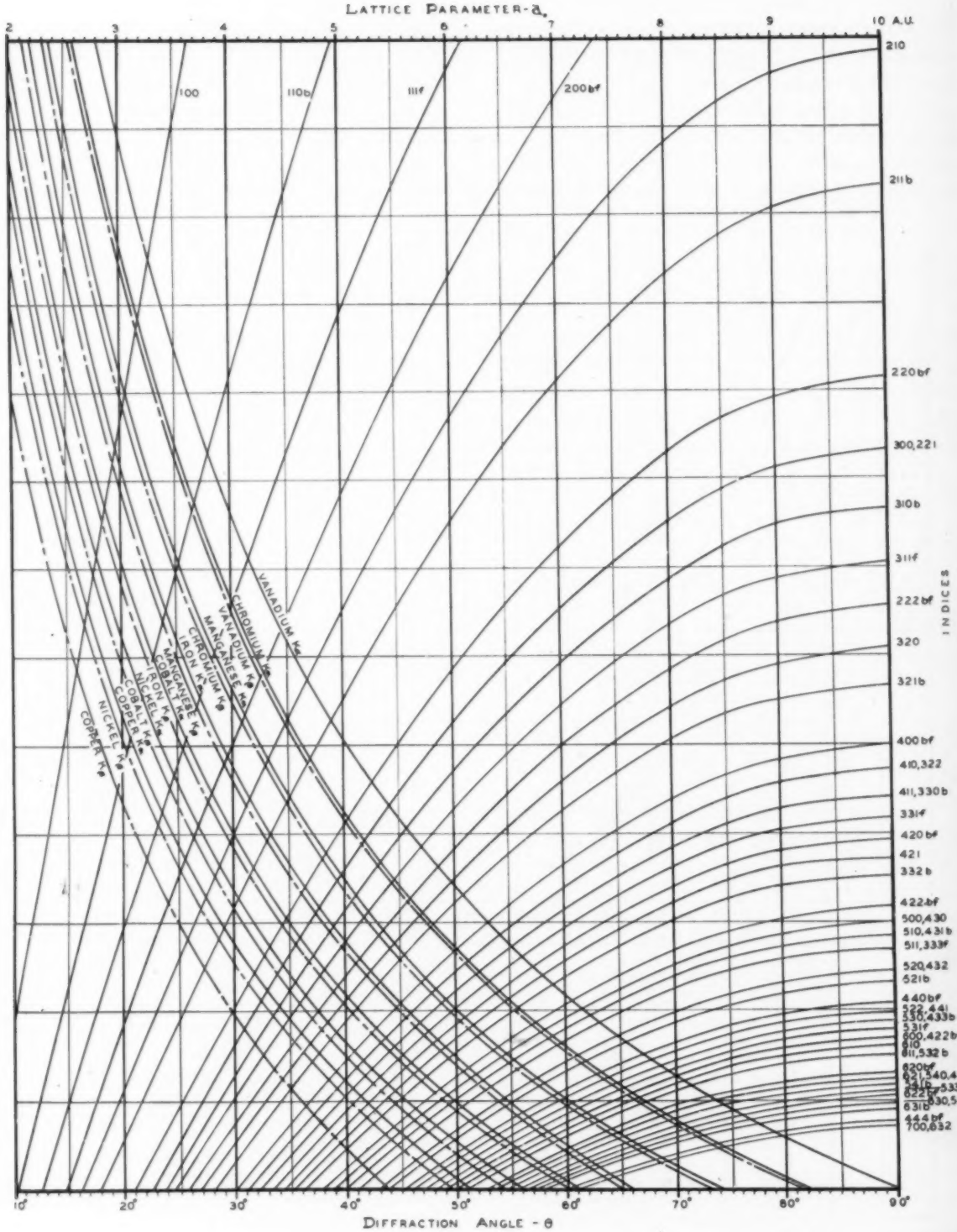

FIG. 2. b=b.c.c. lines, f=f.c.c. lines.

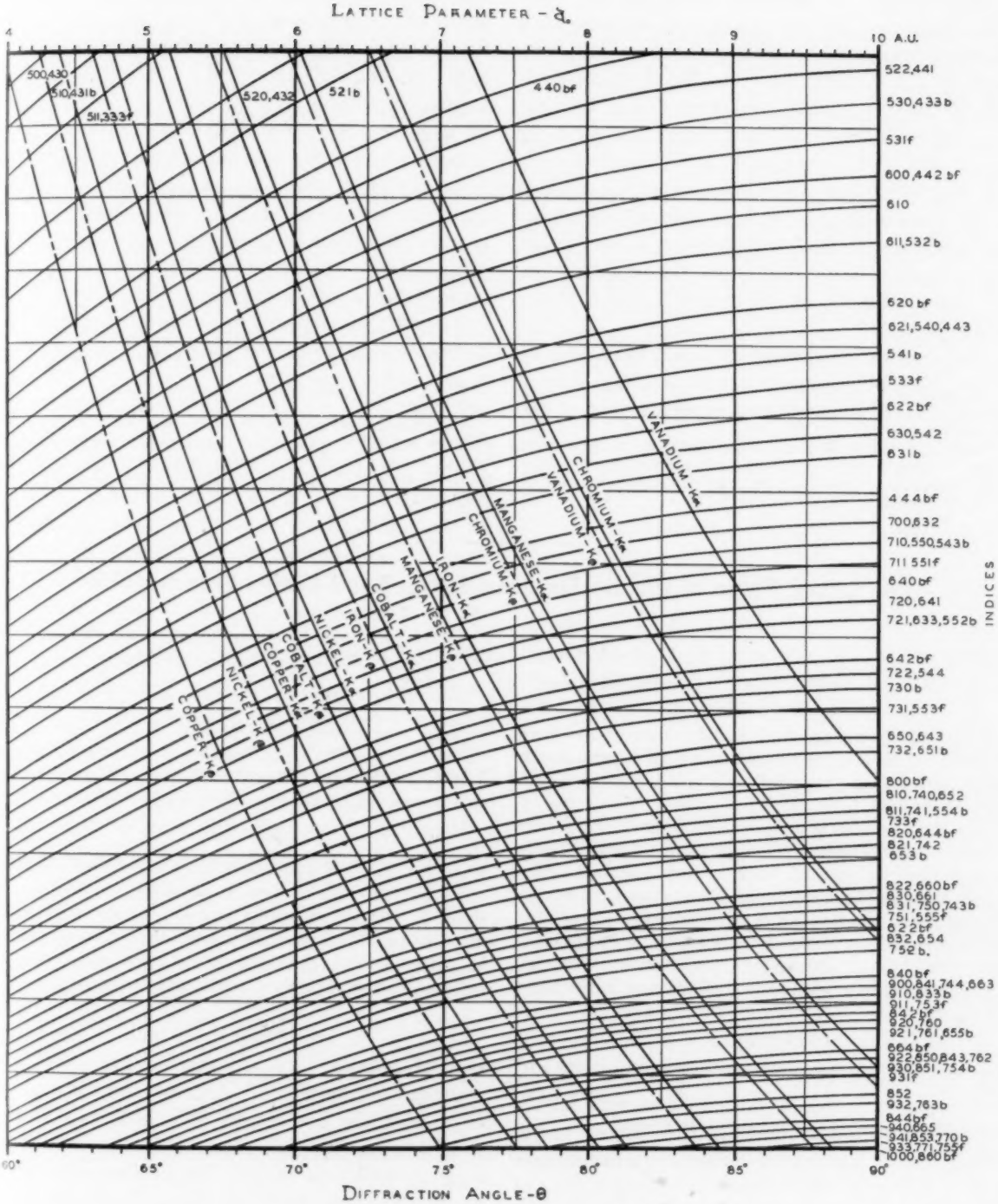

FIG. 3. *b*=b.c.c. lines, *f*=f.c.c. lines.

nation of cubic lattice constants can be readily selected.*

For example, let us determine from Fig. 1 the best radiation for the precise evaluation of a face-centered cubic lattice constant of approximately 3.36A. This is done by drawing horizontal lines (a straight edge may well be used for this purpose) for each radiation-curve at $a_0 \approx 3.36$A. (This value of a_0 is represented by a vertical line.) The intersections made by each of these lines with the "indices-curves" determine the positions of possible diffraction lines. Copper radiation was found to give the best distribution, $K\alpha$-lines occurring at 86° and 67°, and $K\beta$-lines at 66° and 63°.

The indices of diffraction lines may also be found by plotting the θ values obtained from a given pattern on a strip of paper to scale of the charts.† The strip in a horizontal position is next moved vertically (never laterally) until all the marks on it are in reasonable coincidence with the "indices-curves" on the charts as illustrated in Fig. 1. Thus, the lines and lattice-type are easily identified. Furthermore, the lattice constant may also be read directly with an accuracy of better than one percent. In the illustrated example, the lattice was found to be body-centered cubic with an approximate lattice constant of about 3.70A. Beta-lines can be readily identified in similar manner since their χ-value intersects the beta-radiation curve at the same value of the lattice constant.

The author wishes to acknowledge his indebtedness to Professor Ralph R. Hultgren for many useful criticisms.

* Before making the final selection, some consideration must be given to the absorption edge of the material under investigation; for example, copper radiation may not be used for iron samples.

† Transparencies of Figs. 2 and 3 may be made for any camera radius by reducing or enlarging the figures to the proper scale. In this form, the patterns themselves may be used, instead of plotting the diffraction angles on a strip of paper.

The Initial Stage of Plastic Deformation in Lead Under Compression

W. James Lyons
Loyola University, New Orleans, Louisiana
(Received March 19, 1940)

In the steady-creep stage in metals, stress (or resistance to deformation) is related to the velocity of deformation, in accordance with the hyperbolic-sine law, or the exponential law. These laws, however, fail completely to describe the initial stage of plastic deformation in lead. The present series of tests is an investigation of this initial stage in compression. An optical lever system and high speed kymograph have been employed. The photographic records obtained show the progress of deformation with time. The duration of the initial stage increases with the compressing load. For a load of 120.0 kg the duration is about 0.16 sec. It is found that a unique, initial deformation, independent of time, is associated with each load. From measurements on the deformation curves, resistances as functions of time have been calculated. These data indicate a linear relationship between the resistance R and time t:

$$R = l + mt,$$

where l = a parameter of small value, evidently a correction term, and m = rate of increase of resistance. Using this equation and the dynamic constants of the apparatus, deformation curves in good agreement with experiment have been derived. Resistance in the initial stage appears to be only approximately a function of deformation alone

Introduction

THE plastic deformation of metals may be said to occur in three stages, *viz.*, initial, transition (called by Andrade the "β-flow"), and steady creep. The initial deformation takes place within a fraction of a second after application of the deforming force. The later stages, particularly steady creep, have been investigated extensively for many metals. In lead, under both tension and compression, it has been found that the so-called *asymptotic creep rate* is an exponential function of the prevailing stress, at constant temperature.[1] Andrade has given an expression for the length of a lead wire under tension as a function of time, in the transition stage as well as in steady creep.[2] Examination of these relations, however, soon indicates that

[1] L. C. Tyte, Proc. Phys. Soc. **51**, 203 (1939); W. J. Lyons, J. App. Phys. **10**, 651 (1939).
[2] E. N. da C. Andrade, Proc. Roy. Soc. **A84**, 1 (1910); **A90**, 329 (1914).

attempts to apply them to the initial stage would be futile. The initial stage appears simply as a boundary condition in the analytical expression derived for the later stages.

While no experimental investigations of deformation in lead as a function of time in the initial stage appear to have been conducted, numerous attempts have been made to set up relations between deforming force and the resultant initial deformation. The most extensive of these tests have been limited to compression, and have been conducted principally in ballistics laboratories, where lead and copper "crusher" cylinders are used for pressure measurements in gun chambers. On the whole, the results with lead have been unsatisfactory. Those obtained by different methods of compression have been discordant, while those that have been brought into accord involve unverified assumptions which cast doubt on the deforming pressures reported.

Lead cylinders have been calibrated for deforming pressures by two methods, which may be expected to give absolute values.[3] In the *drop-weight* method a known mass is allowed to fall on to the cylinder. From the kinetic energy of the mass at the instant of impact, and the resultant deformation of the cylinder, the resistance of the latter in bringing the mass to rest is calculated. In the *dead-load* method a known load is poised in contact with the uncompressed cylinder. The load is instantaneously released and compresses the cylinder until, it is supposed, the resistance balances the load. The measured deformation, presumably independent of time, is taken to correspond uniquely to the particular load imposed on the cylinder. In their tests on lead, Bogomolov and Kunin[4] found that for the equal deformation of cylinders the computed resistance at room temperature was 86 percent greater by the drop-weight method than that shown with a dead-load. Similarly, the resistances reported for the impact tests of Mason[5] are about 40 percent greater than those found for identical cylinders equally deformed during the first seconds of dead load tests made by the present writer.[6]

The differences in results by these two methods of test were qualitatively explained as being due to the increase in resisting stress with increased deformation velocity, the higher range of velocities occurring in the drop-weight tests. But a quantitative agreement has been lacking, and the energy relations are unsatisfactory. Furthermore, in view of the well-known property of lead for deforming indefinitely under pressure, there arose some doubt as to whether, at the higher loads, the dead-weight methods had been giving a unique deformation not involving time. The present tests were undertaken (1) to determine whether such unique deformations existed, (2) to discover the character of the compression process as a function of time, and (3) to throw some light on the relations between deformation, velocity and stress in the initial stage.

Apparatus and Procedure

The apparatus for compressing and detecting the deformation of the lead cylinders has been previously used and described.[6] A simple tripping device has been added to release instantaneously the lever carrying the compressing load. This device consists essentially of a steel rod about 1 cm in diameter, which fits and moves in a vertical sleeve. The rod supports the lever near the load point, and in turn is supported by a horizontal key passing through the rod and sleeve. The load is released by pulling out the key. By means of a thumbscrew between the rod and lever, the latter may be raised or lowered, to remove all play and assure intimate contact between the test cylinder, piston and lever.

From the results of the previous researches, it was obvious that a high speed method of recording was required. While the optical lever was retained, the telescope and scale were dismantled, and replaced by a kymograph. This consists of the synchronous motor of a Cenco-Harrington timer, mounted on a wooden stand, with its shaft vertical. Above the motor the extended shaft carries a sheet-metal drum about 7.5 cm diameter and 10 cm long. On a 60-cycle a.c. line, the speed of motor and drum is 10 r.p.s. In operation the

[3] In a third method, in which pressures are supplied by powder gases in a gun-chamber, only relative values are obtained, and even their validity may be restricted to a narrow range of conditions.

[4] U. N. Bogomolov and N. F. Kunin, J. Tech. Phys. (U. S. S. R.) **5**, No. 5 (1935).

[5] H. W. R. Mason, Arms and Explosives, January 1, 1918, and February 1, 1918; F. W. Jones, Arms and Explosives, February 1, 1918, pp. 20–22.

[6] W. J. Lyons, J. App. Phys. **9**, 641 (1938).

rotating drum carries a sheet of photographic paper. Light from a strongly illuminated pinhole, passing through a system of lenses, falls on the tilting mirror, and after reflection, comes to a focus on the drum of the kymograph. A photographic record of the motion of the mirror is thus obtained.[7] To avoid fogging the sensitized paper, the entire kymograph was enclosed in a suitable housing, having a vertical slit at the front.

With a drum speed of 10 r.p.s., the resolution of time on the photographic records is 0.0042 sec./cm. This value was used in measurements on the records. Inquiry at the engineering office of the public utility serving the electric line from which the synchronous motor was operated, disclosed that the frequency variation is from 59.9 to 61.25 cycles/sec., with an average of 60 cycles for a 24-hour period. The maximum error introduced into the time-scale by this variation is 2.1 percent, which is within the limits of accuracy to be otherwise expected of the present research. Since tests were made at various hours of the day and on various days of the week, with tests at particular loads widely scattered, it may be assumed that the time-scale errors on the averaged results are much smaller.

Measurements of the lengths of the lead cylinders were made with micrometer calipers before and after compression. On the photographic records the light spot traced a horizontal base-line before compression, and a similar line above it at the completion of the initial stage. Connecting the two is the single deformation curve. The distances between centers of the two horizontal traces were measured, and from these, with the caliper readings, the average magnification of deformation for 26 records was found to be 56.5 ± 0.2. This value was used to translate all measurements made on the records into percent deformations.

Results

Only lead cylinders were tested in this investigation, and they were identical in composition and form with those used in tests previously reported.[6] Records were obtained for the compression of 28 cylinders under seven different loads.

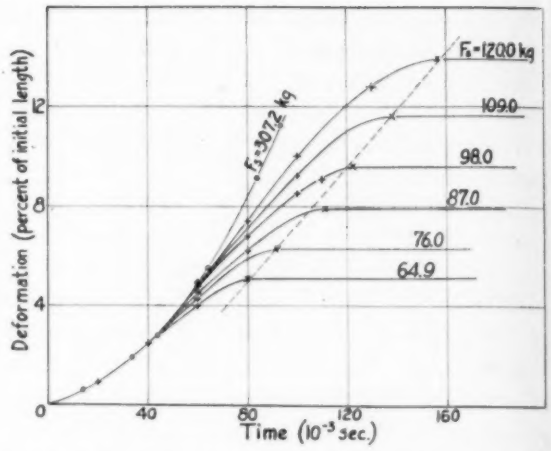

FIG. 1. Deformation in the initial stage as a function of time, for various compressive loads.

The results of all compression tests are summarized graphically in Fig. 1. Each curve is the mean of 3, 4, or 5 photographic traces, depending on the uniformity between the traces for a particular load. In general, the traces for the heavier loads were more uniform. The points at which the traces were measured, and means determined, are indicated by crosses. Below 40 millisec. no real distinction between the various traces is detectable. The loads indicated are those exerted by the piston on the test cylinders in static equilibrium; they are, therefore, the forces prevailing during the intervals represented by the flat portions of the curves.

These flat portions of the curves show clearly that there exists in the initial stage a unique deformation associated with each load. This deformation is independent of time of the order of magnitude encountered in the initial stage. This fact is emphasized by the continuous horizontal band traced on the original records in many revolutions of the drum after the initial stage has been completed.

The instant at which, for each load, the initial stage ended has been indicated on the graph. The location of these points is necessarily accompanied by uncertainty, because the leveling-off of the traces is very gradual. However, when the averages of the best choices were fixed, it was found that they lay very close to a straight diagonal line, as shown.

[7] A 1000-watt lamp illuminates the 1-mm pinhole, the image of which on the drum is 1.6 mm in diameter. Verichrome film was used in the first tests, but Eastman Recording Paper No. 1 was found to give good records, and has been used in all later tests.

The fidelity with which the deformations are recorded depends upon the rear leg of the tilting mirror remaining in contact with the top surface of the piston. This contact is effected solely by gravitational pull at the centroid of the mirror. Several tests were made to determine whether the response of the mirror (acting under gravity) was rapid enough to follow the compression. In these tests, a cylinder was quickly slid from beneath the piston, allowing the latter to fall freely, and with it, the rear leg of the mirror. The four traces obtained were nearly identical; their mean is curve I, Fig. 2. The points at which measurements were made are indicated by crosses. This curve coincides with that for the familiar equation:

$$s = \tfrac{1}{2}at^2, \qquad (1)$$

when a, corresponding here to the acceleration of the rear point of the mirror, has the value 330 cm/sec.^{2}. The graph shows that this acceleration is ample to keep the mirror leg in contact with the piston throughout the compressive process.

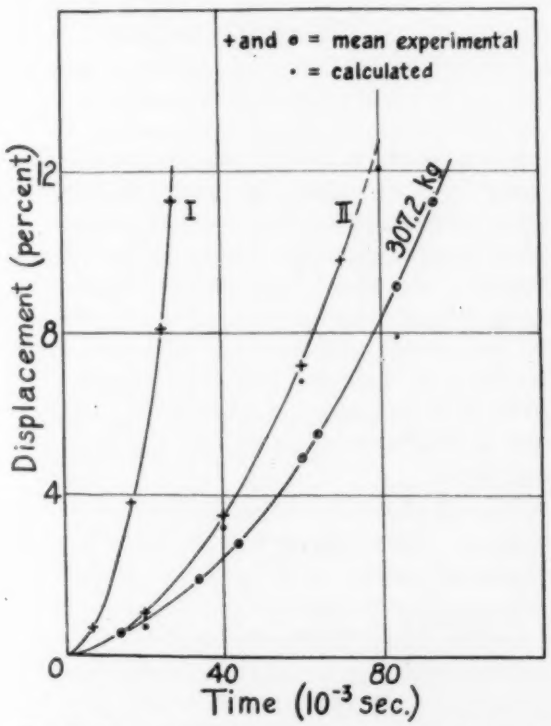

FIG. 2. Curve I: displacement of rear leg of mirror in freely tipping back. Curve II: displacement of piston in the free fall of lever under a 98.0-kg load. For ease of comparison with Fig. 1, displacements are given in percent of initial length of the lead cylinders (0.500 in.), and the *deformation* curve for 307.2 kg is included.

Appearing in Fig. 2 is another curve, designated II. This was obtained as the mean of three trials in which the lever, with a load, was allowed to fall with no lead cylinder beneath the piston to resist the fall. The load was such that it would exert, in static equilibrium, a force of 98.0 kg at the piston. The piston was held securely up against the lever by means of a brass strip to which a stud was soldered near the center. The brass strip was supported at each end by rubber bands passing around the lever bar.

The dots near curve II represent displacements given by Eq. (1) when the acceleration is 47.9 cm/sec.^{2}. As is shown later, this is the acceleration of the piston to be expected under the load conditions used here, when neither friction nor plastic stresses resist the fall of the lever under gravity. The experimental curve is consistently above the dots, implying an acceleration greater than that due to gravity, which was, however, the only force causing the displacement. Friction would tend to bring the curve below the dots. The discrepency here appears to be due solely to the choice of the zero-time on the photo-records. Because of the small slope of the trace in this region, the zero can be fixed only within a range of about ± 2 millisec. of the true value. Curve II was drawn using the zero-times originally chosen on the records, no adjustments being made. However, if the zero of the records is transposed to the left 2 millisec., it is found that the dots fall on the curve. In any case, the constant time-difference between curve and dots at the various displacements indicates that after 10 millisec. the acceleration of the piston is 47.9 cm/sec.^{2}. We may, therefore, conclude that friction in the apparatus is entirely negligible, and that the curves of Fig. 1 have not been distorted by this factor.

Dynamical Theory

An adequate discussion of the results must be based upon the dynamical principles involved in the present method. It should be recognized, that though an unvarying load is applied instantaneously, the deforming force acting on the test cylinder at every instant is not equal to that acting when static equilibrium is attained. The force applied to the lever, and available at any instant to compress the cylinder, is the weight of

the total load on the lever minus the kinetic reaction of the load. Conversely, if we neglect friction, the kinetic reaction is less than the weight because of the stress in the cylinder.[8] The following rigorous equation may be readily deduced for the motion:

$$I\alpha = M_L g\bar{x} + Mgr - Mr^2\alpha - Rr_1, \qquad (2)$$

where I = moment of inertia of lever-bar; α = angular acceleration of lever; M_L and M are masses of lever-bar and weights, respectively; g = acceleration of gravity, $\bar{x}$, r, r_1 are distances from fulcrum, respectively, to centroid of bar, application point of weights, and point of contact with piston, and R = resistances to deformation. The resistance $R = \sigma A$, where σ is the plastic stress, and A is cross-sectional area of the cylinder. For a bar of uniform density and cross section, such as that of the lever, the moment of inertia is $M_L r^2/3$. Substituting this value for I in Eq. (2), and rearranging terms, we obtain

$$R = \frac{M_L g \cdot \bar{x} + Mg \cdot r}{r_1} - \frac{(M + M_L/3)r^2}{r_1^2}\ddot{\epsilon}, \qquad (3)$$

where $\ddot{\epsilon} = \alpha r_1$ = acceleration of deformation. The term

$$\frac{M_L g \cdot \bar{x} + Mg \cdot r}{r_1} = F_s,$$

TABLE I.*

F_s (KG)	$\frac{(M+M_L/3)r^2}{r_1^2}$
64.9	1.30
98.0	2.05
120.0	2.54
307.2	6.75

* With these values of the coefficients, R is in kg and $\ddot{\epsilon}$ in cm/sec.².

the load on the cylinder at static equilibrium.

In the derivation of Eq. (2), R is treated as a force acting on the lever bar, the motion of which is determined by R to the extent indicated by the equation. It is unnecessary to introduce explicitly into the equation a "deforming force"; this force appears as the reaction to R, with which it is at all times in dynamic equilibrium. There arises no question, such as has troubled some investigators,[9] as to whether the resistance or plastic stress in the cylinder keeps pace with the varying deforming pressure. By means of Eq. (3), it is possible to determine the value of the resistance at any instant from the dimensions and motion of the deforming mechanism, provided $\ddot{\epsilon}$ can be measured accurately. Likewise, $\ddot{\epsilon}$ may be computed when R is known, as was done to locate the dots associated with curve II, Fig. 2. In this case, $R = 0$.

[8] We may neglect the mass of the piston, since its inertial effects are negligibly small compared to those of the other masses in the system.

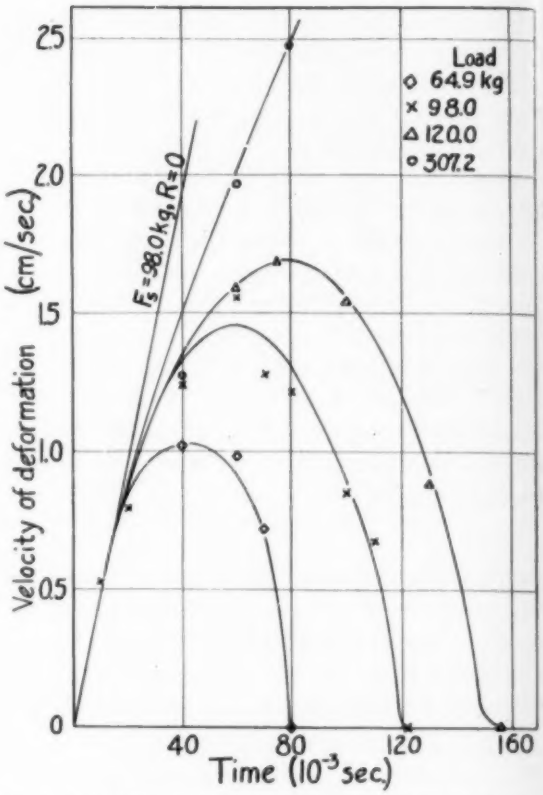

FIG. 3. Velocities of deformation as functions of time, as obtained from measurements on Fig. 1.

The values for the coefficient of $\ddot{\epsilon}$ in Eq. (3) have been calculated for four of the loads used, and are set out in Table I.

DISCUSSION OF RESULTS

An examination of Fig. 1 discloses that the compressions under the various loads attain the maximum velocity (slope) in about half the durations of the respective initial periods. Thereafter the velocity decreases, the deceleration

[9] Jones, reference 5.

increasing with time. This is shown graphically in Fig. 3 for four loads. Measurements of slopes at various times on the original of Fig. 1, converted to velocities in cm/sec., are indicated by crosses, etc. Through these points the best-fitting, smooth curve has been drawn for each load. To promote its reliability the 98.0-kg curve, in addition, has been drawn so that the graphical integration of its included area over any interval gives a deformation in satisfactory agreement with the corresponding curve of Fig. 1.

Also plotted is the graph for the load $F_s = 98.0$ kg, $R = 0$. The acceleration being uniform, the graph is a straight line with a slope of 47.9 cm/sec.^{2}. It might be pointed out that, as Eq. (3) will show, the slope of lines for other loads, with $R = 0$, would not have this same value. However, the difference is small.

These curves strongly suggest that the resistance of the cylinders does not become appreciable before the first 10 millisec. Thereafter the effect of the resistance is observable. It increases with time, as indicated by the decreasing slopes. This behavior is in accord with the opinion that the resistance is a function of the deformation and velocity. At the apex of each curve, $\ddot{\epsilon} = 0$, and $R = F_s$, as Eq. (3) shows. However, deformation does not cease at this point, as some writers on ballistics have inferred. In fact, these are the conditions existing in steady creep, where the deformation goes on indefinitely. The velocity must be brought from a small, but finite, value to zero. The resistance of the cylinder in accomplishing this deceleration must rise to a value greater than F_s.

As is suggested by the curvature of these graphs, and as Fig. 4 conclusively shows, R rises continuously until compression ceases. Differentiation of the curves of Fig. 3 gives the acceleration of deformation $\ddot{\epsilon}$ as a function of time. With values of $\ddot{\epsilon}$ thus obtained, R may be calculated at various times. This procedure was followed to obtain the various sets of points in Fig. 4, differentiation being accomplished by slope measurements on Fig. 3. The computed R's are very critical to minor variations in the slopes of the velocity curves. No resistance data for the 307.2-kg load are given in Fig. 4, because it was found that the large slopes occurring in the deformation and velocity curves for this load could not be measured with sufficient accuracy to give reliable values of R.

Several conclusions, of at least qualitative validity, may be drawn from a cursory examination of the lines drawn through the points of Fig. 4. The most obvious is that the resistance to deformation in the initial stage increases very nearly linearly with the time. Furthermore, it appears that the rate is about the same for the three loads. Finally, it is seen that the resistance

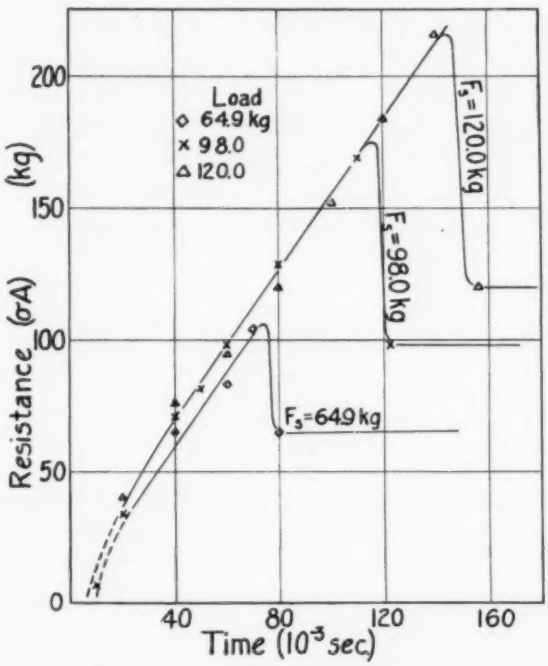

FIG. 4. Resistance to deformation in the initial stage, as computed by Eq. (3) from graphical differentiation of the curves in Fig. 3.

rises to a value about 70 percent above F_s before deformation ceases.

The linearity of the resistance-time relationship may be expressed:

$$R = l + mt, \tag{4}$$

where l = a parameter, and m = rate of increase of resistance. Assuming the validity of this relation, it was combined with Eq. (3) to eliminate R. Successive integration of the resultant equation under the boundary conditions that the deformation $\epsilon = 0$, and velocity $\dot{\epsilon} = 0$ at $t = 0$, leads to the equation:

$$\epsilon = at - bt^2,$$

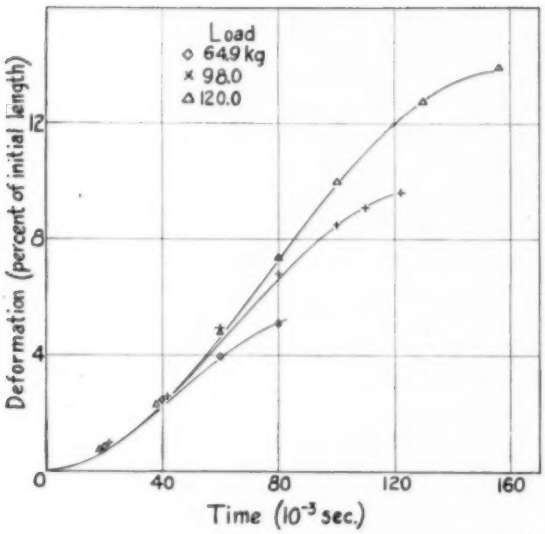

FIG. 5. Hypothetical deformation curves, based on Eq. (4). The experimental data for each load are indicated.

where

$$a=\frac{(F_s-l)r_1^2}{2(M+M_L/3)r^2},$$

and

$$b=\frac{mr_1^2}{6(M+M_L/3)r^2}.$$

By means of Eq. (5), with $m=1.45$ kg/millisec. for all loads, and with l having values given by Table II, the curves shown in Fig. 5 were drawn. Also shown are the measured points for each load, taken from Fig. 1.

In general, the agreement between experiment and hypothesis, reflected by Fig. 5, is good, and may be taken as indicating that Eq. (4) expresses the essential behavior of the resistance to deformation in the initial stage. The regular disposition of the measured points above the theoretical curve in the 20- to 40-millisec. region suggests that for a short period the resistance may lag behind the value given by Eq. (4), by a small amount. As a matter of fact, the measured points fall very close to Curve II, Fig. 2, in which no resistance to motion was offered. This suggests that the earlier portions of the resistance curves in Fig. 4 have the form indicated by the dotted lines.

While the term l appears in Eq. (4) as a preliminary resistance which varies with the compressing load, this need not be its real physical significance. Compared to resistances encountered later in the initial stage, l is very small. The accuracy of the present tests does not justify interpreting a quantity as small as l as anything other than a correction term. The conclusion to be drawn from these data is that the resistance has the value zero at zero time, and rises approximately linearly with time.

Equation (4) indicates that the behavior of resistance is governed by time only. If, in accord with the general theory of plastic deformation,[10] the resistance is a function of the variables ϵ and $\dot{\epsilon}$ together, we can only conclude that in the initial stage for loads of the order used here, the effects of ϵ and $\dot{\epsilon}$ so interact as to give a practically constant m. The present data are not sufficiently critical to exclude the possibility that

$$R=\phi(t^n), \tag{6}$$

where n is different from unity by a small amount.

As Curve II, Fig. 2 shows, the maximum acceleration of the piston (which occurs when no resistance is encountered) is fixed for a given load by the apparatus. This maximum acceleration varies from 45.5 cm/sec.^{2} for a 307.2-kg load on the lever to 49.9 cm/sec.^{2} when the 64.9-kg load is employed. When the lever *alone* is used, the maximum is 66.5 cm/sec.^{2}. It is not unlikely that the value of m is determined by these maxima, which are evidently the initial accelerations when a cylinder is beneath the piston. In the present tests, the initial accelerations were not greatly different, and the m's, accordingly, are indistinguishable. For sensibly greater initial accelerations, we may suppose m to be greater. This assumption would explain the magnitude of the deformations (8 percent is typical) which occur when lead cylinders of the type used here are compressed by explosive processes that are completed in 3 millisec. Because of the large chamber pressures quickly built up, and the small

TABLE II.

F_s (KG)	l (KG)
64.9	0.0
98.0	5.6
120.0	8.4

[10] A. Nadai, *Plasticity* (McGraw-Hill, 1931), pp. 270–75.

mass of the piston (the only inertial part), the initial accelerations are enormously greater than those encountered in the present tests. Accordingly, we would expect the slope m to be many times larger than 1.45 kg/millisec., so that in a few milliseconds sufficient resistance is built up to stop the compression. A rough calculation indicates that resistances of the order given by Fig. 4 for 3 millisec. would allow deformations exceeding 100 percent under pressures commonly encountered in ballistic research.

That the behavior of resistance as portrayed by Fig. 4 is consistent with the energy conservation law is shown by Fig. 6. Here resistances at various times from the *curve* of Fig. 4 have been plotted against deformations from Fig. 1 for two loads. The area beneath the curve $OCDB$ represents the work done against the resistance of the cylinder. The area beneath the line ACB, on the other hand, represents the potential energy lost by the compressing weights. Since frictional losses could be and were ignored in deriving the values of R plotted in Fig. 4, we should expect area $OCDBE$ = area $OABE$, unless the values of R are spurious for other reasons. Measurements show that the areas OAC and CDB are very nearly equal.

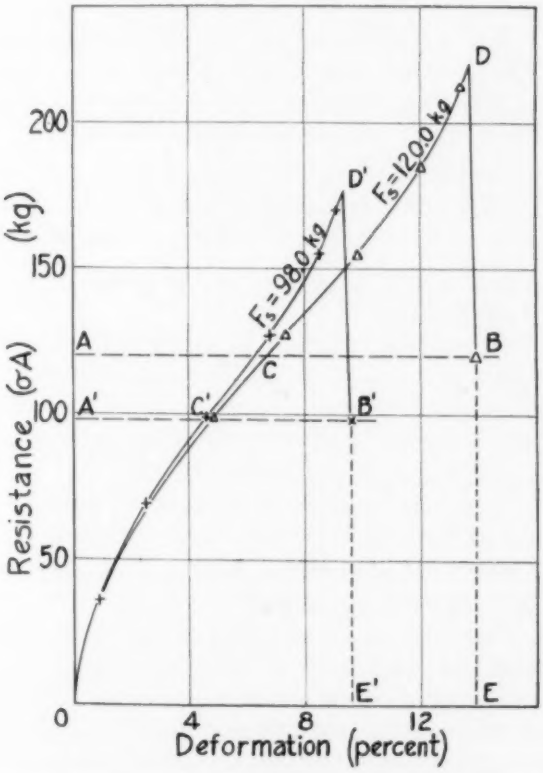

FIG. 6. Resistance as a function of the deformation of a cylinder. The data are taken from Figs. 1 and 4.

It is significant that Fig. 6 does not confirm the general validity of the principle that the rise of the resistance is determined solely by the deformation, which would be represented by a single curve for all loads. The law holds approximately up to about 5 percent, at which point the deformation velocity of the smaller load begins to fall off. This suggests that after it has reached a maximum, the velocity is inversely related to the resistance at a given deformation.

While the present tests have established indubitably the existence of unique deformations in the initial stage, it has been found that these deformations, for every load employed, are larger than those found in the writer's previous investigation[6] in 1938. In the 1938 tests, the load was lowered gradually, by hand, on to the piston, while in the present tests a tripping device applied the load instantaneously, so that it had zero velocity at the instant deformation started. Evidently, the application of a compressing load to a cylinder with an initial velocity has the same effect as an increase in the initial acceleration. In either case, it appears, the rate at which resistance rises with time increases. Thus the compression is stopped before the deformation becomes as great as would be allowed by a slower rise in resistance. These views furthermore are in accord with the divergence, previously noted, between Mason's impact data and those of the writer's 1938 tests, and are essentially the same as the assumption made by Bogomolov and Kunin to explain their results.

The writer gratefully acknowledges the cooperation of Dr. R. L. Womer, and Mr. Lewis Walkup of the Western Cartridge Company. They have selected and supplied much literature, otherwise inaccessible, pertaining to the subject of this article.

The Influence of Initial Stress on Elastic Waves*

MAURICE A. BIOT
Columbia University, New York, New York

(Received March 27, 1940)

A rigorous treatment is given of the problem of wave propagation in an elastic continuum when the influence of the initial stress is taken into account. After a short review of the theory various cases of initial stress are considered. It is shown that a uniform hydrostatic pressure does not change the laws of propagation. A hydrostatic pressure gradient produces a buoyancy effect which causes coupling between rotational and dilatational waves. Bromwich's equations for the effect of gravity on Rayleigh waves are derived from the general theory and the physical transition from Rayleigh waves in a very rigid medium to pure gravity waves in a liquid is discussed. The case of the vertical uniform stress is also considered and it is shown that the effect of the initial stress on the waves in this case cannot be accounted for by elastic anisotropy alone. Reflections may be produced by a discontinuity in stress without discontinuity of elastic properties.

INTRODUCTION

A SIMPLE experiment will show that initial stress must have an influence on elastic wave propagation. Consider a uniform rod held between two hinges. The oscillations of this rod obey the well-known equation

$$EId^4w/dx^4-\rho\omega^2w=0, \tag{1}$$

where w is the deflection, EI the stiffness, ρ the mass per unit length, $\omega/2\pi$ the frequency and x is the abscissa along the rod. The fundamental mode for the hinged rod of length l is

$$w=A\sin\frac{\pi x}{l}$$

and the corresponding frequency

$$\frac{\omega}{2\pi}=\frac{\pi}{2l^2}\left(\frac{EI}{\rho}\right)^{\frac{1}{2}}. \tag{2}$$

If there is an axial compression P in the rod the equation for the free oscillations becomes

$$EI\frac{d^4w}{dx^4}+P\frac{d^2w}{dx^2}-\rho\omega^2w=0. \tag{3}$$

The shape of the fundamental mode is the same as before but the frequency is now

$$\frac{\omega}{2\pi}=\frac{\pi}{2l^2}\left(\frac{EI}{\rho}(1-P/P_e)\right)^{\frac{1}{2}} \tag{4}$$

with

$$P_e=EI\pi^2/l^2.$$

The axial compression P decreases the frequency. When P approaches P_e, which is the buckling load of the rod, the frequency falls to zero.

If P is negative we have an axial tension in the rod. In that case the frequency is increased. Considering a very slender rod with vanishing stiffness ($EI\to 0$) the frequency becomes

$$\frac{\omega}{2\pi}=\frac{1}{2l}\left(\frac{-P}{\rho}\right)^{\frac{1}{2}}, \tag{5}$$

which is the frequency for a string under a tension $-P$.

When we put the rod under tension it acquires partly the properties of a stretched string. From the viewpoint of wave propagation a tension in the rod increases the velocity of propagation and a compression decreases this velocity.

It is clear that these phenomena must be a particular aspect of the more general case of elastic wave propagation in three dimensions in a body under initial stress.

The effect of initial stress on oscillations and wave propagation has been investigated by a number of writers, but because of the lack of a general and rigorous theory the results are restricted to the case of an initial hydrostatic pressure and are often contradictory or incomplete. L. Brillouin's[1] treatment leads to the conclusion that at sufficiently high pressure the wave

* Publication assisted by the Ernest Kempton Adams Fund for Physical Research of Columbia University.

[1] L. Brillouin, Ann. de physique **4**, 528 (1925).

velocities would reduce to zero. This paradoxical result is due to incorrect assumptions. In connection with problems in geophysics the effect of initial stress on the oscillations of a gravitating sphere has been considered. Correct equations have been derived by Love[2] for the case of an incompressible material under hydrostatic pressure. He also points out that the compressibility must introduce an important effect of buoyancy but does not attempt to establish any theory for this case. By an extension of Love's method Macelwane and Sohon[3] have established equations for the oscillations of a compressible gravitating sphere. These equations may be shown to be particular cases of our general theory if we introduce explicitly the change of body force due to the oscillations of the earth itself. The effect of gravity on Rayleigh waves and the oscillations of an elastic globe was investigated by T. J. I'A Bromwich,[4] applying the equations derived by Love for an incompressible material under hydrostatic pressure. In a recent paper F. Birch[5] has applied Murnaghan's[6] theory of finite strain and shows that the hydrostatic pressure has no effect on the laws of propagation. This paper is restricted not only by the fact that the initial stress is assumed hydrostatic, but also by a condition not mentioned explicitly by the writer, namely that there is no initial pressure gradient. Further restriction is due to Murnaghan's assumption that the material in the unstressed state is homogeneous and isotropic, with a definite potential energy function of the finite strain so that the initial hydrostatic pressure condition is assumed to be obtained from an initial unstressed condition through a reversible process. There is no physical basis for this assumption because it is very likely that the state of hydrostatic pressure inside the earth is produced by a slow process of creep in which viscosity and physical-chemical irreversible processes are predominant.

The present author has derived[7–9] a general theory of elasticity for bodies under initial stress which can be immediately applied to the problem of wave propagation.

No assumption is made on how the initial state of stress is produced. These initial stress components satisfy only the conditions of internal equilibrium. We give a brief review of the theory in the case of two-dimensional strain. The derivation is quite elementary and does not involve the use of tensor calculus. The equations are applied to various cases of initial stress. We find that a homogeneous hydrostatic pressure does not affect the laws of wave propagation. When there is an initial pressure gradient we show that there is coupling between rotational and compression waves. This coupling is due to a buoyancy effect whose presence was suspected by Love[2] and which we derive here in a quantitatively correct form. This effect is of course small for usual earthquake waves, but becomes preponderant if we consider tidal waves or the modes of oscillation of the earth. In the next paragraph we consider the special case of surface waves or Rayleigh waves, assuming an incompressible material with hydrostatic pressure due to gravity.

Our theory in this case leads exactly to Bromwich's equations, but a special feature of the surface waves is pointed out which is not mentioned in Bromwich's paper. Finally, we consider an initial state of stress which is homogeneous but not hydrostatic, i.e., we assume unequal initial principal stresses. This approximates the state of stress near the surface of the earth. It is found in this case that the behavior of the transversal wave alone is affected by the stress. The behavior of these waves cannot be accounted for by elastic anisotropy or a change in elastic coefficients and the existence of stress introduces an essentially new aspect in the nature

[2] A. E. H. Love, *The Mathematical Theory of Elasticity* (Cambridge Univ. Press, 4th edition, 1927), pp. 176–178.
[3] J. B. Macelwane and F. W. Sohon, *Introduction to Theoretical Seismology, Part I Geodynamics* (John Wiley & Sons, New York, 1936).
[4] T. J. I'A Bromwich, "On the influence of gravity on elastic waves and in particular on the vibrations of an elastic globe," Proc. London Math. Soc. **30**, 98–120 (1898).
[5] F. Birch, "The effect of pressure upon the elastic parameters of isotropic solid according to Murnaghan's theory of finite strain," J. App. Phys., **9** 279 (1938).
[6] F. D. Murnaghan, "Finite deformations of an elastic solid," Am. J. Math. April, 1937.
[7] M. A. Biot, "Theory of elasticity with large displacements and rotations," Proc. Fifth Internat. Congress of Applied Mechanics, 1938.
[8] M. A. Biot, "Non linear theory of elasticity and the linearized case for a body under initial stress," Phil. Mag. [7] **27**, 468 (1939).
[9] M. A. Biot, "Théorie de l'Elasticité du second ordre avec application à la théorie du flambage," Ann. de la Société Scientifique de Bruxelles, Serie I **59**, 104 (1939).

of the wave propagation. The velocity of propagation depends on the stress and it is possible to obtain reflections in a medium which has uniform elastic properties but contains discontinuities of initial stress. These facts must have their importance for the interpretation of data in methods of seismic prospecting.

General Theory

Consider a state of initial stress such that a principal direction is always parallel with the z axis, while the small additional strains are assumed to constitute a state of plane strain in the xy plane.

The initial stress is defined by the components S_{11}, S_{22} and S_{12} referred to rectangular axes x, y. They satisfy the equilibrium conditions

$$\begin{aligned} \frac{\partial S_{11}}{\partial x}+\frac{\partial S_{12}}{\partial y}+\rho(x, y)X(x, y)=0, \\ \frac{\partial S_{12}}{\partial x}+\frac{\partial S_{22}}{\partial y}+\rho(x, y)\,Y(x, y)=0, \end{aligned} \tag{6}$$

where ρ is the specific mass and X, Y the components of the body force per unit mass. An elastic element of coordinates x, y acquires the coordinates $\xi=x+u$, $\eta=y+v$ after deformation and rotates through an angle

$$\omega=\tfrac{1}{2}(\partial v/\partial x-\partial u/\partial y). \tag{7}$$

The stress components after deformation referred to *directions which rotate with the material* are

$$\begin{aligned} \sigma_{11}&=S_{11}+s_{11}, \\ \sigma_{22}&=S_{22}+s_{22}, \\ \sigma_{12}&=S_{12}+s_{12}. \end{aligned} \tag{8}$$

The components s_{11}, s_{22} and s_{12} of the stress increment depend only on the strain. This stress may be referred to the original x, y directions and the components then become in first approximation

$$\begin{aligned} \sigma_{xx}&=s_{11}-2S_{11}\omega, \\ \sigma_{yy}&=s_{22}+2S_{22}\omega, \\ \sigma_{xy}&=s_{12}+(S_{11}-S_{22})\omega. \end{aligned} \tag{9}$$

These are the stresses at the point ξ, η along the x and y directions.

These components satisfy the dynamical equilibrium relations

$$\begin{aligned} \partial\sigma_{xx}/\partial\xi+\partial\sigma_{xy}/\partial\eta+\mu(\xi, \eta)X(\xi, \eta)&=\mu(\xi, \eta)\partial^2u/\partial t^2, \\ \partial\sigma_{xy}/\partial\xi+\partial\sigma_{yy}/\partial\eta+\mu(\xi, \eta)\,Y(\xi, \eta)&=\mu(\xi, \eta)\partial^2v/\partial t^2, \end{aligned} \tag{10}$$

where $\mu(\xi, \eta)$ is the specific mass after deformation.

Now we can express these equations in terms of the independent variable x, y by using transformations of the type

$$\frac{\partial\sigma_{xx}}{\partial\xi}=\frac{\partial\sigma_{xx}}{\partial x}\frac{\partial x}{\partial\xi}+\frac{\partial\sigma_{xx}}{\partial y}\frac{\partial y}{\partial\xi}, \quad \text{etc.} \tag{11}$$

The partial derivatives of x, y with respect to ξ, η are in first approximation

$$\begin{aligned} \frac{\partial x}{\partial\xi}&=\frac{1}{D}\left(1+\frac{\partial v}{\partial y}\right), & \frac{\partial x}{\partial\eta}&=-\frac{1}{D}\frac{\partial u}{\partial y}, \\ \frac{\partial y}{\partial\xi}&=-\frac{1}{D}\frac{\partial v}{\partial x}, & \frac{\partial y}{\partial\eta}&=\frac{1}{D}\left(1+\frac{\partial u}{\partial x}\right), \end{aligned} \tag{12}$$

where D is the Jacobian

$$D=\frac{d(\xi, \eta)}{d(x, y)}=\begin{vmatrix} 1+\dfrac{\partial u}{\partial x} & \dfrac{\partial u}{\partial y} \\ \dfrac{\partial v}{\partial x} & 1+\dfrac{\partial v}{\partial y} \end{vmatrix}. \tag{13}$$

Using these relations and the property

$$\rho(x, y) = D\mu(\xi, \eta),$$

expressing the conservation of mass Eqs. (10) become

$$\begin{aligned}
&\frac{\partial \sigma_{xx}}{\partial x}+\frac{\partial \sigma_{xy}}{\partial y}+e_{yy}\frac{\partial \sigma_{xx}}{\partial x}+e_{xx}\frac{\partial \sigma_{xy}}{\partial y}-(e_{xy}-\omega)\frac{\partial \sigma_{xy}}{\partial x}-(e_{xy}+\omega)\frac{\partial \sigma_{xx}}{\partial y}+\rho X(\xi, \eta)=\rho\frac{\partial^2 u}{\partial t^2},\\
&\frac{\partial \sigma_{xy}}{\partial x}+\frac{\partial \sigma_{yy}}{\partial y}+e_{yy}\frac{\partial \sigma_{xy}}{\partial x}+e_{xx}\frac{\partial \sigma_{yy}}{\partial y}-(e_{xy}-\omega)\frac{\partial \sigma_{yy}}{\partial x}-(e_{xy}+\omega)\frac{\partial \sigma_{xy}}{\partial y}+\rho Y(\xi, \eta)=\rho\frac{\partial^2 v}{\partial t^2},
\end{aligned} \tag{14}$$

in which $e_{xx}=\partial u/\partial x$, $e_{yy}=\partial v/\partial y$, $e_{xy}=\frac{1}{2}(\partial v/\partial x+\partial u/\partial y)$ are the strain components. We now substitute the values (9) for σ_{xx}, σ_{yy}, σ_{xy} and drop terms of higher order than the first; the above equations become

$$\begin{aligned}
&\frac{\partial s_{11}}{\partial x}+\frac{\partial s_{12}}{\partial y}+\rho u\frac{\partial X}{\partial x}+\rho v\frac{\partial X}{\partial y}+\rho\omega Y-2S_{12}\frac{\partial \omega}{\partial x}+(S_{11}-S_{22})\frac{\partial \omega}{\partial y}\\
&\qquad+e_{yy}\frac{\partial S_{11}}{\partial x}+e_{xx}\frac{\partial S_{12}}{\partial y}-e_{xy}\left(\frac{\partial S_{11}}{\partial y}+\frac{\partial S_{12}}{\partial x}\right)=\rho\frac{\partial^2 u}{\partial t^2},\\
&\frac{\partial s_{12}}{\partial x}+\frac{\partial s_{22}}{\partial y}+\rho u\frac{\partial Y}{\partial x}+\rho v\frac{\partial Y}{\partial y}+\rho\omega X+(S_{11}-S_{22})\frac{\partial \omega}{\partial x}+2S_{12}\frac{\partial \omega}{\partial y}\\
&\qquad+e_{yy}\frac{\partial S_{12}}{\partial x}+e_{xx}\frac{\partial S_{22}}{\partial y}-e_{xy}\left(\frac{\partial S_{12}}{\partial y}+\frac{\partial S_{22}}{\partial x}\right)=\rho\frac{\partial^2 v}{\partial t^2}.
\end{aligned} \tag{15}$$

In order to obtain these equations account must be taken of the initial equilibrium conditions (6) and the identities

$$\begin{aligned}
\partial e_{xx}/\partial y&=(\partial/\partial x)(e_{xy}-\omega),\\
\partial e_{yy}/\partial x&=(\partial/\partial y)(e_{xy}+\omega).
\end{aligned} \tag{16}$$

We remember that the stress increments s_{11}, s_{22}, s_{12}, depend only on the strain. They may be taken as linear functions of the strain components

$$\begin{aligned}
s_{11}&=B_{11}e_{xx}+B_{12}e_{yy}+B_{13}e_{xy},\\
s_{22}&=B_{21}e_{xx}+B_{22}e_{yy}+B_{23}e_{xy},\\
s_{12}&=B_{31}e_{xx}+B_{32}e_{yy}+B_{33}e_{xy}.
\end{aligned} \tag{17}$$

Assuming the existence of a potential energy function of the strain it is possible to prove[8] that the elastic coefficients must satisfy the relations

$$\begin{aligned}
B_{12}+S_{11}&=B_{21}+S_{22},\\
B_{13}-S_{12}&=B_{31}+\tfrac{1}{2}S_{12},\\
B_{23}-S_{12}&=B_{32}+\tfrac{1}{2}S_{12}.
\end{aligned} \tag{18}$$

It is only in case of initial hydrostatic pressure ($S_{11}=S_{22}$, $S_{12}=0$) that the elastic coefficients will be symmetric ($B_{ij}=B_{ji}$).

The boundary conditions along an element dx, dy of the boundary contour are found to be[7]

$$\begin{aligned}(s_{11}-S_{12}\omega)dy-(s_{12}-S_{22}\omega)dx&=dF_x,\\(s_{12}+S_{11}\omega)dy-(s_{22}+S_{12}\omega)dx&=dF_y,\end{aligned}\tag{19}$$

where dF_x, dF_y are the projections of the force acting on the boundary element dx, dy.

For a three-dimensional theory the following equations may be derived as above. We find

$$\sum^{\nu}\frac{\partial S^{\nu i}}{\partial x^{\nu}}-\rho\sum^{\mu}\omega_{\mu}{}^{i}X^{\mu}+\rho\sum^{\mu}u^{\mu}\frac{\partial X^{i}}{\partial x^{\mu}}+\rho\Delta X^{i}+\sum^{\mu\nu}\left(S^{\nu i}\frac{\partial\omega_{\nu}{}^{\mu}}{\partial x^{\mu}}+S^{\mu\nu}\frac{\partial\omega_{\mu}{}^{i}}{\partial x^{\nu}}\right)-e\rho X^{i}-\sum^{\mu\nu}e_{\mu}{}^{\nu}\frac{\partial S^{\mu i}}{\partial x^{\nu}}=\rho\frac{\partial^{2}u^{i}}{\partial t^{2}}.\tag{20}$$

With the following notations: x^{ν} = the Cartesian coordinates, u^{ν} = the displacements, X^{ν} = the components of the initial body force, ΔX^{ν} the increment of body force due to the motion, $\omega_{\nu}{}^{\mu}=\frac{1}{2}(\partial u^{\mu}/\partial x^{\nu}-\partial u^{\nu}/\partial x^{\mu})$, $e_{\nu}{}^{\mu}=\frac{1}{2}(\partial u^{\mu}/\partial x^{\nu}+\partial u^{\nu}/\partial x^{\mu})$, $e=\sum^{\nu}e_{\nu}{}^{\nu}$. The derivation of these equations for the statical case is given in references 8 and 9. We have introduced here explicitly the increment of body force ΔX^{ν} due to the motion itself this term must be taken into account if we wish to state correctly the equations of motion of a gravitating body.

We consider now various cases of initial stress conditions and examine the corresponding behavior of elastic waves for each case. For simplicity we restrict ourselves to two-dimensional strain.

Uniform hydrostatic pressure

In this case

$$S_{11}=S_{22}=\text{const}\ S_{12}=0.$$

Moreover a uniform pressure implies $X=Y=0$. In this case Eqs. (15) become

$$\begin{aligned}\partial s_{11}/\partial x+\partial s_{12}/\partial y&=\rho\partial^{2}u/\partial t^{2},\\\partial s_{12}/\partial x+\partial s_{22}/\partial y&=\rho\partial^{2}v/\partial t^{2}.\end{aligned}\tag{21}$$

These equations are the same as the classical ones for a body in an unstressed state. The influence of the pressure appears only in the elastic coefficients of the material.

Hydrostatic pressure with uniform pressure gradient

Such a case will occur in a material under the action of gravity when the influence of creep has been acting a sufficiently long time so that the stress condition at every point has become isotropic. This condition must be approximately realized in the earth.

Taking the y axis positive downward we have

$$X=0,\quad Y=g,$$

where g is the acceleration of gravity. Also $S_{11}=S_{22}$ and $S_{12}=0$. From (6) we derive

$$\partial S_{11}/\partial x=\partial S_{22}/\partial y=0,$$

$$\partial S_{22}/\partial y=\partial S_{11}/\partial y=-\rho g.$$

We assume the specific mass to be uniform (ρ = constant). With these conditions Eqs. (15) become

$$\begin{aligned}\frac{\partial s_{11}}{\partial x}+\frac{\partial s_{12}}{\partial y}+\rho g\frac{\partial v}{\partial x}&=\rho\frac{\partial^{2}u}{\partial t^{2}},\\\frac{\partial s_{12}}{\partial x}+\frac{\partial s_{22}}{\partial y}-\rho g\frac{\partial u}{\partial x}&=\rho\frac{\partial^{2}v}{\partial t^{2}}.\end{aligned}\tag{22}$$

These equations are different from the classical ones for an initially unstressed medium. The additional terms are due to the existence of a pressure gradient. In order to investigate the behavior of the waves for this case, let us assume the stress-strain relations to be Hooke's law for an isotropic medium

$$\begin{aligned}s_{11}&=\lambda e+2Ge_{xx},\\s_{22}&=\lambda e+2Ge_{yy},\\s_{12}&=2Ge_{xy}.\end{aligned}\tag{23}$$

By substitution in Eqs. (22) we find

$$\begin{aligned}G\nabla^{2}u+(G+\lambda)\frac{\partial e}{\partial x}+\rho g\frac{\partial v}{\partial x}&=\rho\frac{\partial^{2}u}{\partial t^{2}},\\G\nabla^{2}v+(G+\lambda)\frac{\partial e}{\partial y}-\rho g\frac{\partial u}{\partial x}&=\rho\frac{\partial^{2}v}{\partial t^{2}}.\end{aligned}\tag{24}$$

We derive the following equations for the dilatation e and the rotation ω by the usual method

$$(2G+\lambda)\nabla e^2+2\rho g\partial\omega/\partial x=\rho\partial^2 e/\partial t^2,$$
$$G\nabla^2\omega-2\rho g\partial e/\partial x=\rho\partial^2\omega/\partial t^2.$$

These equations show the existence of coupling between longitudinal and transversal waves. This coupling is due to the existence of an initial pressure gradient. The physical meaning of this coupling is as follows. Consider a dilatational plane wave propagating in the horizontal direction. At a point where the material is compressed it is denser and therefore has a negative buoyancy, while in the region of positive dilatation the buoyancy is positive. The dilatational wave is therefore associated with a periodic distribution of vertical buoyancy force which generates a transversal wave. Conversely a transversal wave propagating in the horizontal direction produces a dilatational wave. In this case a portion of the material which is horizontal in the initial state undergoes a rotation and the initial pressure gradient acquires a horizontal component of alternating sign which causes a dilatational wave. The effect increases with the wave-length and we may verify that for the case of the earth it can only acquire an importance in the study of tidal waves with a wave-length of the order of 1000 km or larger.

Influence of gravity on Rayleigh waves

It was shown by Rayleigh that elastic waves may propagate along the surface of elastic bodies the amplitude of the wave decreasing exponentially with depth. It is clear that such waves at the surface of the earth must be influenced by gravity. The effect must increase with the wave-length, and also when the rigidity of the medium becomes smaller. In fact, we can imagine materials less and less rigid, such as jelly, in which gravity would have a predominant effect, and consider finally the limiting case of a liquid in which the rigidity is zero and the waves such as ocean waves are due entirely to gravity. As the velocity of the latter depends on the wave-length, we may expect that one of the effects of gravity on Rayleigh waves is to make their velocity of propagation depend on the wave-length. The theory of this effect was first attempted by Bromwich.[3] It is interesting to verify that his equations may be derived from our general theory provided we introduce the assumption that the initial state of stress is hydrostatic.

We introduce the same simplifying assumption as Bromwich, namely that the material is incompressible. This eliminates the dilatational wave. We then add the assumption that the initial state of stress is a hydrostatic pressure with a pressure gradient due to gravity, and apply therefore the above Eqs. (24). We may write Hooke's law for an incompressible material as follows:

$$\begin{aligned} s_{11}&=-p+2Ge_{xx},\\ s_{22}&=-p+2Ge_{yy},\\ s_{12}&=2Ge_{xy}, \end{aligned} \tag{25}$$

where p is the increment of hydrostatic pressure. Substituting these values in Eqs. (24) and taking into account the condition of incompressibility $\partial u/\partial x+\partial v/\partial y=0$ we find

$$\begin{aligned} G\nabla^2 u-\frac{\partial}{\partial x}(p-\rho gv)&=\rho\frac{\partial^2 u}{\partial t^2},\\ G\nabla^2 v-\frac{\partial}{\partial y}(p-\rho gv)&=\rho\frac{\partial^2 v}{\partial t^2}. \end{aligned} \tag{26}$$

Assuming the x axis to coincide with the free surface, the boundary conditions (19) for $y=0$ are $s_{22}=s_{12}=0$ or

$$\begin{aligned} 0&=-p+2Ge_{yy},\\ 0&=2Ge_{xy}. \end{aligned} \tag{27}$$

Putting $p_1=p-\rho gv$, the wave equation becomes

$$\begin{aligned} G\nabla^2 u-\partial p_1/\partial x&=\rho\partial^2 u/\partial t^2,\\ G\nabla^2 v-\partial p_1/\partial y&=\rho\partial^2 v/\partial t^2, \end{aligned} \tag{28}$$

and the boundary condition

$$\begin{aligned} -p_1+2Ge_{yy}&=\rho gv,\\ 2Ge_{xy}&=0. \end{aligned} \tag{29}$$

The quantity p_1 may be interpreted physically as the pressure increment due to the waves at a fixed point (x, y), while p is the pressure at a point originally of coordinates x, y but displaced

with the material at the coordinates $x+u$, $y+v$. The case $G=0$ corresponds to a liquid medium and Eqs. (28) become the hydrodynamical equations of an incompressible fluid for small oscillations. Eqs. (28) and (29) are identical with those considered by Bromwich. He also derived Eq. (31) below for the velocity.

We can verify that we may write the following solution for Eqs. (28)

$$u=(Ale^{-ly}+Cre^{-ry})\sin(lx-\alpha t),$$
$$v=(Ale^{-ly}+Cle^{-ry})\cos(lx-\alpha t), \qquad (30)$$
$$p_1=-A\alpha^2\rho e^{-ly}\cos(lx-\alpha t)$$

with

$$r=l(1-\zeta^2)^{\frac{1}{2}}, \quad \zeta^2=\alpha^2\rho/Gl^2.$$

This solution also verifies the condition $\partial u/\partial x+\partial v/\partial y=0$ of incompressibility. From the boundary conditions (29) we derive

$$(2Gl^2-\alpha^2\rho+\rho gl)A+(2Glr+\rho gl)C=0,$$
$$2l^2A+(l^2+r^2)C=0.$$

Elimination of A and C yields

$$(2-\zeta^2)^2-\frac{\rho g\zeta^2}{Gl}=4(1-\zeta^2)^{\frac{1}{2}}. \qquad (31)$$

The quantity ζ in this equation is the ratio of the velocity of the Rayleigh wave $v=\alpha/l$ to the velocity of a shear wave $v_t=(G/\rho)^{\frac{1}{2}}$

$$\zeta=v/v_t.$$

Eq. (31) therefore yields the velocity of the Rayleigh wave as a function of the dimensionless parameter $\rho g/Gl$. This parameter represents the influence of gravity and it can be seen that the velocity increases with the wave-length $2\pi/l$, but as shown already by Bromwich the correction for waves at the surface of the earth is small even for very large wave-length.

For a very small wave-length ($l=\infty$) the equation yields the root $\zeta^2=0.912$ which is the value found by Rayleigh. For an increasing wave-length the value of the root increases until $\rho g/Gl=1$ for which $\zeta=1$.

Consider, for instance, the case of the earth. We assume $g=981$ cm/sec., $\rho=3$ g/cm^3, $G=(1.5)10^{11}$ dynes/cm^2 then $\rho g/Gl=1$ for a wave-length

$$2\pi/l=3200 \text{ km}.$$

This shows that even for a wave-length equal to half the earth's radius the increase of velocity is of the order of 5 percent.

The limiting case $\rho g/Gl=1$ occurs when the velocity $(g/l)^{\frac{1}{2}}$ of the gravity waves is equal to the velocity $(G/\rho)^{\frac{1}{2}}$ of the shear waves.

It is of interest to investigate what happens when the material becomes less and less rigid and the rigidity G tends to zero. For values $\rho g/Gl>1$ the solution above breaks down and it is impossible to satisfy the boundary condition with a real solution. We therefore introduce a solution of the following type:

$$u=(Ale^{-ly}-C\mu\sin\mu y)\sin(lx-\alpha t),$$
$$v=(Ale^{-ly}+Cl\cos\mu y)\cos(lx-\alpha t), \qquad (32)$$
$$p_1=-A\alpha^2\rho e^{-ly}\cos(lx-\alpha t)$$

with

$$\mu=l\left(\frac{\alpha^2\rho}{Gl}-1\right)^{\frac{1}{2}}.$$

Introducing these expressions in the boundary conditions (29) we find

$$-2Al^2-C\alpha^2\rho/G=0,$$
$$A(\alpha^2\rho-2Gl^2-\rho gl)-C\rho gl=0.$$

Elimination of A and C yields

$$(2Gl^2/\alpha^2\rho-1)(lg/\alpha^2-1)=0, \qquad (33)$$

which can be considered as an equation for l. There are two solutions. One,

$$lg/\alpha^2=1,$$

depends on gravity. The velocity of the corresponding waves is $\alpha/l=(g/l)^{\frac{1}{2}}$ and is equal to that of the gravity wave. This solution is valid only if $g\rho/Gl>1$.

It is a combination of a pure gravity wave with a transversal plane wave coming from the depth of the material and being reflected at the surface at an angle $\tan^{-1}(l/\mu)$ with the vertical. The relative amplitude of this wave is

$$\frac{C(\mu^2+l^2)^{\frac{1}{2}}}{Al}=-2\left(\frac{Gl}{\rho g}\right)^{\frac{1}{2}}.$$

It decreases with the rigidity. This indicates that a pure gravity wave for wave-lengths or rigidities such that $\rho g/G\lambda>1$ cannot persist, but must lose

energy by radiation of a transversal wave inside the material. This loss of energy vanishes when $G=0$, i.e., the material becomes a liquid, and we are left with the gravity wave alone.

The other solution of Eq. (33) is

$$2Gl^2/\alpha^2\rho=1.$$

It is independent of gravity. The reason for this is that $A+C=0$ and the displacement $v=0$ at $y=0$, i.e., the free surface stays a plane. The velocity of this wave is

$$\alpha/l=(2G/\rho)^{\frac{1}{2}},$$

i.e., 40 percent higher than that of a pure transversal wave. Since $A=-C$, such a wave when excited must dissipate very quickly by radiation inside. The phenomena pointed out here will influence those modes of oscillation of the earth which have a wave-length above 1000 km.

Medium under initial vertical compression

We first consider a state of uniform initial stress and take the principal directions of this initial stress along the x and y axes. Then $S_{12}=0$ and the components S_{11}, S_{22} are constant values of the principal initial stresses. Eqs. (15) become

$$\begin{aligned}\frac{\partial s_{11}}{\partial x}+\frac{\partial s_{12}}{\partial y}+(S_{11}-S_{22})\frac{\partial \omega}{\partial y}&=\rho\frac{\partial^2 u}{\partial t^2},\\ \frac{\partial s_{12}}{\partial x}+\frac{\partial s_{22}}{\partial y}+(S_{11}-S_{22})\frac{\partial \omega}{\partial x}&=\rho\frac{\partial^2 v}{\partial t^2}.\end{aligned}\tag{34}$$

These equations are also different from the classical ones for an unstressed initial state. It is seen that the additional terms depend only on the difference between the principal stresses $S_{11}-S_{22}$ and on the rotation. Hence *only the rotational waves* are affected by this stress condition.

We assume that the vertical and horizontal directions are directions of elastic symmetry, and consider the general stress-strain relations (17). Because $S_{12}=0$ and the assumption of symmetry we have

$$B_{13}=B_{31}=B_{23}=B_{32}=0.$$

Hence the stress-strain relations become

$$\begin{aligned}s_{11}&=B_{11}e_{xx}+B_{12}e_{yy},\\ s_{22}&=B_{21}e_{xx}+B_{22}e_{yy},\\ s_{12}&=B_{33}e_{xy}.\end{aligned}\tag{35}$$

From (18) we still have $B_{12}-B_{21}=S_{22}-S_{11}$. Therefore there are four distinct elastic constants in these relations. Introducing these relations in Eqs. (34) we derive

$$\begin{aligned}G\nabla^2 u+(B_{12}+G)\frac{\partial e}{\partial x}+(B'-2G)\frac{\partial^2 u}{\partial x^2}\\ +(S_{11}-S_{22})\frac{\partial \omega}{\partial y}=\rho\frac{\partial^2 u}{\partial t^2},\\ G\nabla^2 v+(B_{21}+G)\frac{\partial e}{\partial y}+(B''-2G)\frac{\partial^2 v}{\partial y^2}\\ +(S_{11}-S_{22})\frac{\partial \omega}{\partial x}=\rho\frac{\partial^2 v}{\partial t^2},\end{aligned}\tag{36}$$

with

$$B_{33}=2G,\quad B'=B_{11}-B_{12},\quad B''=B_{22}-B_{31},$$
$$e=e_{xx}+e_{yy}.$$

Consider now a transversal plane wave propagation in the horizontal direction

$$u=0,\quad v=\cos(lx-\alpha l).$$

By substitution in Eqs. (36) we find the velocity

$$V_h=\frac{\alpha}{l}=(G+\tfrac{1}{2}(S_{11}-S_{22}))^{\frac{1}{2}}/\rho^{\frac{1}{2}}.$$

A similar wave propagating in the vertical direction would have the velocity

$$V_v=(G-\tfrac{1}{2}(S_{11}-S_{22}))^{\frac{1}{2}}/\rho^{\frac{1}{2}}.$$

For instance if there is a vertical compression P in the material

$$S_{22}=-P,\quad S_{11}=0,$$

the velocity in the horizontal direction is greater than in the vertical. This effect is essentially due to the existence of the initial stress, because if this initial stress is zero or if it is a hydrostatic pressure then the two velocities are the same in spite of the elastic anisotropy of the material.

Note that this phenomenon is the same if we put

$$S_{22}=0, \quad S_{11}=-P.$$

The initial condition is then a horizontal tension $-P$ and the velocity of shear waves propagating in the horizontal direction is

$$V_h=\left(\frac{G-\frac{1}{2}P}{\rho}\right)^{\frac{1}{2}}.$$

If we put $G=0$ in this formula we do not find the velocity in a membrane or a string under tension. This is because the wave in a membrane is not a shear wave but a bending wave. For the viewpoint of the theory of elasticity a bending wave is the combination of two waves of the Rayleigh type at both free boundaries.[10] If we calculate the velocity of these bending waves and then put $G=0$ we find

$$V_h=(-P/\rho)^{\frac{1}{2}},$$

which is the velocity of a wave in a membrane under tension P.

This analysis shows that propagation and reflections of elastic waves in a material under initial stress must follow laws which cannot be explained by elastic anisotropy or a change in elastic constants. In fact, because the velocity of propagation depends on the total initial shear, a discontinuity in shear may produce a reflection even if there is no discontinuity in elastic constants.

[10] S. P. Timoshenko, "On the transverse vibrations of bars of uniform cross section." Phil. Mag. **43**, 125 (1922).

Equations of Finite Differences Applied to Torsional Oscillations of Crankshafts*

MAURICE A. BIOT
Columbia University, New York, New York
(Received April 8, 1940)

From the viewpoint of torsional oscillations an internal combustion engine with a long crankshaft is generally considered to be equivalent to a uniform shaft carrying equidistant identical disks. It is here shown that advantage can be taken of the regularity of such a system to simplify the calculation of torsional oscillations. This is done by applying a mathematical method known as the *calculus of finite differences*. The procedure leads to a frequency equation (2.7) of remarkable symmetry in which appear as parameter the number n of cylinders in line and two simple functions K_1 and K_2 of the frequency which characterize the dynamical properties of the machines coupled at both ends of the crankshaft. These characteristic functions are of the nature of mechanical impedances, but due to their physical interpretation as a spring modulus (or spring constant) generalized to dynamic phenomena, the appellation *dynamic modulus* is being preferably used in the present paper. The concept of dynamic modulus is briefly introduced in the first section, while the second deals with the establishment of the frequency equation and an artifice for its rapid graphical solution avoiding the necessity of plotting an oscillatory function. Numerical applications to Diesel engines are treated in the last section. An example is also given of an extreme case where the fundamental frequency has a very low value and a special method is used for the calculation of this frequency.

1. Mechanical Impedance and Dynamic Modulus

IN the theory of electric networks the concept of impedance has proved to be a highly useful tool for both the analytical treatment and the comprehension of electrical phenomena. Its use has been extended to the field of mechanics by the introduction of so-called equivalent networks or, as in acoustics, by defining the mechanical impedance as the ratio of force to velocity. The latter definition is very useful in compound electromechanical systems and in those for which the amount of dissipated or radiated energy is one of the important features. However, in systems without or with negligible dissipation constituted, for instance, by a combination of masses and springs, it seems preferable to introduce as mechanical impedance the ratio of force to displacement. When there is no dissipation this ratio is a real quantity which can be either positive or negative. It generalizes the concept of spring constant to the case of harmonic mo-

* Publication assisted by the Ernest Kempton Adams Fund for Physical Research of Columbia University.

tion. In order to distinguish this type of impedance from the other we use the appellation *dynamic spring constant* or simply *dynamic modulus*. The following example illustrates the above definition.*

An elastic rod AB of torsional spring constant k is clamped at B and carries at A a disk of moment of inertia I (Fig. 1). In order to produce an harmonic oscillation of the disk of frequency $\omega/2\pi$ and of amplitude θ we must apply to the disk a torque

$$M=(k-I\omega^2)\theta.$$

This may be written

$$M=K\theta \tag{1.1}$$

with

$$K=k+Ip^2 \quad p=i\omega \quad i=\sqrt{-1}.$$

The quantity K is the dynamic modulus of the system at A. It becomes equal to the static modulus k of the rod for small frequencies, it vanishes at resonance and is negative for higher frequencies.

In the case of a shaft carrying two disks and free to rotate in bearings as illustrated in Fig. 2, it is readily verified that the dynamic modulus K_2 at the left end is obtained by the following steps. The dynamic modulus K' at the left of

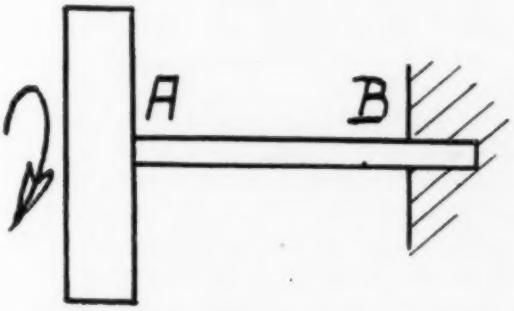

FIG. 1. Example of mechanical impedance.

the system (k, I) alone is given by

$$1/K'=1/k+1/Ip^2. \tag{1.2}$$

If we add the mass I_1 the dynamic modulus becomes K''

$$K''=K'+I_1p^2 \tag{1.3}$$

and adding the spring k_1 the dynamic modulus K_2 is given by

$$1/K_2=1/k_1+1/K''. \tag{1.4}$$

The law of formation of the dynamic modulus† is the well-known series-parallel combination rule for the electrical impedance of a ladder-type

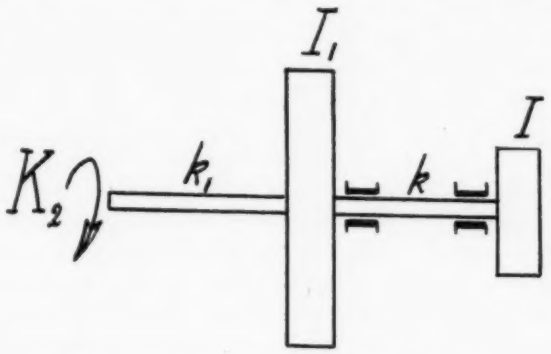

FIG. 2. Example of mechanical impedance.

network. From (1.2), (1.3), (1.4) we find

$$K_2=\cfrac{1}{\left[\cfrac{1}{k_1}+\cfrac{1}{-I_1\omega^2+\cfrac{1}{1/k-1/I\omega^2}}\right]}. \tag{1.5}$$

The physical meaning of this quantity K_2 is that a harmonic torque of given frequency $\omega/2\pi$ acting on the left end of the system produces an amplitude at that point which would be the same as if the torque were driving an elastic rod clamped at the other end and of spring constant equal to K_2. Also if we put $K_2=0$ we obtain the frequency equation for the free oscillations of the system, while $1/K_2=0$ is the frequency equation when it is rigidly clamped at the left end.

2. Frequency Equation

Using the concept of dynamic modulus and a mathematical method known as the *calculus of finite differences* we are now going to show that it is possible to establish a frequency equation of remarkable simplicity.

Following the usual procedure we represent

* Further developments on mechanical impedances, the concept of dynamic modulus and the application of the calculus of finite differences to engineering problems will be found in a textbook by Dr. Th. von Karman and the author (*Mathematical Methods in Engineering* (McGraw Hill Book Co., Inc., New York, 1940)).

† A similar rule for the combination of springs is indicated in J. P. Den Hartog, *Mechanical Vibrations* (McGraw Hill Book Co., New York, 1934), p. 41.

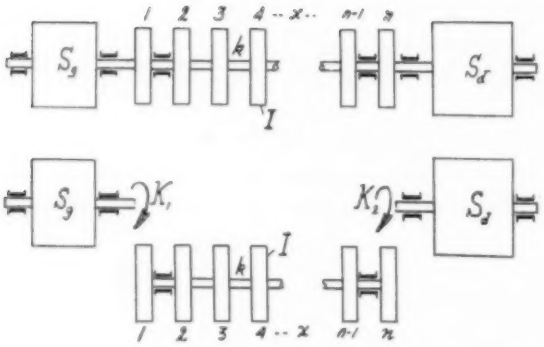

FIG. 3. Schematic representation of an internal combustion engine and its end impedances.

schematically the crankshaft rods and pistons by a uniform shaft carrying as many disks as there are cylinders in line. (Fig. 3). Let n be the number of disks (or cylinders in line) numbered from 1 to n, I their moment of inertia and θ_x the amplitude of oscillation of a disk numbered x. It is well known that the amplitudes of three successive disks satisfy the equation

$$I\omega^2\theta_x = k(-\theta_{x-1}+2\theta_x-\theta_{x+1}), \qquad (2.1)$$

where ω is the angular frequency of the oscillation and k the torsional spring constant of a section of the shaft between two disks.* If we put $\alpha^2 = I\omega^2/k$ Eq. (2.1) may be written

$$\theta_{x-1}-(2-\alpha^2)\theta_x+\theta_{x+1}=0. \qquad (2.2)$$

There are $n-2$ such equations for $x=2, 3, \cdots, n-1$. In order to express the corresponding relations for the end disks we assume that a machine of dynamic modulus K_1 is coupled at the left end of the shaft and a machine of dynamic modulus K_2 at the right end. Then the amplitudes of oscillation θ_1 and θ_2 satisfy the equations,

$$\begin{aligned}\theta_2-(1-\alpha^2+K_1/k)\theta_1&=0\\ \theta_{n-1}-(1-\alpha^2+K_2/k)\theta_n&=0.\end{aligned} \qquad (2.3)$$

The recurrence Eq. (2.2) is called an *equation with finite differences of the second order*. Such an equation may be treated by methods similar to those used in the solution of differential equations, with relations (2.3) playing here the role of "boundary conditions."

Let us first assume that $|\alpha|<2$. In that case the so-called general solution of Eq. (2.2) is known to be

$$\theta_x = A\cos\mu x + B\sin\mu x, \qquad (2.4)$$

where A and B are arbitrary constants and μ is related to the frequency by the relation

$$\omega = 2(k/I)^{\frac{1}{2}}\sin\mu/2. \qquad (2.5)$$

The arbitrary constants A and B are determined by substituting the general solution (2.4) into the boundary conditions (2.3). Putting $K_1/k-1=M$, $K_2/k-1=N$ we find

$$\begin{aligned}&A(1+M\cos\mu)+BM\sin\mu=0\\ &A[\cos\mu(n+1)+N\cos\mu n]\\ &\quad+B[\sin\mu(n+1)+N\sin\mu n]=0.\end{aligned} \qquad (2.6)$$

These are two simultaneous equations for A and B. A more detailed derivation is given in the Appendix at the end of the paper. The elimination of A and B between these two equations yields the frequency equation,

$$\begin{aligned}&\sin\mu(n+1)+(M+N)\sin\mu n\\ &\quad+MN\sin\mu(n-1)=0.\end{aligned} \qquad (2.7)$$

We have assumed $|\alpha|<2$ or $\omega=2(k/I)^{\frac{1}{2}}$ which means that the frequency Eq. (2.7) yields only the natural frequencies of the system which are lower than $2(k/I)^{\frac{1}{2}}$. In most practical cases however this range will be sufficient as it will actually cover all the frequencies of the system or at least the greatest number of them and the most important ones. The limiting value $\omega_c=2(k/I)^{\frac{1}{2}}$ of the frequency has an important physical significance as regards the response of the crankshaft to vibrations. In the terminology of electric wave filters ω_c is called the *cut-off frequency*. In fact the crankshaft is the mechanical equivalent of a low pass filter and it reflects all torsional waves of frequency higher than the cut-off frequency. For a frequency approaching this limiting value the mode of vibration in the crankshaft is such that two successive cranks oscillate in opposite phases.

* As pointed out by R. Grammel [see for instance: *über einige dynamische Probleme bei Kolben motoren* Schriften der Deutschen Akademie der Luftfohrtforschung (1939)] due to the existence of play between bearings and crankshaft journals, the model should include a slight coupling between the disks x and $x+2$. This can also be treated by the method of finite differences. It is believed however that the classical method of perturbations might yield more quickly the corrected modes and frequencies. Another correction which can be obtained by the method of perturbations is due to the fact that the moments of inertia of the disks include a periodic function of time.

In principle, in order to find the roots of the frequency equation it would be sufficient to plot the left side of Eq. (2.7) as a function of μ or ω and note the abscissas where the curve intersects the horizontal axis. This procedure however, is generally cumbersome because the function to plot is highly oscillatory and requires the calculation of a great number of points. This difficulty may be avoided and the numerical work considerably simplified by the following artifice.

We notice that the frequency equation may be written in complex form by putting

$$\begin{aligned} e^{\mu i/2}+Me^{-\mu i/2}&=A_1e^{\varphi_1 i}\\ e^{\mu i/2}+Ne^{-\mu i/2}&=A_2e^{\varphi_2 i}. \end{aligned} \tag{2.8}$$

The left side of the frequency Eq. (2.7) is then the imaginary part of $A_1A_2e^{(\mu n+\varphi_1+\varphi_2)i}$. An equivalent form of the frequency equation is therefore

$$\mu n+\varphi_1+\varphi_2=\text{multiple of } \pi, \tag{2.9}$$

where φ_1 and φ_2 are functions of μ given by

$$\begin{aligned} \varphi_1&=\tan^{-1}\left[\left(\frac{2k}{K_1}-1\right)\tan\frac{\mu}{2}\right],\\ \varphi_2&=\tan^{-1}\left[\left(\frac{2k}{K_2}-1\right)\tan\frac{\mu}{2}\right]. \end{aligned} \tag{2.10}$$

In Eq. (2.9) the left side represents a smooth function of μ generally near to a straight line. This form of the frequency equation is therefore well fit for solution by graphical methods and interpolation. The procedure will be made clear by the numerical examples below.

The method is of course not limited to the calculation of frequencies lower than the cut-off frequencies. If $|\alpha|>2$ the general solution of the difference equation (2.2) is

$$\theta_x=A(-1)^x\cosh\mu x+B(-1)^x\sinh\mu x, \tag{2.11}$$

where μ is related to ω by the relation,

$$\omega=2(k/I)^{\frac{1}{2}}\cosh\mu/2.$$

Proceeding as we have done above this leads to a frequency equation similar to (2.6) this time with hyperbolic instead of circular function.

The shape of the modes of vibration in the crankshaft may be calculated below the cut-off frequency by (2.4) and above by (2.11). Using, for instance, the first condition (2.6) we may write (2.4) in the form

$$\theta_x=C\sin(\mu x+\beta) \tag{2.12}$$

with

$$\tan\beta=(1-K_1/k)\sin\mu/[1+(K_1/k-1)\cos\mu]$$

and C an arbitrary constant. The torsional mode of order r is found by substituting the values μ_r and ω_r, roots of the frequency equation and corresponding to that mode.

3. Applications

Example 1

We consider the case of a crankshaft with n cranks free at both ends. Then $K_1=K_2=0$. The frequency Eq. (2.7) may be written

$$\sin\mu(n+1)-2\sin\mu n+\sin\mu(n+1)=0$$
$$\text{or}\qquad \sin\mu n=0.$$

The roots are $\mu=p\pi/n$ ($p=0, 1, 2, \cdots, n$). The values $p=0$ and $p=n$ must be excluded because they do not correspond to any motion of the crankshaft. The $(n-1)$ natural frequencies are therefore given by the formula

$$\omega_p=\omega_c\sin p\pi/n,\qquad p=1, 2, \cdots, n-1.$$

The spectrum of frequencies is represented in Fig. 4. We notice that the highest frequencies have a tendency to gather in the vicinity of the

Fig. 4. Frequency spectrum of a 12-cylinder in-line engine without end impedances.

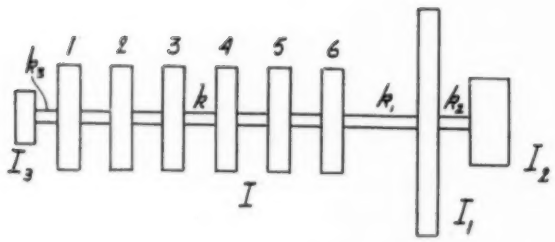

FIG. 5. Six-cylinder Diesel with pump flywheel and pulley.

cut-off frequency $\omega_c = 2(k/I)^{\frac{1}{2}}$. This is a general feature in the oscillations of long crankshafts. It is also of interest to consider the frequency equation in the form (2.9). We may write in this case $\varphi_1 = \varphi_2 = -\pi/2$ then the Eq. (2.9) becomes

$$\mu n = \text{multiple of } \pi.$$

In this case the left side of the equation as a function of μ represents a straight line.

Example 2

A six-cylinder Diesel installation is represented in Fig. 5. The numerical data are:*

$I = 3920$ lb. in. sec.^{2}	$k = 730\times10^6$ in. lb./rad.
$I_1 = 139800$ lb. in. sec.^{2}	$k_1 = 402\times10^6$ in. lb./rad.
$I_2 = 26400$ lb. in. sec.^{2}	$k_2 = 1334\times10^6$ in. lb./rad.
$I_3 = 708$ lb. in. sec.^{2}	$k_3 = 2070\times10^6$ in. lb./rad.

The dynamic modulus K_1 at the left end of the crankshaft is given by

$$1/K_1 = 1/k_3 - 1/I_3\omega^2$$

and $2k/K_1$ expressed as a function of μ by means of relation (2.5) is

$$\frac{2k}{K_1} = \frac{2k}{k_3} - \frac{I}{2I_3 \sin^2 \mu/2}.$$

Introducing this in the first formula (2.10) we calculate φ_1 as a function of μ. In the same way we calculate $2k/K_2$ where K_2 is the dynamic modulus at the right end of the crankshaft. This may be calculated as a function of μ in the following steps

$$\omega^2 = 4k/I \sin^2 \mu/2$$
$$1/K' = 1/k_2 - 1/I_2\omega^2$$
$$K'' = -I_1\omega^2 + K'$$
$$2k/K_2 = 2k/k_1 + 2k/K''.$$

* The numerical data for this engine are taken from S. Timoshenko, *Vibration Problems in Engineering* (D. Van Nostrand, New York, 1939), p. 150.

Introducing this function in the second formula (2.10) we calculate φ_2. Calculations need only be made in the range $0 < \mu < \pi$. The frequency equation

$$6\mu + \varphi_1 + \varphi_2 = \text{multiple of } \pi$$

will be solved graphically by plotting the left side as a function of μ. The values of the functions φ_1, φ_2 are given in Table I.

The curve representing $6\mu + \varphi_1 + \varphi_2$ is plotted in Fig. 6; the intersections of this curve with the horizontals of ordinates $0, \pi, 2\pi, 3\pi, 4\pi, 5\pi$, yield the roots of the frequency equation (3.6). These roots are in degrees,

$$\mu_1 = 12.75 \qquad \mu_2 = 37.5 \qquad \mu_3 = 63.7$$
$$\mu_4 = 91.2 \qquad \mu_5 = 129 \qquad \mu_6 = 149.$$

The corresponding frequencies are derived from the formula $\omega = \omega_c \sin \mu/2$ where $\omega_c = 2(k/I)^{\frac{1}{2}} = 866$; the natural frequencies are

$$f_1 = \frac{866}{2\pi} \sin \frac{12.75}{2} = 15.3 \text{ sec.}^{-1}$$
$$f_2 = \frac{866}{2\pi} \sin \frac{37.5}{2} = 44.3 \text{ sec.}^{-1}$$
$$f_3 = \frac{866}{2\pi} \sin \frac{63.7}{2} = 72.4 \text{ sec.}^{-1}$$
$$f_4 = \frac{866}{2\pi} \sin \frac{91.2}{2} = 98.3 \text{ sec.}^{-1}$$
$$f_5 = \frac{866}{2\pi} \sin \frac{129}{2} = 124 \text{ sec.}^{-1}$$
$$f_6 = \frac{866}{2\pi} \sin \frac{149}{2} = 132 \text{ sec.}^{-1}.$$

TABLE I.

μ	φ_1	φ_2	$6\mu+\varphi_1+\varphi_2$
0	−90	−90	−180
5	−8.20	−89.3	−67.5
10	5.75	−88.2	−22.4
15	14.7	−87.3	17.4
20	22.1	−86.3	55.7
30	34.8	−83.7	131
45	46.5	−82.2	234
60	56.0	−79.5	336
75	63.5	−76.3	437
90	69.1	−75.4	533
105	73.6	−74.1	629
120	77.6	−73.6	724
150	84.1	−78.2	905
280	90	−90	1080

These are the six natural frequencies of the system below the cut-off frequency whose value is in this case 138 sec.$^{-1}$. The system has actually eight natural frequencies, there are therefore two more frequencies higher than 138 but their practical importance is not great. They could however eventually be calculated by the procedure indicated above [cf. Eq. (2.11)].

The complete calculation of the six frequencies requires about two or three hours of slide rule work. The method is very well fit to discuss rapidly the effect on the frequencies of a structural change of the system. If, for example, the

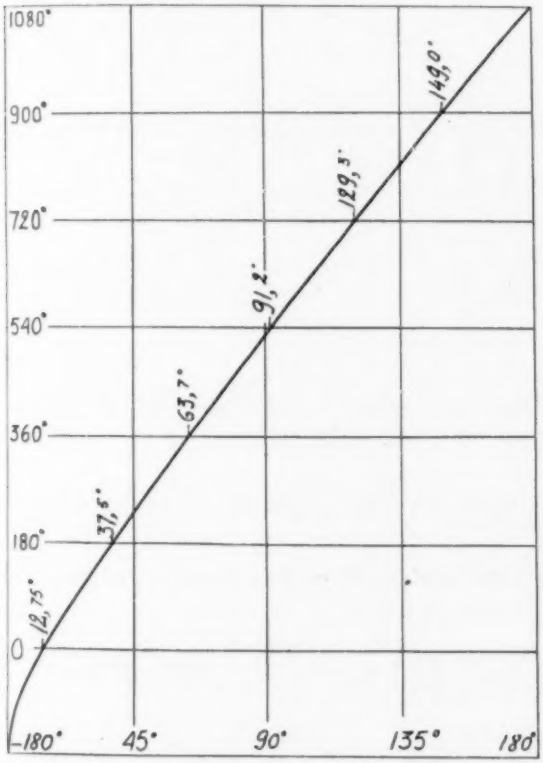

FIG. 6. The function $6\mu+\varphi_1+\varphi_2$ for the engine in Fig. 5 plotted as function of μ.

number of cylinders were 12 instead of 6, the 12 natural frequencies below 138 would be obtained without repeating all the calculations by solving the equation

$$12\mu+\varphi_1+\varphi_2=\text{multiple of } \pi,$$

where the functions φ_1 and φ_2 are numerically the same as above.

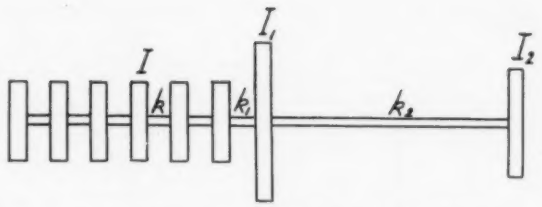

FIG. 7. A six-cylinder Diesel ship drive with flywheel and propeller.

Example 3

We consider the six-cylinder Diesel ship drive represented in Fig. 7. The propeller is driven by a long shaft. The data are.*

$$k=k_1=675\times10^6 \text{ in. lb./rad.}$$
$$k_2=13.5\times10^6 \text{ in. lb./rad.}$$
$$I=2560 \text{ lb. in. sec.}^2$$
$$I_1=75000 \text{ lb. in. sec.}^2.$$

Since $K_1=0$ we may take for φ_1 the constant value $\varphi_1=-90°$ while φ_2 is calculated as a function of μ as in the previous example. We find the values given in Table II.

The curve representing $6\mu-90+\varphi_2$ as a function of μ is plotted in Fig. 8. The intersections of this curve with the horizontals of ordinates 0, π, 2π, 3π, 4π, 5π, 6π yield seven roots of the frequency Eq. (2.8)

$$\mu_2=14.9 \qquad \mu_3=42.0 \qquad \mu_4=69.5$$
$$\mu_5=97.0 \qquad \mu_6=124.5 \qquad \mu_7=152.$$

The lowest root μ_1 determined by the horizontal of abscissa 0 cannot be evaluated easily by this method unless the function φ_2 is calculated very accurately in the interval 0–5°. This is not very convenient and it is preferable in this case to use directly the frequency equation in the form (2.7). Since $K_1=0$ it may be written

$$\omega^2 I\frac{\sin \mu n}{2 \sin (\mu/2) \cos \mu(n-\tfrac{1}{2})}=K_2.$$

For small values of μ the factor

$$\lambda(\mu)=\frac{\sin \mu n}{2 \sin (\mu/2) \cos \mu(n-\tfrac{1}{2})}$$

is approximately equal to n and the frequency equation becomes

$$n\omega^2 I=K_2.$$

* The numerical data of this engine are taken from J. P. Den Hartog, *Mechanical Vibrations* (McGraw Hill Book Co., New York, 1934), p. 208.

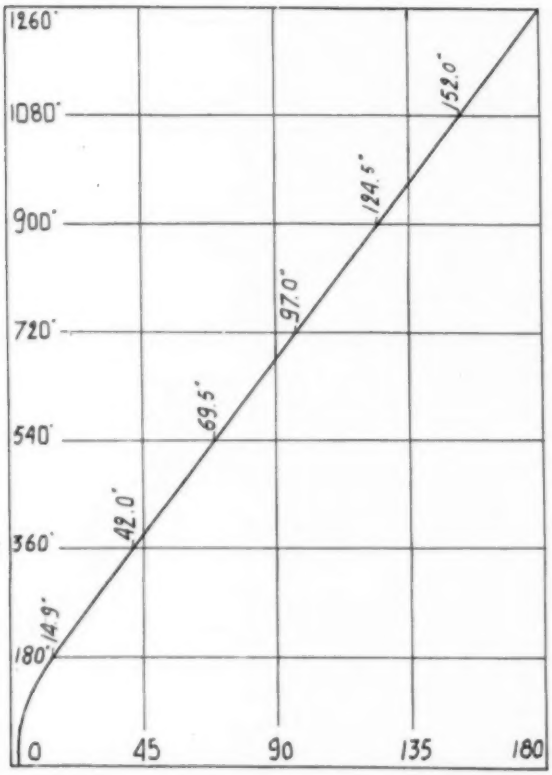

FIG. 8. The function $6\mu+\varphi_1+\varphi_2$ for the engine in Fig. 7 plotted as function of μ.

It is clear that this equation is the frequency equation for the case of a rigid crankshaft. The factor λ plays the role of a correction factor taking into account the elasticity of the crankshaft. Introducing the numerical data and putting $z=2\sin\mu/2$ the frequency equation may be written

$$0.02\lambda+0.7736-(10.15\lambda+275)z^2+275\lambda z^4=0.$$

A first approximation for the lowest root is found by putting $\lambda=6$. Neglecting the term in z^4 we find

$$z^2=\frac{0.02\times6+0.7736}{10.15\times6+275}=2.65\times10^{-3}$$

$$z=5.15\times10^{-2}.$$

This corresponds to an angle $\mu=2.95°$. Introducing this value of μ in the factor λ we find $\lambda=6.09$. This yields the second approximation

$$z^2=\frac{0.02\times6.09+0.7736+6.09\times275\times(2.65)^2\times10^{-6}}{10.15\times6.09+275},$$

$$z=5.19\times10^{-2},\quad \mu_1=2.98°.$$

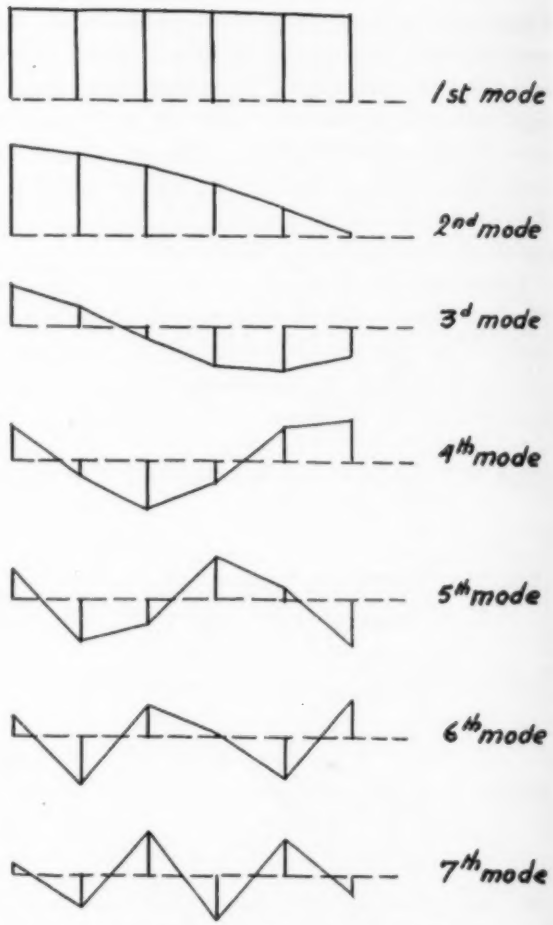

FIG. 9. The shape of the torsional modes in the crankshaft of the engine in Fig. 7 for the seven natural frequencies of the system.

This second approximation is quite satisfactory. The lowest frequency is

$$f_1=\frac{z}{2\pi}\left(\frac{k}{I}\right)^{\frac{1}{2}}=\frac{5.19\times10^{-2}}{2\pi}\times512=4.24\ \text{sec}^{-1}.$$

TABLE II.

μ	φ_2	$6\mu-90+\varphi_2$
0	−90	−180
5	158.1	98.1
10	173.8	143.8
15	180.07	180.07
20	184.35	214.35
30	191.65	281.65
45	200.0	380.0
60	208.2	478.2
75	216.1	576.1
90	224.1	674.1
105	231.6	771.6
120	239.4	869.4
150	254.7	1064.7
180	270	1260

The other frequencies are

$$f_2=\frac{1024}{2\pi}\sin\frac{14.9}{2}=21.2 \text{ sec.}^{-1}$$

$$f_3=\frac{1024}{2\pi}\sin\frac{42.0}{2}=58.4 \text{ sec.}^{-1}$$

$$f_4=\frac{1024}{2\pi}\sin\frac{69.5}{2}=92.8 \text{ sec.}^{-1}$$

$$f_5=\frac{1024}{2\pi}\sin\frac{97.0}{2}=122 \text{ sec.}^{-1}$$

$$f_6=\frac{1024}{2\pi}\sin\frac{124.5}{2}=145 \text{ sec.}^{-1}$$

$$f_7=\frac{1024}{2\pi}\sin\frac{152}{2}=158 \text{ sec.}^{-1}.$$

In this case we obtain all seven natural frequencies of the system. The modes of vibration in the crankshaft are easily calculated from formula (2.12). Since $K_1=0$ we have

$$\tan\beta=\frac{\sin\mu}{1-\cos\mu}=\cot\frac{\mu}{2}.$$

Hence $\beta=\pi/2-\mu/2$ and the modes are given by

$$\theta_x=\sin\left(\mu x+\frac{\pi}{2}-\frac{\mu_r}{2}\right)=\cos\left[\frac{2x-1}{2}\mu_r\right].$$

The values are plotted in Fig. 9 and recorded in Table III.

TABLE III.

CRANK	$r=1$ 1ST MODE	$r=2$ 2ND MODE	$r=3$ 3RD MODE	$r=4$ 4TH MODE	$r=5$ 5TH MODE	$r=6$ 6TH MODE	$r=7$ 7TH MODE
$x=1$	0.999	0.990	933	819	662	466	241
$x=2$	.996	.916	453	−258	−819	−994	−682
$x=3$	.991	.773	−258	−996	−469	656	939
$x=4$	.983	.573	−838	−422	933	087	−987
$x=5$	.972	.325	−987	707	241	−945	798
$x=6$	.959	.061	−629	906	−992	819	−422

APPENDIX

The solution (2.4) is based on the following trigonometrical identities

$$\begin{aligned}\sin(x+1)\mu-2\sin x\mu\cos\mu+\sin(x-1)\mu=0\\ \cos(x+1)\mu-2\sin x\mu\cos\mu+\cos(x-1)\mu=0.\end{aligned}\tag{a}$$

If we choose μ so that

$$\begin{aligned}\cos\mu&=1-\tfrac{1}{2}\alpha^2\\ \text{or}\qquad \alpha&=2\sin\mu/2,\end{aligned}\tag{b}$$

we may verify from the identities that the expression

$$\theta_x=A\cos\mu x+B\sin\mu x\tag{c}$$

satisfies the $n-2$ equations,

$$\theta_{x-1}-(2-\alpha^2)\theta_x+\theta_{x+1}=0,\tag{d}$$

whatever the values of the constants A and B. These constants may be adjusted in such a way that expression (c) also satisfies the Eq. (2.3) which may be written

$$\begin{aligned}\theta_2-2\theta_1\cos\mu-M\theta_1=0\\ \theta_{n-1}-2\theta_n\cos\mu-N\theta_n=0.\end{aligned}\tag{e}$$

Substitution of expression (c) in these equations yield

$$\begin{aligned}A[\cos 2\mu-2\cos\mu\cos\mu-M\cos\mu]+B[\sin 2\mu-2\sin\mu\cos\mu-M\sin\mu]=0\\ A[\cos(n-1)\mu-2\cos n\mu\cos\mu-N\cos n\mu]+B[\sin(n-1)\mu-2\sin n\mu\cos\mu-N\sin\mu]=0.\end{aligned}\tag{f}$$

This may be simplified by taking identities (a) into account

$$\begin{aligned}\cos 2\mu-2\cos\mu\cos\mu&=1\\ \sin 2\mu-2\sin\mu\cos\mu&=0\\ \cos(n-1)\mu-2\cos n\mu\cos\mu&=\cos(n+1)\mu\\ \sin(n-1)\mu-2\sin n\mu\cos\mu&=\sin(n+1)\mu.\end{aligned}$$

Equations (f) then take the form (2.6) in the text.

Theory of Frequency Controlled Oscillators

SAMUEL SABAROFF*
Moore School of Electrical Engineering, University of Pennsylvania, Philadelphia, Pennsylvania
(Received February 17, 1940)

A solution of the oscillator equation is obtained in which is indicated the basic mechanism involved in the frequency control of oscillators. The well-known fact that control of an oscillator is possible when the ratio of controlling frequency to oscillator frequency is m/n, where m and n are integral, is theoretically demonstrated.

AN oscillator is said to be frequency controlled when a fixed ratio is maintained between a controlling frequency and the frequency of the controlled oscillator. Of the several methods used to control the frequency of an oscillator the simplest and most generally used scheme is to inject the controlling signal into the oscillator circuit. As either frequency is made to approach the other, a point is reached at which the frequencies remain in synchronism or control for a fairly large variation in any of the oscillator parameters. The condition of control is also possible when the ratio of controlling signal frequency to oscillator frequency is m/n where m and n are integral.[1-4] It is assumed in the following that the controlling signal is injected directly into the nonlinear element so that the complication of a circuital intervention is minimized.

It is intended in this paper to present a formulation of the basic action involved in the frequency control of oscillators. The circuit on which the analysis is based is shown in Fig. 1 in which g is the nonlinear element necessary for the maintainance of oscillations. The exact form of g will be discussed later, but for the present it will be assumed to have a small and slow time variation.

Simple circuit analysis gives

$$v=L\frac{di_1}{dt}+ri_1=\frac{1}{C}\int i_2dt=\frac{i_3}{g}. \qquad (1)$$

From (1) and the relation $i_1+i_2+i_3=0$, the following differential equation is obtained

$$\frac{d^2v}{dt^2}+s\frac{dv}{dt}+v\omega^2\left(1+\frac{s}{\omega Q}+\frac{1}{\omega^2}\frac{ds}{dt}\right)=0, \qquad (2)$$

where

$$s=(gL+rC)/LC,$$
$$\omega^2=(1-r^2C/L)/LC,$$
$$Q=L\omega/r.$$

Equation (2) is similar in form to the equation representing the motion of a string of variable density and tension. An approximate solution of this problem in which the density and tension vary slowly has been found,[5] corresponding in this case to a slowly varying value for s. The solution of Eq. (2) is therefore

$$v=V\frac{e^{-\frac{1}{2}\int s\,dt}}{\left(1+\frac{s}{\omega Q}+\frac{1}{\omega^2}\frac{ds}{dt}\right)^{\frac{1}{4}}}\times\cos\left[\omega\int\left(1+\frac{s}{\omega Q}+\frac{1}{\omega^2}\frac{ds}{dt}\right)^{\frac{1}{2}}dt\right]. \qquad (3)$$

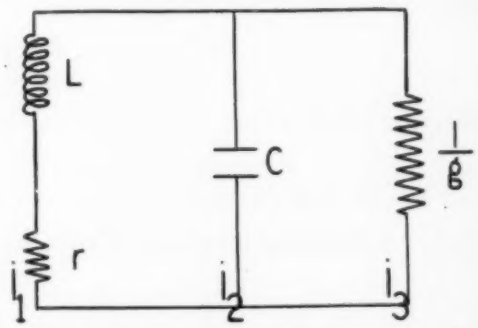

FIG. 1. Circuit for analysis of frequency control of oscillators.

* This paper was completed while the author was a graduate student in the Moore School; he is now transmitter engineer, station WCAU.

[1] I. Koga, "A new frequency transformer or frequency changer," Proc. I. R. E. **15**, 669 (1927).

[2] Victor J. Andrew, "A simplified frequency dividing circuit," Proc. I. R. E. **21**, 982 (1933).

[3] E. V. Appleton, "The automatic synchronization of triode oscillators," Proc. Camb. Phil. Soc. **21**, 231 (1922).

[4] S. Sabaroff, "Frequency controlled oscillators," Communications **19**, No. 2, p. 7 (1939).

[5] John C. Slater and Nathaniel H. Frank, *Introduction to Theoretical Physics* (McGraw-Hill, 1933), p. 146.

Ordinary oscillator analysis shows that in the absence of any external disturbing force and assuming sinusoidal operation, the steady state condition requires that the value of s be equal to zero.[6] However, a frequency controlled oscillator infers the presence of a controlling signal so that s no longer equals zero. For the purpose of this paper s will be assumed small, with particular attention drawn to the frequency variations in (3).

The approximate solution of (2) now becomes,

$$v = V \cos\left(\omega t + \frac{1}{2Q}\int s dt\right). \tag{4}$$

The form of s is nonlinear by virtue of the presence of g, and can be represented by

$$s = \sum_{0}^{h=\infty} a_h (v+e)^h, \tag{5}$$

where e is the controlling signal and is equal to $E \cos(pt)$. Equation (5) is to be averaged over the high frequency terms only.

A typical sum of the difference frequency cross products is

$$s = \sum_{0}^{k=\infty} b_k \cos\left[k(m\omega - np)t + \frac{mk}{2Q}\int s dt\right], \tag{6}$$

where m and n are integral.

It is sufficient to consider the first two terms of (6) only, thus

$$s = b_0 + b_1 \cos\left[(m\omega - np)t + \frac{m}{2Q}\int s dt\right], \tag{7}$$

where m and n are, respectively, the orders of the oscillator and controlling signal harmonics that by intermodulation produce (7).

Equation (7) can be written in the following form

$$\Delta\omega = \Delta\omega_0 \cos\left(qt + m\int \Delta\omega dt\right), \tag{8}$$

where

$$\Delta\omega = (s - b_0)/2Q,$$
$$\Delta\omega_0 = b_1/2Q,$$
$$q = m(\omega + b_0/2Q) - np.$$

It is evident that $\Delta\omega$ is the instantaneous deviation of the oscillator frequency due to the presence of the controlling signal and $\Delta\omega_0$ is the maximum possible oscillator frequency deviation. The parameter q is a measure of the tuning of either the oscillator or the controlling frequency or both as one or the other is varied to secure control. If the instantaneous frequency of the oscillator be referred to its mth harmonic, (8) becomes

$$\Delta\omega_m = \Delta\omega_{0m} \cos\left(qt + \int \Delta\omega_m dt\right), \tag{9}$$

where

$$\Delta\omega_m = m\Delta\omega, \quad \Delta\omega_{0m} = m\Delta\omega_0.$$

Eq. (9) is an integral equation in the transcendental form. Fortunately it is capable of exact solution. Let $x = qt$, $y = \int \Delta\omega_m dt$, and $A = q/m\Delta\omega_0$, then (9) is

$$dy/dx = \cos(x+y)/A. \tag{10}$$

A is directly proportional to q and now becomes the measure of the oscillator or controlling signal tuning. Further let $x+y=z$, then the indicated solution is

$$y = \int \frac{\cos(z)}{A + \cos(z)} dz. \tag{11}$$

Equation (11) is now in a suitable form for integration.[7] The solution is

$$y = z - \frac{A}{(1-A^2)^{\frac{1}{2}}} \log\left[\frac{\tan(z/2) + [(1+A)/(1-A)]^{\frac{1}{2}}}{\tan(z/2) - [(1+A)/(1-A)]^{\frac{1}{2}}}\right]. \tag{12}$$

The constant of integration has been omitted since it can easily be shown to equal zero.

After inserting the proper values for x and y, (12) can be reduced to the following

$$\Delta\omega_m = -\Delta\omega_{0m} \frac{1 + A\cos[\Delta\omega_{0m} t (A^2-1)^{\frac{1}{2}}]}{A + \cos[\Delta\omega_{0m} t (A^2-1)^{\frac{1}{2}}]}. \tag{13}$$

[6] Balth. van der Pol, "The non-linear theory of electric oscillations," Proc. I. R. E. 22, 1051 (1934).

[7] Integrals 304 and 239 in *A Short Table of Integrals* by B. O. Peirce, third revised edition (Ginn and Co., 1929).

Equation (13), when expanded in a Fourier series becomes

$$\Delta\omega_m = -A\Delta\omega_{0m}\left[1-\left(\frac{A^2-1}{A^2}\right)^{\frac{1}{2}}\right]+2\Delta\omega_{0m}(A^2-1)^{\frac{1}{2}}\sum_{1}^{a=\infty}(-A)^a\left[1-\left(\frac{A^2-1}{A^2}\right)^{\frac{1}{2}}\right]^a\cos\left(a\Delta\omega_{0m}t(A^2-1)^{\frac{1}{2}}\right). \tag{14}$$

For $A^2 \gtrless 1$, the average value of $\Delta\omega_m$ from (14) is

$$\overline{\Delta\omega_m} = -A\Delta\omega_{0m}\left[1-\left(\frac{A^2-1}{A^2}\right)^{\frac{1}{2}}\right]. \tag{15}$$

It is apparent from (13) and (14) that when $A^2>1$, the instantaneous change in the harmonic frequency is periodic with an average deviation given by (15). It can easily be shown that the average deviation is toward the controlling frequency as the controlling frequency and oscillator frequency are made to approach each other.

As A^2 approaches unity the average deviation increases and reaches a maximum at $A^2=1$. For values of A^2 less than unity Eq. (13) becomes

$$\Delta\omega_m = -\Delta\omega_{0m}\frac{1+A\cosh\left[\Delta\omega_{0m}t(1-A^2)^{\frac{1}{2}}\right]}{A+\cosh\left[\Delta\omega_{0m}t(1-A^2)^{\frac{1}{2}}\right]}. \tag{16}$$

It is evident from (16) that as A^2 is slowly made less than unity the passage of time will make the hyperbolics very large. The deviation as $t\to\infty$ then becomes

$$\Delta\omega_m = -A\Delta\omega_{0m}, \tag{17}$$

thus establishing the condition of control.

The average harmonic deviation has been plotted in Fig. 2. Control is maintained over the straight portion of the curve. It is easy to show that the phase change of the oscillator harmonic is 180° over the region of control. It should be remembered that the oscillator deviation is the harmonic deviation divided by the harmonic number.

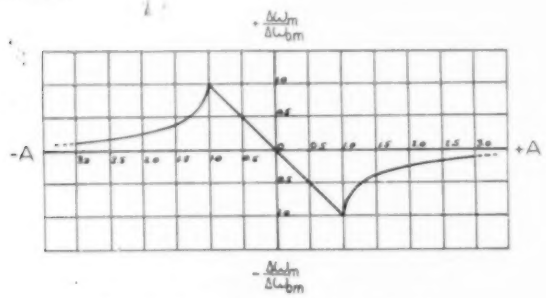

FIG. 2. Average harmonic deviation.

A is equal to zero when the tuning of the oscillator is such as to bring it to the midpoint of the region of control. At this point therefore $m(\omega+b_0/2Q)-np=0$ or

$$\frac{m}{n}=\frac{p}{\omega+b_0/2Q}. \tag{18}$$

It is evident from (18) that control of an oscillator is possible when the ratio of the controlling frequency to the oscillator frequency is m/n where m and n are integral.

In conclusion it may be stated that the basic theory underlying the frequency control of oscillators has been described. Secondary effects, of which hysteresis is one, have not been here considered. Indications are that a general solution in which such effects are incorporated will be quite involved and will necessitate further consideration of the various factors approximated or omitted in the above analysis.

I wish to thank Dr. C. C. Chambers and Dr. J. G. Brainerd of the Moore School for their discussion and advice in the preparation of this paper.

Studies in Lubrication

VIII. Lubrication of Plane Sliders

F. Morgan, M. Muskat, and D. W. Reed
Gulf Research & Development Company, Pittsburgh, Pennsylvania
(Received May 7, 1940)

The coefficient of friction has been experimentally determined in the thick film region of lubrication for both fixed angle and pivoted plane sliders as a function of the lubricant viscosity μ, the relative speed of sliding U, and the load W. Three steel, brass, or bronze sliders of one centimeter length and width constituted the stationary surfaces; the moving surface was of steel. Deviations between experiment and theory for the fixed angle wedges at low values of $\mu N/W$ may be explained on the basis of variations and inaccuracies in the sliders themselves. However, in the case of the pivoted sliders the experimental results are in excellent agreement with theory, and, in fact, provide for the first time an absolute and quantitative direct empirical check of the hydrodynamic theory of lubrication.

IN the previous papers of this series both experimental and theoretical investigations have been described regarding the behavior of journal bearings under thick film lubrication conditions. The available theory was extended so as to be applicable to practical journal bearings of finite width, and the implications of this theory were tested experimentally. These tests proved that within the errors inherent in the experiments or in the approximations of the analysis the physical hydrodynamic theory of lubrication, first proposed by Reynolds, satisfactorily explains the important features of the thick film lubrication of journal bearings.

Both practical experience and theoretical analysis have shown, however, that lubrication difficulties, as experienced under actual operating conditions, are much more likely to occur when a system is in the state of thin film rather than thick film lubrication. From a practical point of view, therefore, the investigation of the thin film region should be of even greater interest than that of the thick film type of lubrication. To undertake such a study with actual journal bearings would, of course, be the most natural procedure. Unfortunately, however, serious difficulties are encountered upon attempting to carry out such researches. Among these difficulties are: (1) the development of negative pressure regions in the lubricant film which lead to rupture of the film and thus destroy the ideal geometry which must be assumed in the analysis of such systems; (2) the difficulty of obtaining accurate bearing surfaces with reproducible clearances between the journal and bearing in order to repeat the experiments; and (3) the expense of providing the numerous separate journal bearing systems which would be required in any thorough investigation.

The problem of providing a number of identical or equivalent journal bearing systems in any single investigation arises from the fact that during the course of thin film experimentation the bearing surfaces will of necessity undergo changes and possibly severe deterioration. For by the nature of the problem thin film conditions will exist only when the lubricant film does not separate the bearing surfaces completely and metal to metal contact actually takes place. A single experiment therefore may result in completely ruining the surface for any further experimentation. To check the reproducibility of original results it is then necessary to begin afresh with new bearing surfaces.

It is for these reasons that our original program of research on journal bearing systems has been shifted, after completing the study of the thick film region, to the investigation of plane sliding surfaces. For one thing the plane slider is particularly adapted to studies of the hydrodynamic theory as the question of negative pressures should not arise even when operating under thin film conditions. Furthermore with the pivoted wedge type of slider the only geometrical factor, besides the length and width of the surface, is the position of the pivot line. This may be deter-

mined with reasonable accuracy and with no great difficulty. Finally, while accurate plane surfaces are by no means easily obtained, the possibility of preparing reproducible flat bearings is decidedly greater than that for cylindrical bearings, and the costs of replacements are even of a lower order of magnitude.

Although the theory of the viscous lubrication of plane sliders of finite width was developed by Michell[1] in 1905, apparently few experimental studies of the various associated phenomena have been attempted. It is true, of course, that such sliders have been widely accepted in practice. And the unqualified success which they have attained, even in the most difficult installations, has been sufficient to establish the main features of the theory.

In 1919 H. A. S. Howarth[2] made tests, on a large bearing testing machine, which were primarily intended to yield information on the effects upon the bearing surfaces of running at very low speeds. While the coefficient of friction was not accurately measured, the trend of the curves obtained indicate that operation was, for the most part, confined to the region of comparatively thin film lubrication. In all cases the babbitt bearing shoes were found to improve with use. Michell[3] has cited experiments on a pivoted journal bearing for which the coefficient of friction was observed to vary approximately as $(\mu U/W)^{\frac{1}{2}}$—where μ is the lubricant viscosity, U the relative surface speed, and W the load. Under certain conditions, which presumably were satisfied, the theory of plane slider bearings has been shown[3] to be equally applicable to pivoted journal bearings. Kingsbury[4] obtained results for sliders of finite width with the electrical model which were shown to be in good agreement with the pressure distribution calculated for the theory of Michell. In none of these cases, however, has an attempt been made to study experimentally the behavior of the coefficient of friction as a function of the viscosity, the speed, the load, and the geometrical properties of the system in the light of the theoretical implications.

[1] A. G. M. Michell, Zeits. f. Math. Phys. **52**, 123–137 (1905).
[2] H. A. S. Howarth, Trans. Am. Soc. Mech. Eng. **41**, 685 (1919).
[3] See A. G. M. Michell, *The Mechanical Properties of Fluids* (D. Van Nostrand Co., New York), p. 143.
[4] A. Kingsbury, Trans. Am. Soc. Mech. Eng., A. P. M. **53**, 59 (1931).

While a study of the thin film type of lubrication is, as previously indicated, of greater practical interest than an experimental investigation of the thick film region, it is nevertheless useful to obtain information as to how well experiment can be expected to agree with theory in a region where the predictions of the latter are available. Before the more difficult thin film study is attempted, it is also desirable to know just where deviations between theory and experiment begin to be noticeable. In fact until such information is available theory and experiment cannot be said to disagree. These experiments are therefore considered to be significant from the point of view of comparison with theory and of reproducibility although they are only of a preliminary nature with regard to the ultimate investigation of thin film lubrication conditions.

Experimental Apparatus

A photograph of the testing machine is shown in Fig. 1. A schematic diagram of the essential parts is shown in Fig. 2. The hardened and lapped steel plate A, 11 inches in diameter, which formed the lower bearing surface was driven through gears at B and C by a variable speed transmission. The speed of the plate was variable from 0 to about 115 r.p.m. The sliders D, which were three in number, were held rigidly in place in a heavy casting E with three legs. The load was applied directly above the sliders by means of a second similar tripod F. The minimum load of about 13 pounds consisted of the two spiders and the load carrying apparatus; the maximum load was about 65 pounds. The auxiliary load G rotated with the tripods but was suspended by ball-bearing gimbals so that it was free to hang in a vertical position. The torque was determined by the rotation produced in a piano wire H which at the same time tended to centralize the tripod arrangement. For torque measurements the wedges were returned to their zero position, as indicated by a lamp and scale, by means of a torsion head I. In order that no extra load should be applied to the sliders through the wire itself, the upper tripod was connected to the torsion wire through a spline joint J. All vital friction parts were protected from dust by a transparent case K.

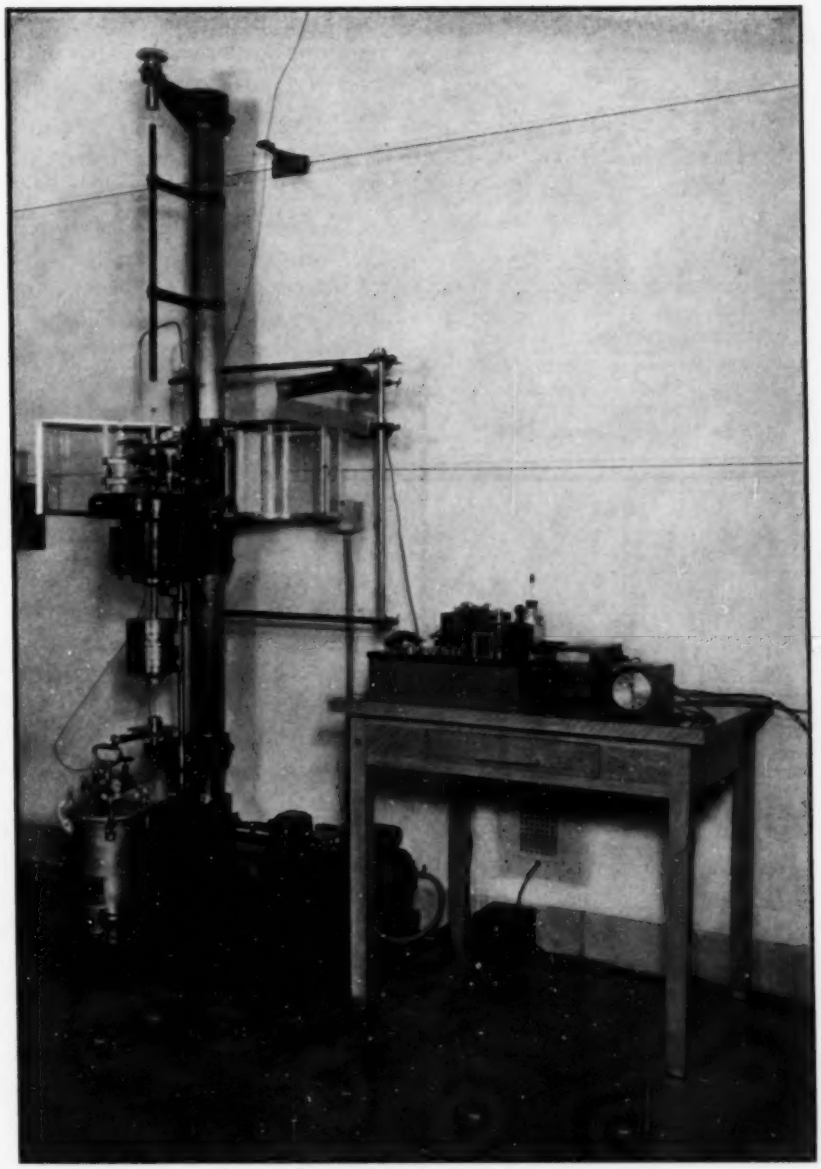

FIG. 1. Testing machine.

Temperatures were measured with copper-constantan thermocouples fixed in the material of the sliders. In no case did the observed temperature differ appreciably from that of the room. Viscosities corresponding to measured temperatures were used in all calculations.

The lubricants were Gulfcrest Oil A, Gulfgem Oil A, and Mineral Seal Oil with viscosities of 60.6, 15.9, and 4.86 centipoises, respectively, at 70°F. The oil in each case was filtered through chamois skin at L immediately before it was distributed to the wedges.

In some of the experiments additional sliders with small clearances were arranged to collect and distribute the lubricant in front of the wedges. These extra sliders were held in place by the framework of the machine and were entirely independent of the torsion measuring apparatus. Although the moving surface frequently appeared to be entirely devoid of lubricant when

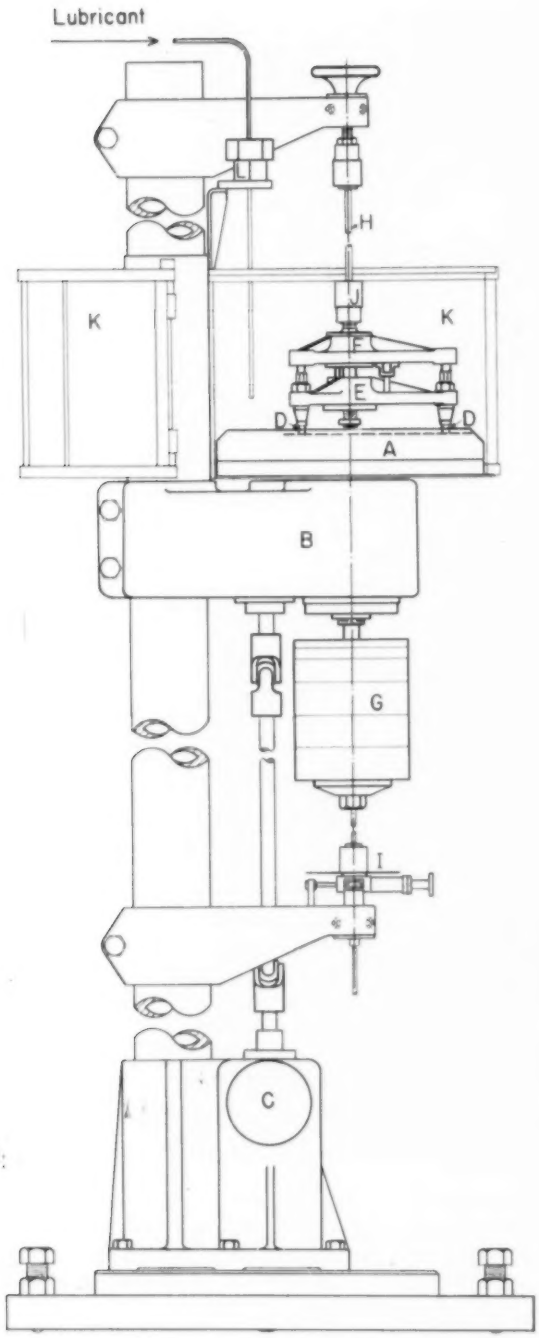

FIG. 2. Schematic diagram of the essential parts of the testing machine.

going under a wedge, the addition of the distributors in most cases had practically no effect on the torque. At high speeds, however, the collectors were beneficial as some tendency to starve the wedges was observed. This behavior is readily understood. At higher speeds more oil is required but less time is available for it to spread over the surface and into the track left by the preceding wedge.

EXPERIMENTAL RESULTS

The first experiments were performed with fixed angle wedges, but the results were not entirely satisfactory as the accurate measurement of very minute angles on such small surfaces (one cm on a side) proved quite difficult. Angles on steel wedges were finally determined by measuring the angle of deviation of reflected light when the wedges were turned through 180°. The accuracy was considerably impaired by uncertainty in the seating of the wedges against the holder. For the better wedges the angle perpendicular to the angle of tilt was extremely small. Both brass and steel sliders were used.

Wedges were later made self-aligning by pivoting about knife edges formed at right angles to the direction of motion. The important geometrical property in the case of such wedges is the position of the pivot line or the center of pressure line with respect to the trailing edge. This distance could be determined with much greater accuracy than could the angle with the previous wedges. The knife edges were of steel; the sliding surfaces were of both steel and bronze.

The theory for both types of sliders has been given in a previous paper.[5] The observations on fixed sliders will here be presented first. These will be followed by data for pivoted wedges.

Fixed angle sliders

As shown in the previous paper,[5] hydrodynamic theory predicts that for sliders having fixed angles all data should lie on a single curve when f/m is plotted against $\mu Uw/Wm^2$, as long as the ratio of slider length to slider width remains constant. Here the coefficient of friction is denoted by f, the slope of the slider by m, μ is the coefficient of viscosity, U, the linear speed of the moving plate, w, the slider width, and W, the total load. As before $\mu Uw/W$ will be denoted by S. Since m is very difficult to measure accurately, it has been found convenient to plot the experi-

[5] M. Muskat, F. Morgan, and M. W. Meres, "Studies in lubrication VII," J. App. Phys. **11**, 208–219 (1940).

mental values obtained for f against those for S and to compare the curves so obtained with the theoretical curves for appropriate values of the slope.

Data were obtained for four sets of fixed angle wedges. The experimental data for the first of the sliders are shown by the points in Fig. 3, where $10^3 f$ has been plotted against $10^6 S$. The average angle in this case was found to be approximately two minutes of arc when measured by reflected light. The probable error was quite large, however. In order to make a comparison between theory and experiment the theoretical curve of $f/\sqrt{S}$ *vs.* S/m^2 has been plotted in Fig. 4. On the same sheet $f/\sqrt{S}$ as determined from the experimental curve of Fig. 3 has been plotted against S. The value of the slope of the slider necessary to make the curves coincide was then calculated for various values of the ordinate. The third curve of Fig. 4 gives the resultant value of the slope m as a function of S. For large values of S the slope evidently approaches a value of about 0.436×10^{-3} radian, or 1.5 minutes of arc. This value in turn has been used in constructing the theoretical curve in Fig. 3.

The data of Fig. 5 for three other sets of sliders were interpreted in the same way. The points correspond to experimental data while the curves were drawn from theory for slopes determined as in Fig. 4. Curve I is for a slider slope of 0.95 minute of arc ($m=0.280\times10^{-3}$ radian), while curves II and III correspond to slopes of 2.06 and 7.57 minutes, respectively. The experimental data corresponding to curve I were obtained with brass sliders; the other sliders were of steel.

In practically all of the curves of m *vs.* S, m was observed to increase rapidly with S when S was small and then apparently to reach a maximum value when S became sufficiently large. Some correlation between the change of the slope, m, and the electrical resistance between the sliders and the rotating plate was also noted. At low values of S the resistance was quite low, but as S increased the resistance was observed to increase also, and finally to become too high to be measured with the instruments available.

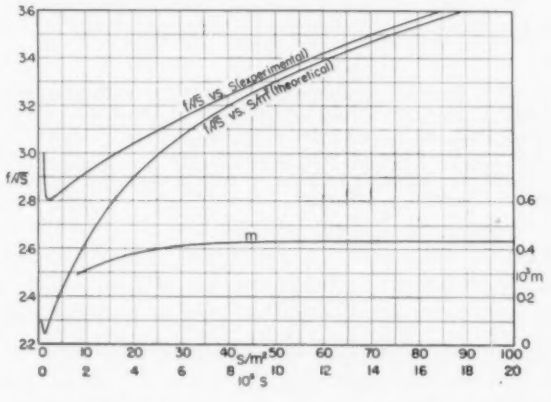

FIG. 4. $f/\sqrt{S}$ curves for square sliders of fixed angle. Experimental curve derived from Fig. 3. m = effective slope of sliders.

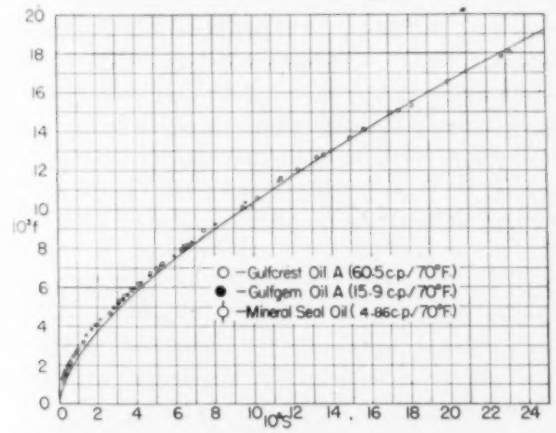

FIG. 3. Friction coefficients for square steel sliders of fixed angle. Solid curve calculated theoretically for slider slope of 1.50 minutes of arc. Points correspond to experimental data. $S=\mu Uw/W$. μ = lubricant viscosity; w = slider width = 1 cm; U = speed of moving surface; W = load per slider.

Two explanations appear possible to explain the deviation of the experimentally determined points from the theoretical curve as illustrated by Fig. 3. Either the effective value of the slope of the sliders decreases as S decreases or the contributions to the torque due to actual metallic contact between the sliding surfaces become more and more important. Although an increasing electrical conductivity, presumably due to metallic contact, seems to correspond to an observed torque increase in some cases, calculations of minimum film thicknesses, both for the above wedges and for self-aligning wedges, indicate that the first assumption is the more probable. Thus, while the minimum film thickness for the lowest value of S in the case of Fig. 3 is found by calculation to be about 0.34×10^{-4} in., the deviation is already quite considerable when the thickness is

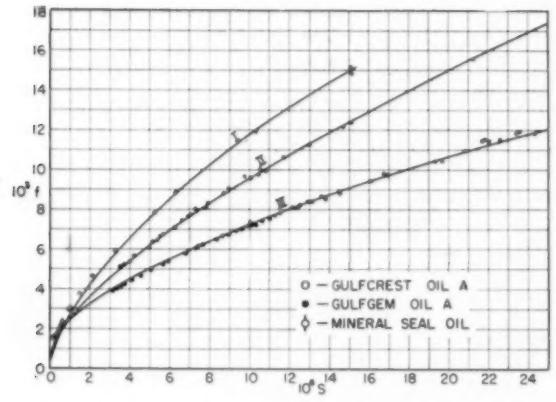

FIG. 5. Friction coefficients for square sliders of fixed angles. I, calculated theoretically for slider slope of 0.95 minute; II, calculated for slope of 2.06 minutes; III, calculated for slope of 7.57 minutes. Points correspond to experimental data. Remainder of notation as in Fig. 3.

as great as 1.7×10^{-4} in. The behavior is entirely different, however, for curve III of Fig. 5 where the minimum film thickness is about 1.4×10^{-4} in. and the deviation is in the opposite direction. Moreover, the sliders in the case of Fig. 3 were probably better than those of Fig. 5. The agreement, to be shown later, between theory and experiment for the self-aligning sliders is further evidence that the deviations are due principally to variations and inaccuracies in the sliders of a given set. The contributions due to such variations may be expected to become relatively more important as the wedge angles and minimum film thicknesses become smaller.

The solid curves in Figs. 3 and 5 basically can be expected to apply only to a single wedge. Since, in actually performing the experiments, no convenient method of holding one wedge was found, three were tested simultaneously. Consequently, in the above figures, it is perhaps not surprising that the agreement is no better, because the experimental results for a set of three wedges are compared with the theory for a single slider.

If the observed deviations between theory and experiment are due to variations in the angles of the sliders, the most obvious way to get better agreement would be to improve the quality of the sliders. Plans were originally made actually to measure and compare the angles by means of interference fringes produced on an optically flat surface. This procedure was abandoned, however, when it became apparent that by a change of slider design comparison between theory and experiment would be possible with much less labor and expense. The method consisted in replacing the fixed angle wedges by self-aligning sliders. The necessity for measuring extremely small angles was consequently eliminated. The position of the pivot point was required instead, but this measurement could be made with reasonable accuracy.

Self-aligning sliders

Figure 6(a) is a drawing of one of the types of self-aligning sliders, showing the method of pivoting. The knife edges and seats were of hardened steel and all were finished by grinding. In order that changes might more easily be made in the effective pivot positions, some of the sliders were made of steel with provisions for inserts of other material as shown in Fig. 6(b). One set of the 41.5 percent sliders (distance of pivot from trailing edge/length of slider $=\Delta x/L=0.415$) and the 20 percent sliders were of this type, bronze being used for inserts. The others were made entirely of steel. As in the case of the fixed angle wedges the moving plate was always of steel. Knife edges of brass were tried but failed to work satisfactorily due to locking in one position. When this occurred the observed torque was many times the torque normally observed.

The experimental results obtained when f is plotted against $\sqrt{S}$ for sliders which have the ratio $\Delta x/L$ equal to 0.415 are shown in the upper curve of Fig. 7. Within experimental error the points lie on the given straight line which passes through the origin of coordinates, as is required theoretically.[5] The data for sliders having a $\Delta x/L$ ratio of 0.318 are shown in the lower curve of Fig. 7. The slopes of the lines are 2.66 and 2.26.

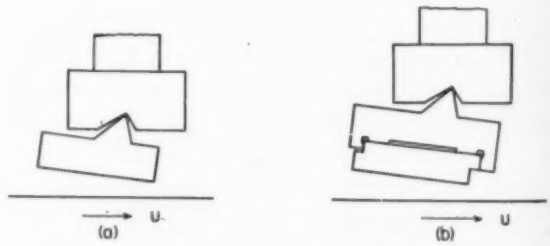

FIG. 6. Types of self-aligning sliders used in the experiments.

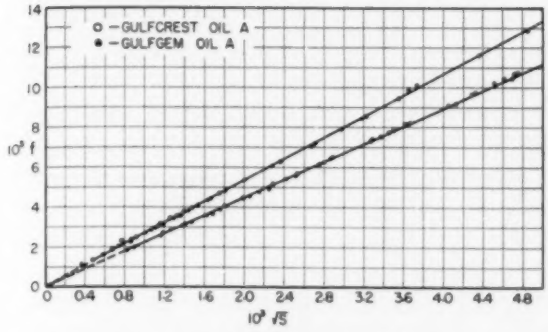

FIG. 7. Experimental friction coefficients for square pivoted sliders. Upper curve, $\Delta x/L=0.415$; lower curve, $\Delta x/L=0.318$; $\Delta x/L=$(distance of pivot from trailing edge)/(length of slider). Remainder of notation as in Fig. 3.

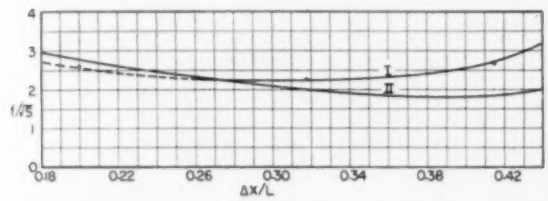

FIG. 8. The variation of the friction coefficient f with the pivot position for self-aligning sliders. I, theoretical curve for square slider. Dashed portion of curve extrapolated. II, theoretical curve for infinitely wide slider. Points correspond to experimental data of Figs. 7 and 9.

In the theoretical analysis of the lubrication of sliders of finite width it was found that for pivot positions relatively close to the trailing edge the friction coefficients should become even smaller than those for the infinitely wide slider. Since this result, at first thought, appears contrary to one's intuitive conception regarding the end effects in lubrication systems, a direct experimental test of this particular point was made. For this purpose a square slider with $\Delta x/L=0.20$ was chosen, for which case the theory definitely indicates a friction coefficient lower than that for the infinitely wide slider, as indicated by the curves of Fig. 8. The experimental results are shown in Fig. 9. Again, as in the previous cases, the curve of f *vs.* $\sqrt{S}$ is a straight line passing through the origin as predicted theoretically. Moreover the slope of this curve, namely 2.59, which is plotted as the circle at $\Delta x/L=0.200$ in Fig. 8, clearly falls below the value for the infinitely wide slider by an amount far greater than might be attributed to experimental error. While the quantitative value of the theoretical slope of this slider has not been calculated analytically

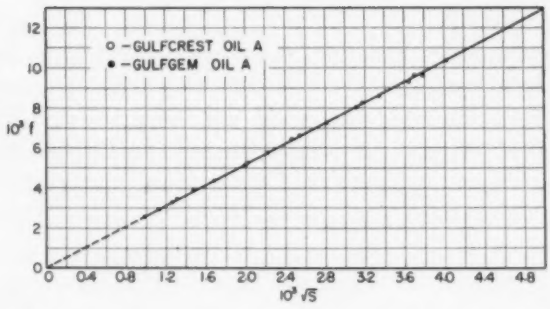

FIG. 9. Experimental friction coefficients for square pivoted sliders. $\Delta x/L=0.200$. Notation as in Fig. 7.

the observed slope does fall upon a reasonable extrapolation of the calculated curve and therefore may be considered as confirming completely the theoretical prediction. The slopes for $\Delta x/L=0.415$ and 0.318 are also plotted for comparison in Fig. 8.

Data have been obtained for lower values of $\sqrt{S}$ but the location of these points depends to a considerable degree upon the previous history of the sliders and a discussion of this phase of the subject will be reserved for a later paper. This phenomenon, which reflects the incipience of thin film conditions, also gave rise to the lower limits of the values of S to which reproducible data could be obtained with sliders of fixed angle. The actual values of these limits depended on the magnitude of the slider slopes for comparable degrees of finish of the sliding surfaces

CONCLUSIONS

It is felt that the above results provide a satisfactory confirmation of the hydrodynamic theory of thick film lubrication. While the data for the sliders of fixed angle deviate somewhat from the theoretical curves in the region of small values of S, the discrepancies as a whole may be explained as being due either to the lack of identity in the slopes of the three individual sliders, or the gradual incidence of thin film conditions. In all cases the major part of the data for the larger values of S agree with the theoretical predictions within the experimental errors.

In the case of the self-aligning, or pivoted, sliders the agreement is even more striking. There the data coincide with the theoretical predictions in absolute magnitudes without the use of any

adjustable or arbitrary constants. The only parameters entering the experiments are the directly measurable dimensions of the sliders and the distance of the pivot line from the trailing edge. With these predetermined, no further adjustment is possible for bringing the experimental data and theoretical predictions into agreement. Yet without such adjustment the measurements confirm in every detail the predictions of the theory.

The authors wish to express their appreciation to Dr. Paul D. Foote, Executive Vice President of the Gulf Research & Development Company, for permission to publish this paper.

Rectilinear Electron Flow in Beams

J. R. PIERCE
Bell Telephone Laboratories, New York, New York
(Received March 25, 1940)

Electrodes are devised by means of which rectilinear electron flow according to well-known space charge equations can be realized in beams surrounded by charge-free space. It is shown how these electrodes can be used in the design of electron guns having desirable characteristics.

I. INTRODUCTION

THE purpose of this paper is to show how rectilinear electron flow according to certain known space charge equations can be realized in regions more limited than those usually associated with the equations. Thus it will be shown how parallel electron flow can be realized in the form of a beam surrounded by charge-free space. This beam, or region containing electron flow, may be of constant thickness perpendicular to the flow, with the boundaries between the beam and the charge-free region in the form of planes, or it may be of constant circular cross section, the boundary being cylindrical. In a similar manner, rectilinear electron flow may exist in which the electrons move radially in the region between segments of cylinders or spheres, the beam occupying a wedge-shaped or conical region. By the means proposed, edge effects in vacuum tubes can be eliminated and electron guns of predictable performance and desirable characteristics can be constructed.

II. PARALLEL ELECTRON FLOW

The assumptions for all sorts of flow are essentially those made by Child[1] in deriving equations which are used to describe parallel motion of electrons. According to these assumptions, electrostatic forces only are considered, the magnetic effects of the electron current and of currents in return circuits being disregarded. Thermal velocities are likewise disregarded, the electron velocity at any point being specified by a potential φ, taken as zero at zero velocity. The charge density is regarded as continuous, and its magnitude is obtained by dividing the current density j (which is constant throughout the flow) by the velocity as specified by φ. Assuming the parallel flow to be in the x direction, Poisson's equation may be written

$$d^2\varphi/dx^2 = j/p_0(2e\varphi/m)^{\frac{1}{2}}, \tag{1}$$

$$\partial\varphi/\partial y = \partial\varphi/\partial z = 0. \tag{2}$$

In Eq. (1), j is in amperes/cm^2, φ is in volts, e/m in coulombs/gram seven ($e/m = 1.768 \times 10^{15}$), and p_0 is the permittivity of vacuum ($p_0 = 8.85 \times 10^{-14}$).

Child solved this equation with the boundary condition of zero gradient at zero potential. Others have supplied complete solutions.[2, 3]

[1] C. D. Child, "Discharge from hot CaO," Phys. Rev. **32**, 492 (1911).

[2] C. E. Fay, A. L. Samuel, and W. Shockley, "On the theory of space charge between parallel plane electrodes," Bell Sys. Tech. J. **17**, 49–79 (1938).

[3] B. Salzberg and A. V. Haef, "Effects of space charge in the grid-anode region of vacuum tubes," RCA Review **2**, 336–374 (1938).

III. Parallel Flow With Plane Boundaries

The solutions of (1) have generally been thought of as describing electron flow in the region between infinite parallel plane equipotential surfaces. Such flow can, however, exist in a region bounded by planes parallel to the flow, the space outside this region being free of charge. In such a case, certain fields must exist in the charge-free region outside of the flow, and these fields are determined by conditions at the boundary between the charge-free region and the region occupied by the flow. The nature of the fields outside the flow will now be investigated.

Imagine electron flow according to (1) existing in the region $y<0$, while the region $y>0$ is charge-free. Figure 1 illustrates conditions at the boundary of such flow. As (1) holds for $y<0$, at $y=0$

$$\partial\varphi/\partial y=\partial\varphi/\partial z=0, \tag{2}$$

$$\varphi=f(x), \tag{3}$$

where $f(x)$ is the appropriate solution of (1).

In the charge-free region, $y>0$, the potential must satisfy Laplace's equation subject to boundary conditions (2) and (3) at $y=0$. Failure of the field outside of the beam to satisfy (2) at the beam boundary would require a sheet of charge at the boundary. Failure to satisfy (3) would require a dipole layer at the boundary.

Both the real and the imaginary parts of any analytic function of $x+iy$ are solutions of Laplace's equation. In (3) suppose that x is replaced by $x+iy$, giving

$$\varphi+i\Psi=f(x+iy), \tag{3a}$$

where φ and Ψ are real. φ as given by (3a) is then a solution of Laplace's equation which satisfies (3) at $y=0$.

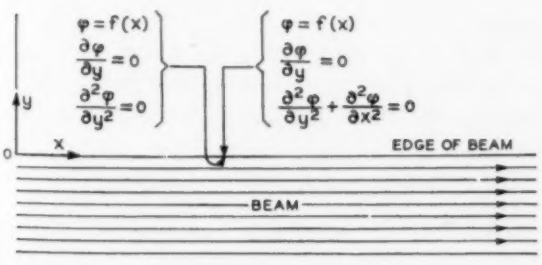

Fig. 1.

As $f(x)$ is a real function, writing $(x-iy)$ instead of $(x+iy)$ gives the conjugate of (3a), or

$$\varphi-i\Psi=f(x-iy).$$

Thus the potential φ as given by (3a) is the same for positive values of y as for negative values, and the field is symmetrical about the x axis. This means that at $y=0$, the y-derivative of φ is zero, satisfying relation (2). Thus φ as given by (3a) is the potential in the region $y>0$.

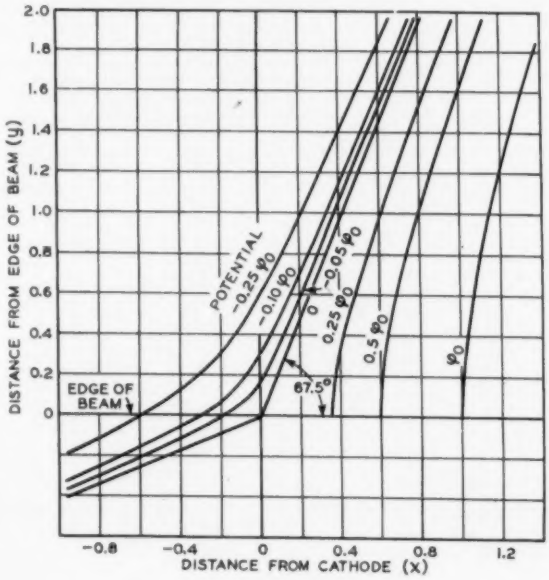

Fig. 2.

The practical interpretation of this is that parallel electron flow according to (1) can exist adjacent to a charge-free region, the boundaries between the flow and the charge-free region being in the form of planes. To realize such flow in a certain region, electrons may enter and leave the region through two parallel grids, to which are joined electrodes corresponding to equipotential surfaces obtained from (3a).

An example of particular interest is the case in which the electrons entering the region come from a cathode forming one boundary, and giving space-charge limited emission. For this case, the gradient is zero at zero potential.* Taking zero

* Smith and Hartman (J. App. Phys. **11**, 3 (1940)) have proposed to attain rectilinear flow under these conditions, for beams of small cross section, by making the potential vary as distance to the 4/3 power along the axis of an electrode system. This will give approximately correct electrode shapes away from the cathode, but cannot be applied to attain rectilinear flow in the vicinity of the cathode.

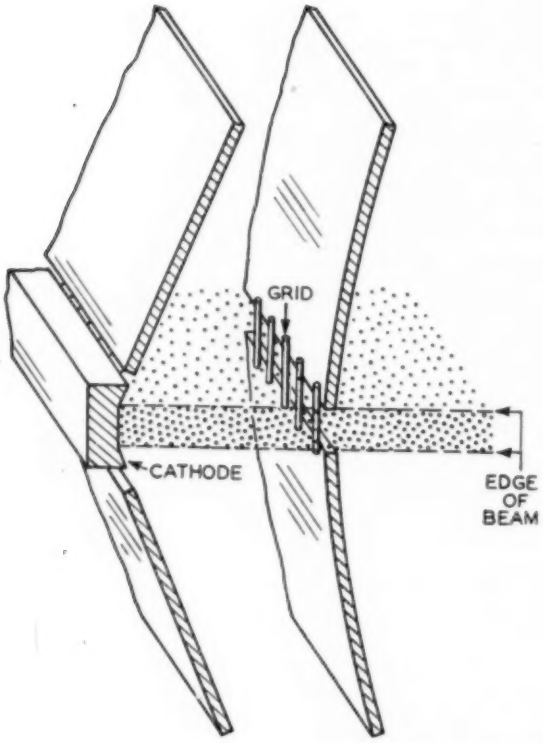

FIG. 3.

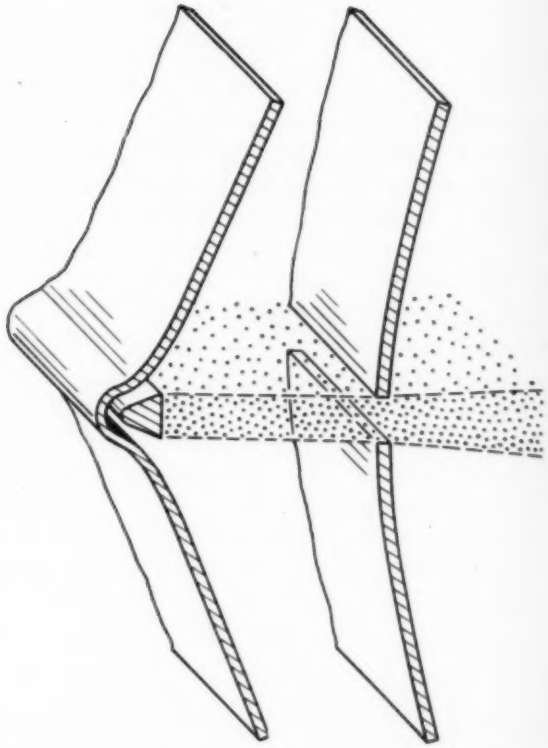

FIG. 4.

potential as at the origin, (1) may be integrated to give

$$\varphi = f(x) = Ax^{4/3}, \tag{4}$$

$$A = \left(\frac{9j}{4p_0(2e/m)^{\frac{1}{2}}}\right)^{\frac{2}{3}} = 5.69\times 10^{3} j^{\frac{2}{3}}. \tag{5}$$

In the charge-free region outside of the beam, according to (3a) the potential is given by φ in the expression

$$\varphi + i\Psi = f(x+iy) = A(x+iy)^{4/3}. \tag{6}$$

Figure 2 shows a plot of equipotential surfaces according to (6). The shape of the equipotentials is independent of the absolute magnitude of the potentials involved and of the units in which distance is measured. Thus, in Fig. 2 potential is indicated in terms of an arbitrary potential, φ_0, assigned to one equipotential surface. The potential of the cathode is taken as zero and distance is measured in arbitrary units, with the origin located at the edge of the cathode. It will be seen that the zero potential surface is a plane which meets the edge of the cathode ($x=y=0$) making an angle of 67.5° with the normal to the cathode (the x axis). Figure 3 shows how a plane cathode and the zero-potential electrode and a positive-potential electrode from Fig. 2 may be combined to give a parallel beam of electrons. The dashed lines indicate the boundaries of the beam.

In Fig. 4, both negative and positive equipotential electrodes are used in producing the beam. In the structure shown, the beam leaves the second electrode through a slit rather than through a grid. When the width of the slit is considerably less than the cathode anode spacing, the electron flow between cathode and anode will be practically the same as though a grid were present. However, the beam emerging from the slit will be divergent because of the lens action at the slit. The focal distance will be practically equal to the focal length of the lens formed by the slit.*,[4]

Equipotentials for other solutions[2, 3] of (1)

* $f=2\varphi/(E_1-E_2)$ where φ is the potential and E_1 and E_2 are the fields at the two sides of the slit.

[4] C. J. Davisson and C. J. Calbick, Phys. Rev. **42**, 580, (1932).

may be obtained in the same manner, and corresponding electrodes may be used in constructing vacuum tubes in which edge effects are eliminated.

IV. Parallel Flow with Cylindrical Boundaries

Electron flow according to (1) may also be obtained in a beam of constant circular cross section, surrounded by a charge-free region in which an appropriate axially symmetrical field exists. The conditions which must be met over the cylindrical boundary between the beam and the charge-free region are

$$\partial\varphi/\partial r=0, \tag{7}$$

$$\varphi=f(z), \tag{8}$$

where r is measured normal to the beam surface and z is distance from the cathode.

The problem of finding an axially symmetrical field outside of a cylinder which satisfies Laplace's equation subject to boundary conditions (6) and (7) at the cylinder may be solved experimentally by means of an electrolytic tank. As the beam and equipotentials are figures of revolution, any sector of the field cut off by planes through the axis of symmetry contains complete information about the entire field. Such a sector of field may easily be represented by current flow in an electrolytic tank.

A suitable tank construction is shown in Fig. 5. The bottom is a tilted plane of nonconducting material. Above the bottom is a wedge-shaped body of electrolyte, bounded by the tilted bottom and the liquid surface. No electrical gradients can exist normal to the bottom or to the surface, so the wedge-shaped electrolyte can represent a sector of an axially symmetrical system. The thin edge of the wedge of electrolyte is the axis of symmetry. Suitable electrodes to establish symmetrical equipotentials would be portions of figures of revolution about this axis. When the angle of the wedge is small, these can be replaced by singly curved electrodes, such as can be bent from flat sheets, with little error. The use of such a tank has been suggested by Manifold and Nicoll.[5]

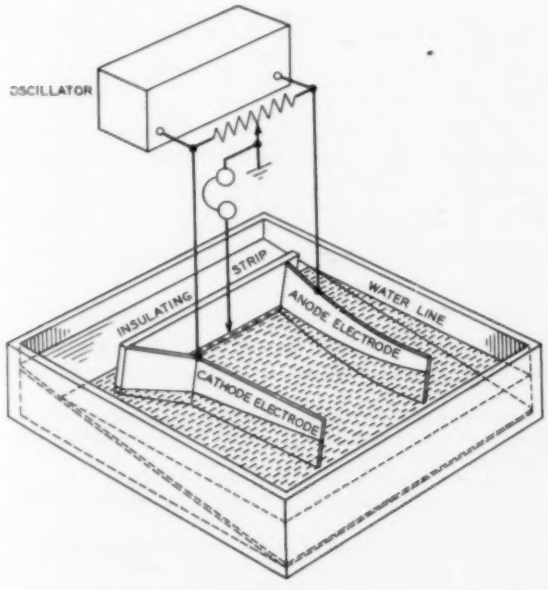

Fig. 5.

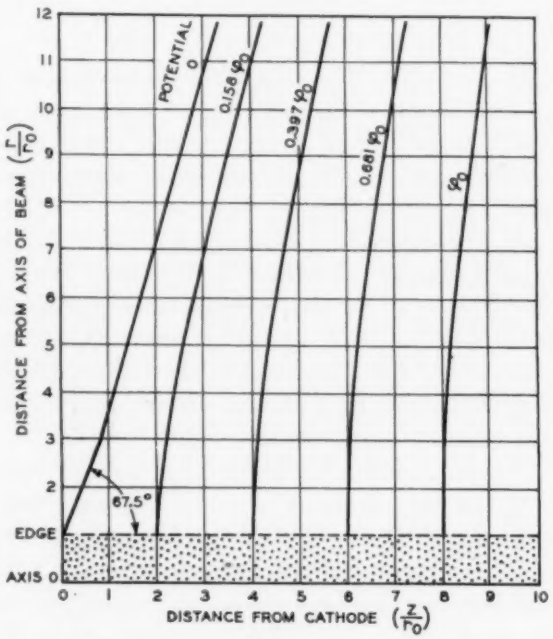

Fig. 6.

In use, a piece of insulating material is inserted in the electrolyte to represent the edge of the beam. This insures that the field normal to the beam boundary will be zero as required by (7). Usually, in obtaining the field two electrodes are used. These electrodes extend from the insulating strip representing the edge of the beam out into

[5] M. B. Manifold and F. N. Nicoll, Nature **142**, 39 (1938).

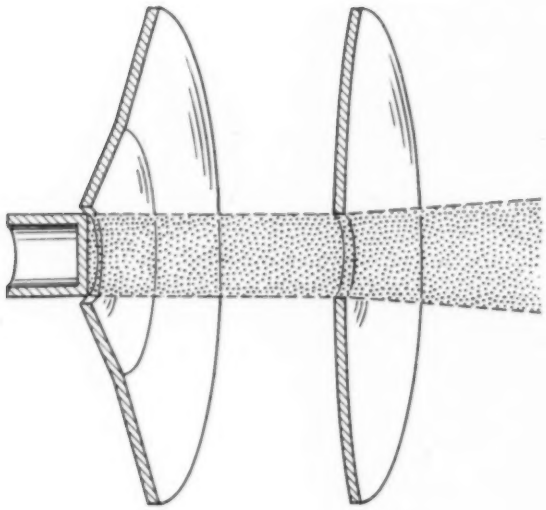

FIG. 7.

the electrolyte. The electrodes are connected to the terminals of an oscillator. A calibrated potentiometer makes it possible to measure potentials along the insulating strip which represents the edge of the beam.

As the condition of zero field normal to the beam boundary is automatically taken care of, the problem of finding suitable electrode shapes is merely that of adjusting the shapes and positions of the electrodes in the tank until the potential along the strip varies as the appropriate function of z as expressed by (8).

Figure 6 shows electrode shapes which were obtained for parallel flow from a space charge limited cathode in a cylindrical beam, according to (5). In Fig. 6, r_0 is the cathode radius, r is the distance from the axis of the beam, and z is the distance along the beam measured from the cathode. In Table I, measured potentials for the electrode system giving the equipotentials shown in Fig. 6 are compared with the desired potential, which varies as $z^{4/3}$. It may be seen that the fit is good.

Figure 7 shows an electron gun design based on the equipotentials in Fig. 6. The focal distance to the right of the aperture in the anode can be calculated by means of the formula for the focal length of a lens formed by a circular aperture.*, [4]

* $f=4\varphi/(E_2-E_1)$.

V. Radial Flow Between Cylinders and Spheres

Besides that described by (1), there are other sorts of rectilinear electron flow in the presence of space charge. Langmuir and Blodgett[6, 7] have presented equations governing radial flow in which the equipotentials are concentric cylinders or spheres. The assumptions made in treating such flow are the same as those used in deriving (1). Langmuir and Blodgett give solutions in series form for the cases in which the gradient is zero at zero potential (similar to Child's solution of (1)).

Such radial flow is usually associated with complete concentric cylindrical and spherical electrodes. However, it can also be realized in regions of limited angular extent between segments of cylinders and spheres, provided that the proper electrodes external to the electron flow are employed.

VI. Radial Flow Between Segments of Cylinders

Converging radial flow in a wedge-shaped region between segments of cylinders is of particular interest. This case may be treated by approximate methods.† In the region $r_0>r>0.25r_0$,

TABLE I.

$z/8r_0$	$(z/8r_0)^{4/3}$	φ/φ_0 MEASURED
0.1	0.046	0.048
.2	.116	.122
.3	.201	.201
.4	.294	.292
.5	.397	.401
.6	.506	.503
.7	.622	.618
.8	.743	.739
.9	.869	.870

where r_0 is cathode radius and r is distance from the center of curvature of the cathode, the following expression gives to a fair approximation the

[6] Irving Langmuir and Katherine Blodgett, "Currents limited by space charge between coaxial cylinders," Phys. Rev. **22**, 374 (1923).

[7] Irving Langmuir and Katherine Blodgett, "Currents limited by space charge between concentric spheres," Phys. Rev. **24**, 49 (1924).

† L. A. MacColl has obtained some equipotentials for the exact solution of this case. The equipotentials are similar in shape to those obtained by the approximate method here presented.

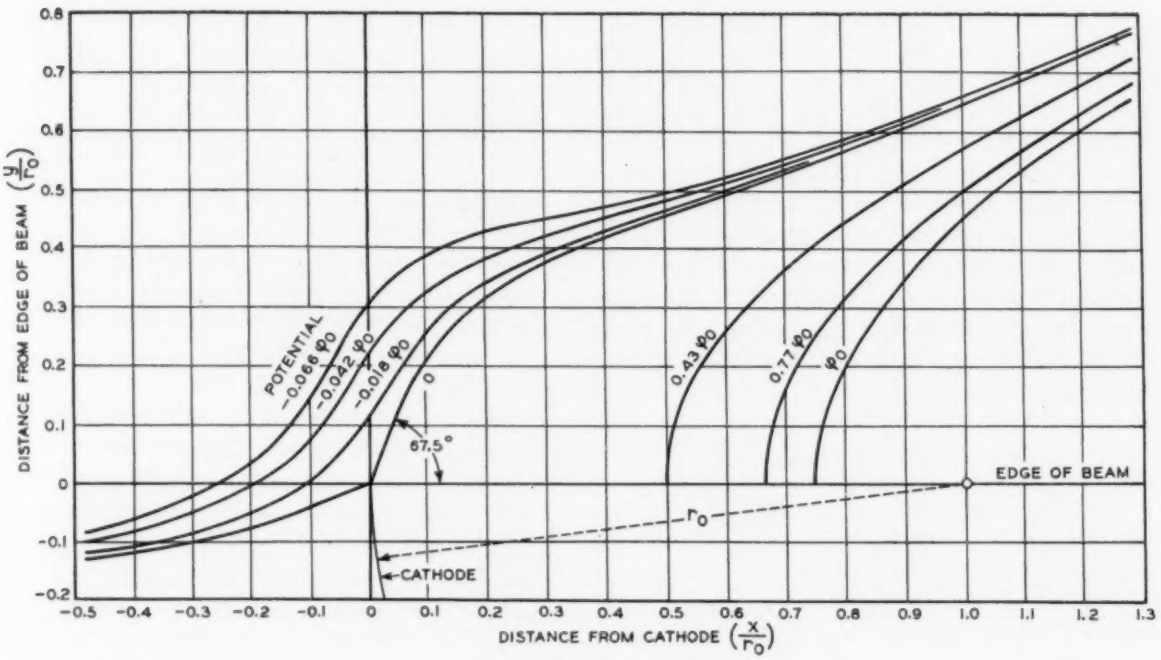

FIG. 8.

potential for converging flow between concentric cylinders

$$\varphi_a = Ax^{4/3}[1+1.63(x/r_0)^2] \qquad (9)$$
$$x = r_0 - r.$$

In Table II φ_a and the true potential φ as given by Langmuir and Blodgett[6] are compared. The factor A has been chosen so that $\varphi = 1$ at $r = 0.25r_0$

When (9) was used to represent the potential, the equipotentials shown in Fig. 8 were obtained. It is seen that these approach one another as they recede from the beam. Thus the field may be well defined by the use of two electrodes conforming to equipotentials. Figure 9 shows a line-focus electron gun based on such equipotentials, using negative potential and positive potential electrodes. Electrons leaving the cathode move along radii until they arrive at the anode, where the beam is $\frac{1}{4}$ its width at the cathode. The electron stream then passes through a slit in the anode, where it suffers a diverging action. As the focal distance of the beam approaching the slit, and the focal length of the lens formed by the slit are both known, the distance to the final focus or crossover can be calculated. A limiting aperture is located at the crossover.

The case of diverging flow may be treated in a similar manner.

TABLE II.

r_0/r	x/r_0	φ	φ_a
1.1	0.091	0.033	0.031
1.2	.167	.077	.073
1.4	.286	.168	.162
1.6	.375	.261	.251
2.0	.50	.43	.42
2.5	.60	.61	.61
3.4	.71	.86	.86
4.0	.75	1.00	.99

VII. Radial Flow Between Segments of Spheres

The analogous sort of spherically symmetrical flow, in which the electrons form a cone-shaped beam between spherical caps, is difficult to treat analytically. As in the case of parallel flow in a beam of circular cross section, appropriate electrodes can be obtained by use of the electrolytic tank. The necessary modification in procedure is that the insulating strip representing the edge of the beam should point toward the position on the axis or waterline of the center of curvature of the cathode. The appropriate variation of potential with distance, for which the electrodes are to be adjusted, can be obtained from the work of Langmuir and Blodgett.[7]

In the spherical case there is a different set of equipotentials for each angle of the cone occupied by the flow. A gun design using a particular pair of electrodes for flow in a cone whose sides have a slope of 0.25 with respect to the axis is shown in Fig. 10. The electrons leave the cathode, which is in the form of a circular spherical cap, and converge along radii to the anode, where the beam is $\frac{1}{3}$ as wide as at the cathode. The beam passes through an aperture in the anode electrode, suffering a calculable divergence. A small aperture limits the size of beam at the crossover.

VIII. Further Consideration

It will be noted that in all the equipotential and electrode shapes (Figs. 2, 6, 8, 10) a zero equipotential meets the cathode edge making an angle of 67.5° with the normal to the cathode surface. This is because in a very small region near the edge of the cathode, the curvatures of the cathode become negligible in all cases and the equations approach (4) and (8) which represent parallel motion between parallel planes.

The absolutely correct electrode shapes, for which the appropriate boundary conditions are satisfied exactly, are unique. There is, however, an infinity of quite dissimilar electrode shapes with which the boundary conditions can be satisfied to a good approximation. An approximate solution may be better in a practical sense than an exact solution, for the approximate solution

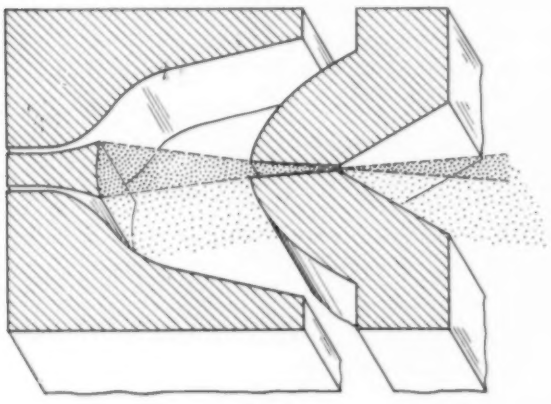

Fig. 9.

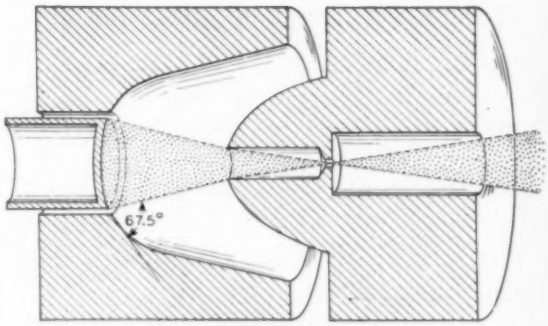

Fig. 10.

allows a certain amount of adjustment of the electrode shapes to meet exigencies of construction.

The equations on which the work is based were derived using certain simplifying assumptions. Thus the idealized electron flow which has been considered cannot be attained exactly, even though the "correct" electrodes are used. Perhaps the most serious divergence of the equations from fact lies in the neglect of thermal velocities. This is most serious in the case of converging flow, as in electron guns, for thermal velocities limit the current density which can be attained according to known relations.[8, 9] Electron guns designed according to the methods outlined have good focusing qualities, however, and with such guns current densities of over one-half of the limiting value imposed by thermal velocities have been attained.

Other practical advantages of these guns are the uniform cathode current density, which makes it possible to take advantage of the maximum allowable emission of the cathode over its entire surface, and the good focusing of electrons emitted from the edge of the cathode, which makes it possible to utilize a large portion of the cathode current in the beam. Thus, guns have been constructed which bring currents of several hundred milliamperes to a sharp crossover, with only a few milliamperes lost on the anode electrode.

[8] David B. Langmuir, "Theoretical limitations of cathode ray tubes," Proc. I. R. E. **25**, Aug. (1937).
[9] J. R. Pierce, "Limiting current densities in electron beams," J. App. Phys. **10**, 715 (1939).

Temperature Measurement with Blocking-Layer Photo-Cells

B. M. Larsen and W. E. Shenk
Research Laboratory, United States Steel Corporation, Kearny, New Jersey
(Received March 13, 1940)

THE authors' predominant interest in temperature measurement problems of the steel plant naturally tends to limit the following discussion of temperature measurements with photo-cells; however, certain aspects of this discussion have more or less general applicability.

When the work was started on this problem about ten years ago in the Research Laboratory of the United States Steel Corporation, the essential need in this field was for an accurate and preferably rapid method of measuring high temperatures which could also be used with recording instruments. The few thermocouples which could stand such temperatures (1300–1750°C or 2400–3200°F) were subject to rapid deterioration under the conditions of most practical applications; optical pyrometers were applicable and reasonably accurate but could not be used with recording instruments; the available total-radiation pyrometers were generally of poor design and subject to more or less serious errors, although they could be used with recorders.

The most promising lines of development seemed then to be (1) refinements in design of total-radiation pyrometers, and (2) the use of photoelectric cells. Since that time, in spite of some developments in thermocouples and protective tubes, and great progress in the design of total-radiation pyrometers, photo-cells have found increasing application in this field and are either essentially equivalent or definitely superior for a number of applications.

Perhaps the earliest specific suggestion for the application of photo-cells for temperature measurement was made by Ives[1] in 1920. We will not attempt to review here the rather scanty literature appearing on the subject since that time.

Nearly all of our work has been done with the so-called "blocking layer" or "rectifier" type of cells, such as the photronic cell made by the Weston Electrical Instrument Company. Such cells usually comprise a layer of selenium, coated on a metal disk, with a thin, transparent layer of gold or platinum sputtered on top. The radiant energy passing through this transparent layer is absorbed near the upper surface of the selenium layer and sets free electrons which tend to flow to the transparent metal film. Compared to the common vacuum type cell with a glass bulb, it has the advantages of (1) ruggedness with respect to handling and rough usage and possession of a size and shape such as to facilitate the design of fixtures for holding and protecting it; and (2) the property of self-generation of its own potential or current, which in many cases simplifies the electrical circuits involved and in other cases helps to avoid certain errors such as those due to variable supply voltage.

Temperature-Voltage Calibration

If the cell is simply shunted with a rather low external resistance of the order of 5 to 300 ohms, either the current flow or the voltage drop across this resistance will approach very near to a linear variation with the intensity of illumination in footcandles. In order to picture the response to a temperature change, the curves of Fig. 1 are helpful. Here the curve on the left shows the

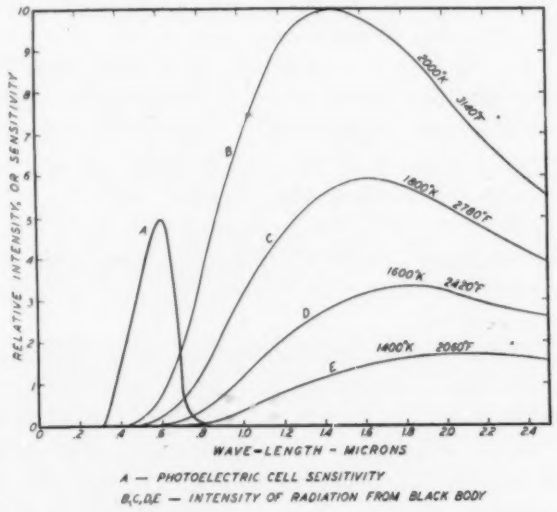

FIG. 1. Distribution of energy in the spectrum of a blackbody, compared with the spectral curve of the photronic cell.

[1] H. E. Ives, U. S. Patent No. 1,449,512, March 27, 1923.

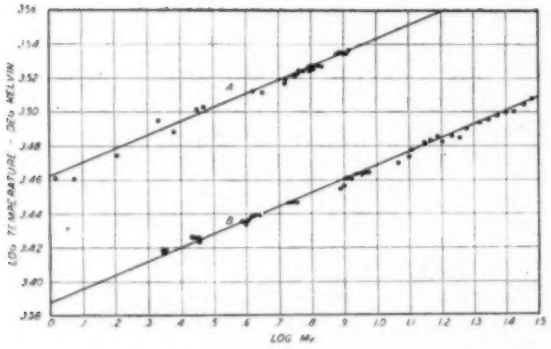

FIG. 2. Calibration curves for two photronic cells, logarithmic scale.

spectral curve for the photronic cell, and on the right are a few spectral emission curves for a "blackbody" at various temperatures. Obviously, the temperature *vs.* output variation for the cell should depend on the relative change in the *common area covered* by *both* the sensitivity curve and the radiation intensity curve for any given blackbody temperature. By rough measurement, this common area turns out to vary with approximately the tenth power of the absolute temperature. This comparison immediately shows up two characteristics of photo-cells used as pyrometers.

(1) The response curve will form a rapidly expanding temperature scale with an increasing accuracy toward higher temperatures, similar to that of an optical pyrometer. Incidentally, the spectral curves of such photo-cells are rather close to that of the human eye.

(2) At furnace temperatures of 2000–3000°F, the relatively small energy content in the short wave-lengths which affect the photo-cell are accompanied by a very much larger amount of useless infra-red radiation, the relative proportion of the latter increasing with decreasing temperature. This is discussed again below in connection with the protection of cells from overheating.

Figure 2 shows calibration data with a "blackbody" radiation source for two different photo-cells in different temperature ranges and with the cells mounted in diaphragm tubes such as to give different included angles in the cone of incident radiation, the data being plotted as the logarithm of the cell output *vs.* the logarithm of the temperature (in degrees Kelvin). The data allow of two parallel lines at a slope of 12.34 so that the potential drop (E) for presumably any cell of this same type with any arbitrary fixture design (assuming the whole cell face is illuminated) and over a fair range of shunting resistance (below a maximum of perhaps 200 to 300 ohms) could be expressed as

$$E = kT^{12.34}. \tag{1}$$

This agrees qualitatively with what we should expect from Fig. 1. In Fig. 3, the curves of Fig. 2 are replotted on ordinary linear scales.

This type of photo-cell in general is subject to uncontrolled variations in manufacture such as to cause differences in sensitivity not only between different cells but also between different areas on any one cell disk. However, it is claimed that for certain types, such as the photronic cell used here, the spectral response curve is the same for various cells of a given type. This means that the constant k above would be the only variable as between different cells of one type, and if the calibration curve for the latter is known, the changes from cell to cell can be adjusted from a check at any single temperature. This is indicated by the parallelism of the lines in Fig. 2, and, in general, we have found it to be true, at least within the limits of accuracy of steel plant measurements.

In the mounting of such cells we have practically always found it preferable to avoid using lenses, and to set the cells at the end of a simple diaphragm tube in such manner that the whole face of the cell is illuminated. In such a unit the potential drop (E) across a shunting resistance (preferably not over 200 to 300 ohms) is given by

$$E = kSD^2T^C/L^2, \tag{2}$$

where C is the slope as in Fig. 2, T is absolute temperature, D is the diameter of the opening in the diaphragm farthest from the cell face, which limits the cone of radiation, L is the distance between this diaphragm and the cell face, S is the sensitivity of the individual photo-cell and k is a constant for all cells of the same type.

Thus it is possible to adjust for differences between cells or for changes in sensitivity of a given cell and for variations in fixture design by simply varying the value of the shunting resistance, and to check by either of two methods:

1. The reading may be compared at any one temperature with that of an optical pyrometer on the source being measured or on some other known radiation source.

2. The cell may be compared with a "standard" cell of the same type on any convenient constant source of radiation.

Advantages and Limitations in Practice

Some of the advantages of such photo-cells for various practical temperature measurement problems are as follows:

1. These cells are very rapid in response to changes in intensity of the incident radiation, rapid enough, for example, to indicate the passage of a rifle bullet across their field of vision. This makes possible certain applications where it is desirable either to (a) measure accurately temperature variations occurring in a period of a few seconds or less or (b) have a very short total "period of exposure" at each measurement. In the recording of such cases it is the temperature recorder speed which limits the over-all period involved.

2. The rapidly expanding temperature scale makes possible a high degree of precision within a limited span near the top of any given temperature range, especially at the higher temperature levels. This is often useful in control of certain processes where a certain rather narrow optimum temperature range is involved in some fashion. A degree of precision equal to the best of optical pyrometer measurements is obtained together with the possibility of recording the data on standard type instruments.

3. The simplicity, cheapness and ruggedness of cells and electrical circuits involved have obvious advantages. For example, there are no cold junction temperature errors involved.

Among the various limitations involved we may mention the following:

1. The cells tend to change or become unstable in response if the disks are heated above about 120°F (50°C). Two sources of such over-heating must be distinguished.

(a) The "ambient temperature" around the cell as a whole must be kept low and in most metallurgical applications this requires a fixture to hold the cell and some air or water-cooling arrangement in this fixture.

(b) The sensitive face of the cell becomes heated to a varying degree above the ambient temperature of its immediate surroundings by the stream of radiant energy from the temperature source being measured, essentially because of the large energy content in the infra-red wave-length range. If, for example, the ambient temperature is up to around 90 to 100°F, the "margin of safety" becomes so small that the incident radiation may overheat the cell face. The amount of incident radiation may be decreased in certain cases by using a smaller limiting diaphragm opening or a longer tube. Beyond the point where this is practical, a special filter glass to absorb the infra-red radiation may be used.

2. The wide spreading temperature scale may be a handicap instead of an advantage in some cases. The scale is quite distorted so that a wide temperature range can in general not be covered very well by one instrument.

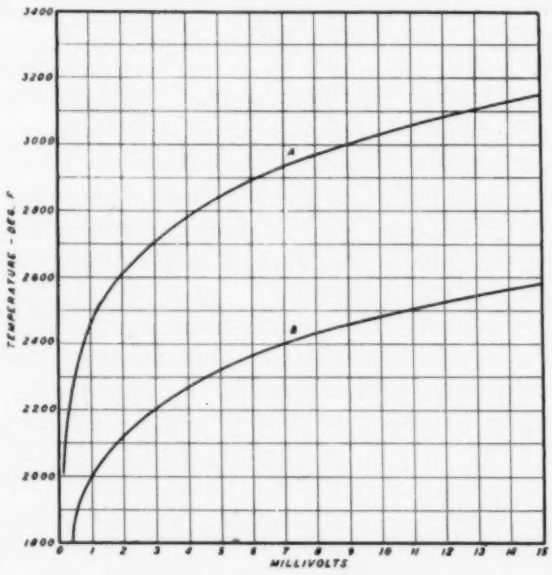

Fig. 3. Calibration curves for the two photronic cells of Fig. 2, ordinary scale.

3. In common with all such radiation type instruments, the "radiation path" must be kept free from all obstructions such as smoke or fumes, or from any change in the effective angular cone of radiation, and there should be no possibility of any radiation by reflection from surfaces of the cell fixture.

4. No great increase in external pressure on the cell should be allowed. The outer contact ring

may be forced down into the sensitive layer, affecting the sensitivity of the cell.

5. Under certain conditions the time lag of the cell may be important. When a large change is made in the total illumination reaching the active surface of the cell, the cell does not come immediately to its final response for the illumination but may take several seconds before essentially the steady-state response has been reached. This lag is called fatigue and is usually numerically designated by the fraction of the change in response by which the cell fails to attain the steady state response corresponding to the changed illumination at the first instant. Fatigue may be positive or negative depending upon whether the response of the cell "undershoots" or "overshoots" the steady-state value. It is usually small (one or two percent) and at worst, since the relation between blackbody temperature and cell response temperature has a large exponent, this lag amounts to a very much smaller temperature lag if the reading is taken without waiting for the steady state to be reached. If the illumination reaching the cell changes by small increments or gradually instead of suddenly from dark to light the error is even less important. Where this small lag is of consequence, cells of practically zero fatigue can be selected.

It is naturally very desirable to avoid the necessity for amplification of the output of these cells, whenever possible. The circuits and instruments become much simpler and many possible sources of error are avoided. At the top of the steelmaking temperature range, between 2800 and 3100°F, it is quite easy to obtain enough voltage or current to operate directly on standard recorders, although even in this range one may choose to employ infra-red filters to help in keeping cell face temperatures low. (It should be noted that the temperature response curve for any given type of cell should be re-determined when any new selective wave-length filter is used, since most of these will have at least some small absorption in the sensitive range of the cell.)

As the temperature drops down to around 2100–2200°F, the cell output drops off very rapidly; the angle of incident radiation must be increased until even with a good infra-red filter it becomes more nearly impossible to keep the cell cool and at the same time obtain enough output to operate directly upon ordinary recorders of sufficient ruggedness to withstand plant environments. In this lower range of perhaps 1800–2200°F, and sometimes also at higher temperatures in such cases where it is necessary to use a small angle of incident radiation, it may therefore be necessary to amplify the cell output, feeding this amplified current into a relatively rugged recording or indicating instrument.

Any amplifier used in such applications should be (a) relatively foolproof in operation and (b) of such design as will have no tendency to distort the temperature-output relationship of the cell or to introduce any extra sources of error. Many of the amplifiers described in recent years have been sadly deficient in the fulfillment of these requirements. The design developed by Gilbert[2] represents an important advance in this line.

Applications

Temperature measurement with such photocells has been applied to combustion chamber, bath, and regenerator zones in commercial open hearth furnaces and to initial rolling and welding temperatures. Especially in certain high speed applications, the combination of precision and speed has been superior to that obtained by any other method. At the present stage of development, it may be said that for applications below a limit of something like 1800–2000°F, temperature recording may better be obtained with thermocouples or total radiation pyrometers. At higher temperature ranges there is not much to choose between either photo-cells or certain modern total-radiation pyrometers for many applications, each having certain advantages. Where either speed or great precision over a relatively narrow temperature range is of predominant importance, however, the photo-cell is probably superior.

Barring accidental breakage or overheating, such cells will tend to give service over periods of a year or more without appreciable changes in calibration. Frequent inspection and checking of cells, fixtures and recorders at intervals of from a day to a week are in general needed with this as

[2] R. W. Gilbert, "A new high speed, high sensitivity photoelectric potentiometer," Rev. Sci. Inst. **7**, 41–44 (1936).

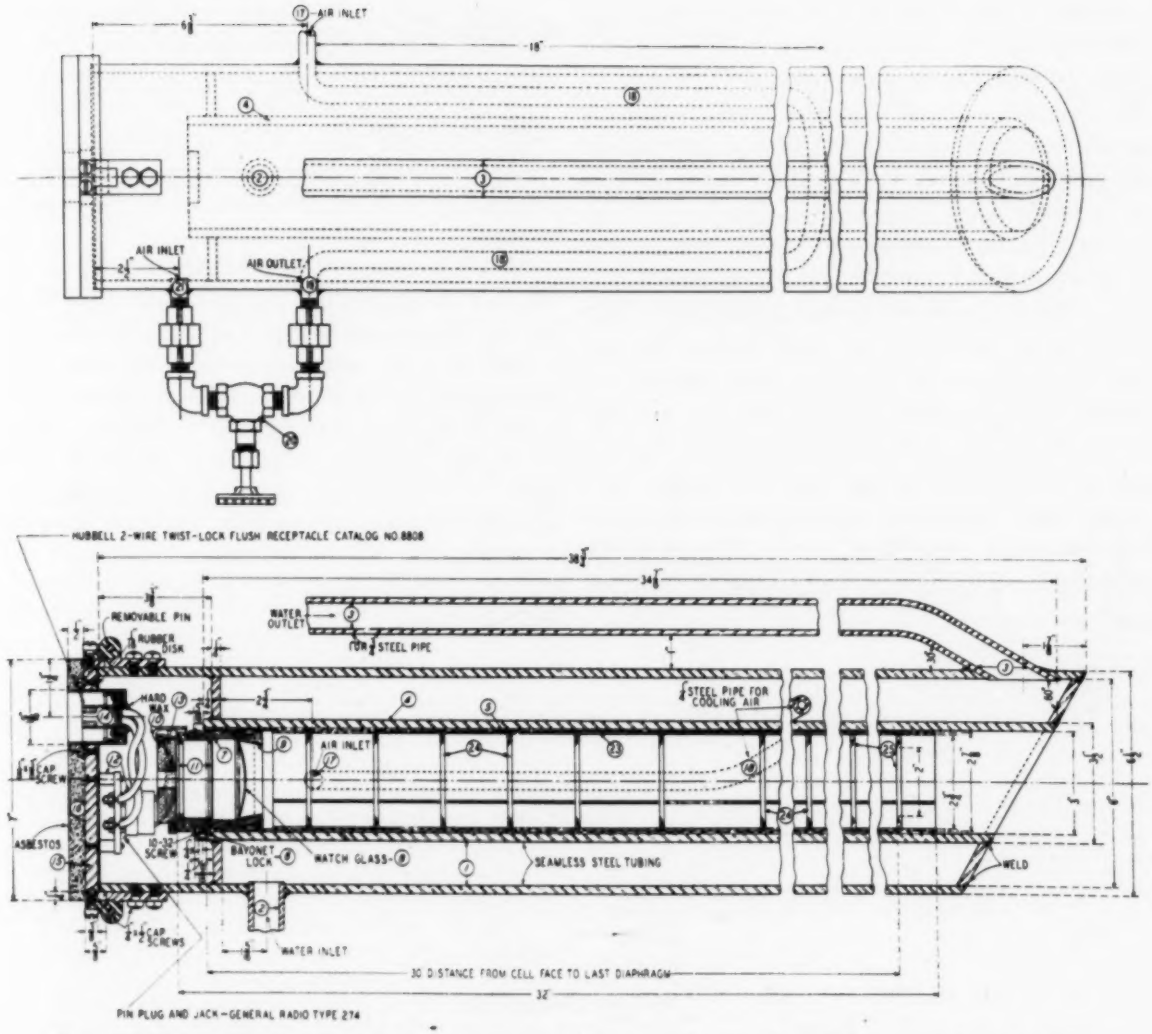

FIG. 4. Water-cooled fixture for photronic cell as used in measuring open-hearth furnace roof temperature.

with most other industrial temperature measuring equipment, however.

To indicate more specifically the severity of conditions under which such cells may be used, we mention the recording of open hearth roof temperature with a cell fixture sighted through the back wall almost above the tapping spout of the furnace. This application happens to include practically all of the possible difficulties in operating measurements with such photo-cells. Figure 4 represents a patented cell fixture[3] developed for this application, and we may briefly indicate certain features merely to indicate the kind of practical difficulties encountered:

(a) An oversize, water-cooled jacket protects against high ambient temperatures and mechanical shock.

(b) The diaphragm tube of stainless steel is arranged with diaphragms set so that no radiation can be reflected from its walls to the cell face and so that the front diaphragm opening defines the cone of radiation. The cell holder is removable and slips back into a fixed position with respect to the front diaphragm. This whole diaphragm tube and cell holder may be removed from the jacket for cleaning or repair.

(c) An inexpensive watch-glass window in the front of the cell holder prevents occasional "shots"

[3] B. M. Larsen and W. E. Shenk, U. S. Patent No. 2,054,382, Sept. 15, 1936.

of steel or slag droplets from the furnace from reaching the filter glass or cell face behind it and is easily replaced when so damaged. The glass filter behind it absorbs infra-red radiation, most of which is dissipated in holder and tube before reaching the cell disk. The diaphragm tube is made sufficiently long and narrow to prevent nearly all shots of steel or slag from reaching the glass window.

(d) An air line is first passed through the water jacket and then into the space behind the cell holder. This cooled air passes through channels in the cell holder, through the diaphragm tube and out toward the furnace opening, serving the double purpose of dissipating the radiant heat energy absorbed in these parts and of keeping the radiation path clear of all dust or fumes which might enter from the furnace chamber or other sources.

Some or all of the troubles indicated above will usually be absent in most applications. It should be noted that while direct or reflected sunlight or artificial illumination usually has a negligible effect on total radiation pyrometer units, such radiation may cause very serious errors in photo-cell pyrometers and must be guarded against in certain applications.

It will perhaps be noted that we have referred mainly to "precision" rather than "accuracy" in the above discussion. For the applications in which we have been interested, it has been more important to obtain relative temperature values with reasonably high precision and with moderate accuracy; for such purposes these cells have been very satisfactory. There is probably room for more exact laboratory studies of the temperature-response characteristics of different cells made to one type by a given method of manufacture.

Calendar of Meetings

August

27–30 American Institute of Electrical Engineers, Los Angeles, California

September

3– 6 American Society of Mechanical Engineers, Spokane, Washington
9–13 American Chemical Society, Detroit, Michigan

October

3– 5 Optical Society of America, Rochester, New York
7–11 National Safety Council, Chicago, Illinois
18–19 Society of Rheology, New York, New York
21–25 American Society for Metals, Cleveland, Ohio
21–26 American Welding Society, Cleveland, Ohio
28–30 National Academy of Science, Philadelphia, Pennsylvania
28–Nov. 2 Conference on Applied Nuclear Physics, Cambridge, Massachusetts

November

15–16 Acoustical Society of America, Chicago, Illinois
22–23 American Physical Society, Chicago, Illinois

Letters to the Editor

Polonium Alloy for Spark Plug Electrodes

Under the same title, Dr. J. H. Dillon discusses some observations of the behavior of spark plugs having standard or auxiliary electrodes containing polonium.[1]

Because of our interest in all phases of applied radioactivity, we have measured the alpha-ray emission of several of these new Firestone plugs, purchased from a large service station on the day of their arrival in Boston. The total polonium content is less than 0.2 $\mu\mu$g, whereas Dr. Dillon, on page 298, states that the "present production plugs" have 108 $\mu\mu$g of polonium (54 $\mu\mu$g per electrode).

On the same page, two other initial activities are given. Choosing the figures in the first paragraph of the discussion, the ionization in the gap (at seven atmospheres pressure), would be 11,000 ion pairs per second, not 40,000. But this ionization is not continuously produced, since there can be only one alpha-ray emitted every three seconds, that is one alpha-ray per 150 revolutions of the motor. These are calculated values, using the usual formulas, tables, and constants on the emission of alpha-rays by solid bodies.[2] The actual retail product measured in our laboratory showed only a small fraction of this claimed activity.

Three types of tests are described by Dr. Dillon: (a) plugs with auxiliary teaser electrodes containing large amounts (1000 $\mu\mu$g) of polonium, tested in a sealed bomb up to 3.75 atmospheres and at plug voltages up to 6000 volts r.m.s., (b) parallel efficiency tests on plugs of standard geometry, tested in a sealed bomb up to 5.75 atmospheres and (c) cranking time tests on three 1936 and 1937 Studebaker motors at -26°C, with 3.75 volts on the ignition system. None of these tests represents the operating service normally met by the motorist. Modern engines operate at about seven atmospheres pressure, and with about 30,000 volts peak on the spark plugs.[3] Under these conditions, the tests of Fig. 1 and Fig. 2 appear to show no difference between the firing of plugs with and without polonium.

In the parallel efficiency tests of Table II, the efficiencies E are ratios of the number of discharges in test plugs and in control plugs. The ignition system voltage is not stated, but by implication it is the normal operating voltage. If so, the control plugs are defective. If not, the tests do not approximate normal operating conditions. Every service station has a spark plug tester which allows one to see the fraction of sparks missed, at normal voltage and pressures up to far above seven atmospheres. The service station operators advise a customer to replace any plug which fires less than 80 to 90 percent of the time at seven atmospheres, even though it fires 100 percent of the time at six atmospheres. Dr. Dillon's highest pressure is 5.75 atmospheres, and the test plug fired 5.7 times as frequently as the control plug. Therefore, the maximum percentage for the control plug is $100/5.7 = 18$ percent!

In discussing Table II, Dr. Dillon says the "increases in total polonium for a given type of ground wire resulted in negligible increases in E." Actually there is either no change (Tests III and IV) or a decrease in efficiency with increasing polonium content (Tests I and II).

Comparing Tests IX and X, a $2.7/0.02 = 135$-fold decrease in efficiency is shown merely by polishing the standard electrodes. The maximum effect due to the absence of polonium is a factor of 5.7 (Test VI), or only $5.7/135 = 4.2$ percent as much effect as polishing the electrode of a new standard plug. Does the motorist draw the conclusion that a full strength polonium electrode will help him only four percent as much as roughening the surface of the electrodes?

The cold starting tests of Table III were conducted at -26°C, with only 3.75 volts on the ignition system. These are the only tests actually made on an engine. Such conditions are met infrequently if at all by the majority of motorists. The Society of Automotive Engineers has set the accepted standards[4] for cold starting service of passenger car batteries. The engine is supposed to start in less than five seconds, and the "medium" battery must be able to supply 300 amperes at 0°F (about -18°C), for this time and maintain a terminal voltage above 4.1 to 4.5 volts.

The data on starting revolutions (Table III), showed an admittedly large spread, that is they were difficult to repeat and even showed reversals (page 298). The actual dispersion of the data, which could easily be given as a probable error in the ratio column is not reported. Also no absolute values of cranking time are reported, and this, as well as the ratios, gives an index of any practical improvement in performance. For example, if normal cranking time is four seconds, it makes little difference to the motorist or to his battery if this is reduced to 2.5 seconds.

Some of the errors and misprints in the text, tables, and figures make reinterpretation necessary. In Fig. 1, the voltage differences at 50 sparks per minute are 610 to 740 volts, not 6100 to 7400 as shown in the figure. In Table II, columns 6 and 9, and in Table III, column 6, the captions apparently should read "previous" instead of "subsequent." In Table III, column 7, either the heading should read "ratio . : . controls *vs.* Po plugs," or all figures should be replaced by their reciprocals, or the Po plugs hinder prompt starting. I cannot confirm the results of Dr. Dillon's calculations on radioactivities, using any of the three different initial activities cited on page 298.

Finally, a word about the use of radium in spark plugs, which Dr. Dillon says would be expensive and dangerous, and which has been previously patented. Taking the highest of his three figures for the initial activity, equivalent alpha-radiation would be obtained by using less than 0.5 cent worth of radium per plug. The industrial hazards of radium are well known, but can be completely controlled if the right precautions are taken. Polonium offers a similar hazard, and equivalent precautions against ingestion must be taken if fatalities are to be avoided.

Because of the 140-day half-period of polonium, the radioactivity of plugs containing it will fall off very rapidly compared with the normal shelf life and operating

life of the average spark plug. Even if new plugs did contain large quantities of polonium, it appears that under practically all starting and driving conditions they have no advantage because modern ignition systems provide many times the voltage required to assure electrical breakdown of the gap in standard spark plugs. The differences between polonium and standard spark plugs are demonstrable only under such extreme conditions that the tests have substantially no bearing on the actual operating conditions met by the motorist.

ROBLEY D. EVANS

Massachusetts Institute of Technology,
Cambridge, Massachusetts,
June 15, 1940.

[1] J. H. Dillon, J. App. Phys. **11**, 291–299 (1940).
[2] R. D. Evans, Phys. Rev. **45**, 29–37 (1934); G. D. Finney and R. D. Evans, Phys. Rev. **48**, 503–511 (1935).
[3] A. B. DuMont, *Oscillographer*, February–March 1940.
[4] Soc. Auto. Eng. 1939 Handbook, p. 103.

Polonium Alloy for Spark Plug Electrodes

This is a discussion of the comments made by Professor Robley D. Evans in the preceding Letter to the Editor on my paper of the above title.[1] Professor Evans' comments will be discussed in order, where possible.

It is interesting to learn of the plugs with low Po content in the electrodes, as tested by Professor Evans. A routine photographic check is made of every coil of electrode wire used in Po spark plugs. In rare instances, coils of wire with low Po concentration have been released for production by error. Possibly the electrodes tested by Professor Evans were from one of these coils. It would be interesting to learn whether both electrodes were employed in his tests and to have his results expressed in terms of the number of alpha-particles emitted per cm^2 per sec. from the alloy. I should appreciate the opportunity of examining some of these electrodes for we are much interested, of course, in maintaining a uniform product. A cloud-chamber photograph of the alpha-particle emission from a 3-in. length of 0.081 in. diameter electrode wire of normal Po concentration is shown in Fig. 1. The sensitive time was 0.1 sec.

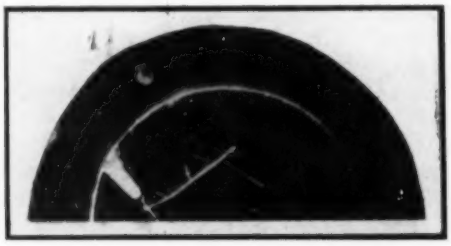

FIG. 1. Alpha-particle tracks from polonium alloy electrode wire.

The third and fourth paragraphs of Professor Evans' letter ignore the fact, specifically stated in my paper, that the principal object of using Po in the electrodes is to improve the cold starting qualities when the motor turns at about 1 r.p.s. rather than at 50 r.p.s. Hence, the correct figure should be 1 alpha-particle per 3 revolutions of the motor. Lacking information as to the details of the calculation and the type of plug tested, the figure 11,000 ion pairs per sec. is difficult to verify. It does not appear to be of sufficient importance to merit further attention.

The tests with the interrupter and the pressure bomb were not intended to reproduce closely the conditions of service and this fact is stated in the paper. The cold starting tests were made under severe conditions actually found in service. Although such conditions are fortunately quite rare, failure of plugs to start under these conditions accounts for a large fraction of consumer complaints. The spark plug manufacturer is vitally interested in eliminating complaints as well as in producing a product which is satisfactory under normal, less severe conditions.

A 4-volt battery was used for the tests of Table II for a reason not important to this discussion. However, if a 6-volt battery had been used, it would have been quite possible to obtain similar data with entirely satisfactory control plugs. Comparison of the results of this paper with service station pressure bomb tests is not justified. It is known to ignition engineers but, unfortunately, not to the majority of consumers, that this sales promotion tester, as often operated, gives very misleading results since it is very sensitive to electrode shape. For example, plugs of a certain common brand are made with sharp edges on the end of the center electrode. Such plugs generally do not cut out at pressures below 200 lb./in.^{2}. The cut out pressure can be reduced by 70 to 100 lb./in.^{2} simply by polishing off the sharp edge. In this manner, a new plug with sharp edges can be made to appear much superior to a perfectly satisfactory used plug with sharp edges burned off, in order to make a sale. Sharp edges on the electrodes, of course, disappear after the first few hundred miles of service and are of no advantage after that period.

Referring to Professor Evans' ninth paragraph, the cranking speed used in the cold starting tests ranged from 15 to 50 r.p.m. Contrary to Professor Evans' opinion, consumer tests and acceptance have shown that motorists *are* interested in a quickly starting motor under severe conditions.

It is regretted that the decimal points in Fig. 1. were omitted and that the heading of column 7 was inverted in meaning, as pointed out by Professor Evans.

Space forbids a thorough discussion of the use of radium in spark plugs but it should be remarked that 0.5 cent/plug is not a negligible item in manufacturing cost.

As remarked by Professor Evans, it is unfortunate that Po decays as rapidly as it does. However, it is well to remember that, from a broad economic standpoint, it is more desirable to utilize a large fraction of the energy of the radioactive material during the normal life of the plug than to use a slowly decaying material, most of which would be discarded with the plug at the end of its service. It should also be noted that impressed voltages are limited by corona and insulation and that conditions do occur when a spark plug may be an unnoticed friend or a maligned enemy, depending on its cold starting properties.

J. H. DILLON

Physics Research Laboratory,
Firestone Tire and Rubber Company,
Akron, Ohio,
June 20, 1940.

[1] J. H. Dillon, J. App. Phys. **11**, 291–299 (1940).

Contributors to This Issue

B. M. Larsen has been on the staff of the United States Steel Corporation Research Laboratory as physical chemist since 1929. He was graduated from the University of Wisconsin in 1921, and then did graduate work at the University of Washington. From 1923 to 1928 Mr. Larsen was with the U. S. Bureau of Mines.

William E. Shenk, who holds a B.S. and an M.S. degree from the Massachusetts Institute of Technology, has been a member of the staff of the United States Steel Corporation Research Laboratory since 1929. His principal activities have been concerned with the development of pyrometric and magnetic apparatus.

E. U. Condon is associate director of the Westinghouse Research Laboratories at East Pittsburgh, Pennsylvania. He received his Ph.D. from the University of California in 1926 and taught theoretical physics at several universities, principally at Princeton, before going to Westinghouse in 1937. Dr. Condon's paper on "Electronic generation of electromagnetic oscillations" was printed in the July issue of the Journal, but his picture and biography were omitted by mistake from that issue.

E. U. Condon

Louis A. Carapella is a Gordon McKay teaching fellow in x-ray metallography in the Graduate School of Engineering at Harvard University, where he received his M.S. degree in 1939. Part of the requirements for his degree were fulfilled at the Massachusetts Institute of Technology.

Samuel Sabaroff worked in the reject-control and factory laboratory of the Philco Radio and Television Corporation from 1931 to 1932 and, since 1932, has been a transmitter engineer with the WCAU Broadcasting Company. Mr. Sabaroff is a graduate of Drexel Institute of Technology and the University of Pennsylvania.

The following contributors to this issue have received mention in earlier issues of the *Journal of Applied Physics:*

Maurice A. Biot, p. 36, Vol. 9, No. 1, 1938.

W. James Lyons, p. 630, Vol. 9, No. 10, 1938.

F. Morgan, p. 391, Vol. 9, No. 6, 1938.

Morris Muskat, p. 391, Vol. 9, No. 6, 1938.

J. R. Pierce, p. 699, Vol. 10, No. 10, 1939.

B. M. Larsen

W. E. Shenk

L. A. Carapella

S. Sabaroff

Necrology

William Wallace Buffum, Treasurer and Director of the Chemical Foundation, Incorporated, died on June 22 after a brief illness. Mr. Buffum was known throughout American scientific circles as an enthusiastic proponent of education and research. While much of his attention was given to helping chemists and physicians with their problems of publication and organization, he also took a vital part in the founding of the American Institute of Physics. He was the first Treasurer of the Institute, his organization supported the Institute financially, and indeed the first office space the Institute had was provided by the Chemical Foundation.

In the developmental stage of the Institute, Mr. Buffum attended all of the Governing Board meetings as Treasurer and invariably contributed both stimulation and judgment to its projects. Not a scientific man himself, Mr. Buffum nevertheless followed the major developments of science including physics and was not only directly instrumental in bringing to scientists much-needed funds for research but also aided them in gaining, through appropriate methods of publicity, a degree of general recognition which has proved invaluable.

Here and There

Council for Defense

An executive committee, composed of Professor Richard C. Tolman, Dr. Max Mason, and Professor E. C. Watson, has been appointed by the trustees of the California Institute of Technology to provide means of mobilizing and coordinating effort in the present national situation. The council will proceed immediately with a survey of the possible contributions which the Institute can make both through individual members of the staff and special facilities in the laboratories. All members of the committee were active in warfare service in 1918. Experts in fields of military significance have offered to devote a large portion of their time to defense work.—*Science*

★

Cornell University Faculty Changes

Dr. Diran H. Tomboulian has been appointed Assistant Professor of Physics at Cornell University, Ithaca, New York. Dr. Robert F. Bacher, Assistant Professor of Physics, has been advanced to the position of Associate Professor.

★

Honorary Degree Conferred

Dr. Lars O. Grondahl of the Union Switch and Signal Company, Swissvale, Pennsylvania, received the honorary degree of Doctor of Science at the 1940 Commencement of Saint Olaf College, Northfield, Minnesota.

★

Cornell College Awards Honorary Degree

Lee A. DuBridge, Dean of the Faculty of Arts and Sciences at the University of Rochester, received the honorary Doctor of Science degree on June 10 at the 87th Commencement of Cornell College, Mt. Vernon, Iowa. Dr. DuBridge is a Cornell College graduate with M.A. and Ph.D. degrees from the University of Wisconsin.

★

Yale University

W. W. Watson, Associate Professor at Yale University, has been promoted to be Professor of Physics and Chairman of the Department of Physics, according to a recent announcement in *Science*. Professor Watson succeeds Professor John Zeleny, who retires this year.

★

Cathode-Ray Symposium Planned

To encourage a still greater exchange of practical information on the rapidly expanding applications of the cathode-ray tube, the Allen B. DuMont Laboratories, Inc., Passaic, New Jersey, are sponsoring a Cathode-Ray Symposium and Prize Contest to extend over the period of one year, beginning June 1, 1940. Contributors to the Symposium are to submit practical information, in form for publication, on any successful application of the cathode-ray tube. Papers received and accepted will be published in the *DuMont Oscillographer*, the Laboratories' publication, and honorariums will be paid to the authors of the published articles. At the close of the Symposium, three papers will be chosen to receive cash awards. A complete set of rules covering the Symposium Prize Contest has been prepared and may be obtained upon request from Allen B. DuMont Laboratories, Inc., Passaic, New Jersey.

★

Standardization of Thermometric Methods in Great Britain

Dr. J. G. Bennett, chairman of an English committee now revising the British Standards Specifications on temperature measurement, has recently made the following announcement in regard to the publication of a revised code of temperature standards:

"A second draft embodying the results of the work of the various sub-committees and panels was completed early in 1939 and was circulated for comment to a small number of selected workers in Great Britain. A large number of valuable suggestions and comments were received and the Committee considered these during the spring and summer of 1939. At the present time a third draft has been completed, and after revision by the Main Committee will be circulated for comment to interested workers at home and abroad. Mr. Bennett, as Chairman of the Committee, will be glad to receive through the American Institute of Physics, the names of any American workers or organizations who may desire to receive the revised draft code, which, it is hoped, will be completed early in 1940."

★

Rochester Optical Society Election

The Rochester Section of the Optical Society of America announces the recent election of the following officers and council for the year 1940–41: President, Brian O'Brien; Vice President, R. Bruce Horsfall, Jr.; Secretary, David L. MacAdam; Treasurer, John W. Gillon; and Council, Henry F. Kurtz, John H. McLeod, Cyril J. Staud, T. Russell Wilkins, and Robert E. Burroughs (*ex officio*).

★

Correction

Because of an error which occurred in checking the list of Modern Pioneer awards made to members of the American Physical Society, the name of Dr. Harry Ferdinand Olson of the RCA Manufacturing Company, Camden, New Jersey, was inadvertently omitted. Dr. Olson was the recipient of a Modern Pioneer award in the Philadelphia area.

Biological Photographers to Meet

The tenth annual convention of the Biological Photographic Association will be held at the Hotel Schroeder, Milwaukee, Wisconsin, September 12, 13, and 14. This society is interested in the further study of photography as applied to the biologic sciences and in the improvement of its technique. Besides informal meetings for the exchange of ideas on still and motion picture photography and on the latest developments in color work, formal papers outlining new methods of technique, exhibits by manufacturers of scientific photographic apparatus and materials, and a salon of natural color and monochrome prints of biologic and clinical subjects are being planned. Further information concerning the convention may be obtained by writing to the Secretary of the Biological Photographic Association, University Office, Magee Hospital, Pittsburgh, Pennsylvania.

★

Mathematical Biophysics

Beginning with the September issue, the *Bulletin of Mathematical Biophysics* will be published by the University of Chicago Press, it is announced by Dr. N. Rashevsky, Editor. The table of contents of the September issue includes the following articles:

A Generalization of Cunningham's Extension of Stoke's Law for a Force on a Sphere, by GALE YOUNG
Physicomathematical Aspects of Some Problems of Organic Form, by N. RASHEVSKY
Contributions to the Mathematical Biophysics of Organic Form III. The Formation of Shell-Shaped Cellular Aggregates, by N. RASHEVSKY
On the Formal Theory of Nerve Conduction, by ALVIN M. WEINBERG
A Note on the Horopter, by ALSTON S. HOUSEHOLDER
A General Fluid Circuit Theory of Active Chloride Absorption, by H. C. PETERS.

★

New Philosophical Society Members

During the annual general meeting of the American Philosophical Society held April 18–20 in Philadelphia, the following were elected to membership in Class I. Mathematical and Physical Sciences: Ira Sprague Bowen, Pasadena; William Francis Giauque, Berkeley; Jerome Clarke Hunsaker, Boston; George Bogdan Kistiakowsky, Cambridge; Robert Sanderson Mulliken, Chicago; Howard Percy Robertson, Princeton; John Clarke Slater, Cambridge; Niels Henrik David Bohr, Copenhagen; Sir William Henry Bragg, London; and Tullio Levi-Civita, Rome.

★

Dr. H. H. Sheldon, Professor of Physics at New York University, which he has served for the past eighteen years, recently in charge of the adult education courses in science, has resigned. He plans to open a consulting service in New York City. Dr. Sheldon is secretary of the Board of Management of the Engineers Club of New York, and has been retained in the past by various industrial organizations. He was for four years science editor of the *New York Herald-Tribune*. Dr. Sheldon expects to continue as managing trustee of the American Institute of the City of New York, whose work he has directed for the past two years.—*Science*

Recent Booklets

The April–May issue of the *DuMont Oscillographer* carries an article entitled "A new cathode-ray oscillograph." The back cover of the issue announces a Cathode-Ray Symposium and Prize Contest being sponsored by the magazine's publishers, the Allen B. DuMont Laboratories, Inc., 2 Main Avenue, Passaic, New Jersey.

A reproduction of Charles Meers Webb's painting of the alchemist appears on the cover of *The Laboratory*, Vol. 11, No. 5, publication of the Fisher Scientific Company of Pittsburgh, Pennsylvania. The first article of this issue describes the new Pyrex Vycor glassware under the heading, "A major achievement in the manufacture of laboratory glassware."

The optical properties of the plastic, Plexiglas, manufactured by Röhm and Haas Company, Inc., 222 West Washington Square, Philadelphia, Pennsylvania, have been discussed in a recent booklet prepared by the manufacturers. This booklet gives the optical constants of this crystal clear plastic and also describes the techniques by which these values were obtained.

Weights and data for copper, brass and bronze products are published in a 33-page booklet by Revere Copper and Brass Incorporated, 230 Park Avenue, New York City. This 1940 *Revere Weights and Data Handbook* is corrected as of May 1, 1940.

The May issue of *Science and Appliance*, published by the Ohio State University Research Foundation, contains notes on the following subjects: "Walls for fire," "Copper-plated hands and feet," "Engineering and management in welding," "Strategic Mg and Mn," and "Notes from the golden anniversary meeting of the Ohio Academy of Science."

Thermocouples, thermocouple wire, lead wire, insulators, protecting tubes, and similar instruments marketed by the Wheelco Instruments Company, 1929–1933 South Halsted Street, Chicago, are illustrated and described in the Company's Bulletin S2-2 now available upon request.

The RCA Manufacturing Company, Inc., Harrison, New Jersey, offers two new booklets: the *RCA Ham Guide* (price $0.15), intended primarily for the use of radio amateurs, gives technical data on RCA transmitting tubes and circuits for utilizing them and also information on the design and operation of amateur transmitters; *RCA 1847 Iconoscope* describes the instrument of that name, which is expected to bring television into the province of the amateur.

A discussion of the electrical and mechanical specifications of the various standard and special Shallcross noninductive, wire-wound resistors is the object of Bulletin 122-W, recently published by the Shallcross Manufacturing Company of Collingdale, Pennsylvania.

Innovations in Instruments

Ultraviolet Lamps

Conti-Glo "Black Lights," sources of light in the region of ultraviolet wave-lengths, for use with the Conti-Glo fluorescent paint products, are now being manufactured in several models by the Continental Lithograph Corporation, 72nd Street at St. Clair Avenue, Cleveland, Ohio. This new line of lamps includes models for spot-lighting, for flood-lighting where a small unit is required, for flood-lighting where a large unit may be used, and for short-period and demonstration purposes. The accompanying photograph shows two of the flood-lighting lamps.

Analytical Balance Brush

Featuring a cellulose fiber brush and an aluminum tubing handle, the "Cello-Lume" brush for use in cleaning small objects in the science laboratory has been recently marketed by the Varniton Company, Box 1541, Station D, Los Angeles, California. It is intended primarily for dusting off dry powders, and is adapted for cleaning analytical balances, microscope lenses, slides, and balance weights. The brush is soft so that it will not harm the objects on which it is used, and it may be washed with soap and water.

Instruments in Plastic Blocks

Sensitive instruments are now being built directly into solid blocks of crystal-clear "Lucite" plastic, it is announced by E. I. duPont de Nemours and Company, Wilmington, Delaware, producers of the methyl methacrylate. These blocks are lightweight and will take knocks that would shatter glass, according to the manufacturers. One of the instruments now manufactured in "Lucite" is a pocket carbon dioxide indicator, marketed by the F. W. Dwyer Manufacturing Company of Chicago. Passages for the absorbent fluid are drilled and reamed directly into the plastic. No glass tubing or delicate moving parts are used. This instrument, which may be used by the industrial engineer to check the fuel efficiency of a plant, admits light from all sides through the plastic, thus facilitating readings.

Brush Method for Electroplating Silver

A process for the application of silver coatings by the brush method is announced by Rapid Electroplating Process, Inc., 1414 South Wabash Avenue, Chicago. A portable kit containing the materials necessary for brush silver plating is on the market. Fundamentally the process does not differ from ordinary commercial plating methods, according to the manufacturers, except that the liquid electrolyte is replaced by a highly-concentrated jelly-like compound which can be picked up by the specially designed brush and applied to the surface to be plated. Silver platings of 0.0002 to 0.001 inch thickness can be applied by this method.

Photoelectric Phonograph

A photoelectric phonograph has been developed by the engineers of the Philco Research Laboratories, according to a recent announcement. In this new type of phonograph the needle has been replaced by a sapphire jewel which floats on the grooves on the record, transmitting the tone vibrations to a tiny mirror swinging freely on an axis. A beam of light, produced by a small bulb and directed at this vibrating mirror, picks up the vibrations and reflects them on a photoelectric cell. The cell, in turn, activated by the vibrating light beam, converts these vibrations electrically into music. The jewel has a life of from eight to ten years, according to the manufacturers. Because of the fact that the friction on the record is less in the photoelectric phonograph than in the needle type, use of the photoelectric phonograph is said to increase the life of records to such an extent that they may be played 1000 times.

Small-Spot Photometer

Response to light values far below the range of conventional photometers is claimed for the new Photrix Small-Spot Photometer with electronic amplification, manufactured by the Photovolt Corporation, 10 East 40th Street, New York City. This instrument operates on a.c. or d.c. and is balanced for line voltage variations without the use of batteries or voltage stabilizers for the power supply. The new photometer is designed particularly for measuring low values of illumination on small areas as required, for instance, if a small spot of an unevenly illuminated surface is to be evaluated. It is possible to use a rugged microammeter as the indicating instrument. The sensitivity of the Small-Spot Photometer is said to be about 1000 times higher than the one of a conventional photometer using a barrier-layer cell directly connected to the same microammeter. This new photometer is a portable unit comprising the instrument proper and the search unit. Two different models of search units are available; one for incident light and one for transparent light. The 100-division scale of the indicating instrument is $3\frac{3}{4}$" long. At the highest sensitivity range each division represents 0.0005 footcandle.

Infrared Photography

For scientific, medical, documentary, and general photography, for photomicrography, and for photoengraving there are available: Eastman Infra-Red Safety Film; Eastman Infra-Red Sensitive Plates; Eastman Infra-Red Process Plates; Kodak Infra-Red Film, for miniature and roll-film cameras.

For spectroscopy, there are seven classes of infrared sensitizing; some of them can be applied to five different types of emulsions. They permit photography of the spectrum to beyond 12,000 Å.

Detailed information about the first group of materials is the basis of the Kodak publication, *Infrared Photography with Kodak Materials*—price, 25 cents; data about the second group are included in *Photographic Plates for Use in Spectroscopy and Astronomy*—free on request.

BE SURE TO VISIT THE KODAK BUILDING AT THE NEW YORK WORLD'S FAIR

EASTMAN KODAK COMPANY

Research Laboratories **ROCHESTER, N. Y.**

THREE OUTSTANDING NEW BOOKS

EXPERIMENTAL COLLEGE PHYSICS. *New second edition*

By MARSH W. WHITE, Pennsylvania State College. In press—ready for fall classes.

Carefully graded and logically arranged, this laboratory manual of 74 thoroughly tested experiments contains not only complete directions for the procedures of the experiments, but also includes an unusually comprehensive discussion of the important underlying theory. Many new experiments have been added.

THE MODERN THEORY OF SOLIDS

By FREDERICK SEITZ, University of Pennsylvania. *International Series in Physics.* 689 pages, 6 x 9. $7.00

In this distinctive new book the author presents a survey of the theory of the properties of all types of crystalline solids. The book is unique in that it covers the theory of all types of solids from a common viewpoint. Besides dealing with the theory of metals, the author treats the properties of salts and other insulators as well, showing the factors which account for differences and similarities of all these materials.

APPLIED X-RAYS. *New third edition*

By GEORGE L. CLARK, University of Illinois. *International Series in Physics.* 675 pages, 6 x 9. $6.00

The author of this well-known book, besides bringing the material up to date, has expanded the text considerably to include the remarkable developments of the past eight years. The chapter on interpretation of X-ray diffraction patterns is entirely new, and new chapters have been added on the measurement of intensity, photochemistry, the biological effects of X-rays, etc.

Send for copies on approval

McGRAW-HILL BOOK COMPANY, Inc.

330 West 42nd Street **New York, N. Y.**

Linde

RARE GASES AND MIXTURES

NEON
ARGON
HELIUM
KRYPTON
XENON
MIXTURES

. . . *Spectroscopically Pure*
. . . *Easily removed from bulb without contamination*

Scientific uses for Linde rare gases include—

1. The study of electrical discharges.
2. Work with rectifying and stroboscopic devices.
3. Metallurgical research.
4. Work with inert atmospheres, where heat conduction must be increased or decreased.

Many standard mixtures are available. Special mixtures for experimental purposes can be supplied upon request.

The word "Linde" is a trade-mark of

The Linde Air Products Company

Unit of Union Carbide and Carbon Corporation

30 East 42nd Street UCC Offices in
New York, N. Y. Principal Cities

IMPROVED "SPOTLIGHT" GALVANOMETERS

Rubicon MULTIPLE REFLECTION galvanometers have recently been improved through a redesign of the optical system. The definition of the line-image is now so sharp that readings can be estimated to .1 of a millimeter division.

These sturdy, self-contained galvanometers are available with sensitivities as high as .0006 microampere per millimeter. The scales, which are 100 mm. long, are remarkably proportional. Send for Bulletin 320.

RUBICON COMPANY

ELECTRICAL INSTRUMENT MAKERS

29 North Sixth Street Philadelphia, Pa.

Baker Special THERMOCOUPLES

Besides the standard platinum-rhodium vs platinum thermocouples, we make many others with much higher values of thermoelectromotive force. We do not guarantee for them a definite e.m.f. nor can they be used at the high temperatures possible with platinum-rhodium vs platinum. They are for measuring temperature changes in the lower ranges. Wire sizes down to .001" — smaller in some cases. Some typical couples are:

COUPLE	E. M. F. per °C in Range 0-100°C Microvolts
Platinum-Iridium vs Gold-Palladium	+ 47
Chromel P vs Constantan	+ 63
Silver vs Bismuth	+ 76
Bismuth-Tin vs Bismuth	+126

We shall be glad to tell you more about these couples and many other metals and alloys. Just a card from you will bring the information.

BAKER & CO., INC.

113 Astor Street Newark, N. J.

JAGABI "LUBRI-TACT" LABORATORY RHEOSTATS

Lubricated sliding contact. Four sizes, seventy-six different ratings carried in stock.

Also Compression Carbon Rheostats.

Bulletin 1620-R.

JAMES G. BIDDLE CO.

ELECTRICAL AND SCIENTIFIC INSTRUMENTS

1211-13 ARCH STREET PHILADELPHIA, PA.

EPPLEY STANDARD CELLS

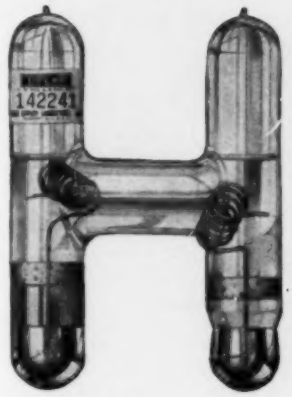

For more than 20 years the leading American manufacturers of industrial temperature control apparatus have used Eppley Standard Cells in their recorders, pyrometers and other instruments utilizing the potentiometric system of measurement.

We feel that this almost universal adoption of the Eppley Standard Cell is the result of high standards of quality and reliability, achieved and maintained through years of painstaking research, which still continues in an endeavor to render American industry a service of ever-increasing value.

When you purchase an instrument containing an Eppley Standard Cell you are obtaining maximum standard cell efficiency and reliability. The best testimonial to this fact is 20 years acceptance by American manufacturers.

EPLAB

THE EPPLEY LABORATORY, INC.

SCIENTIFIC INSTRUMENTS

NEWPORT, R.I.

U.S.A.

REPORTS ON
PROGRESS IN PHYSICS
VOLUME VI (1939)

A COMPREHENSIVE REVIEW by qualified physicists under the general editorship of J. H. AWBERY, B.A., B.Sc.

434 pages *Illustrated* *$5.25 post free* *Bound in cloth*

The steady demand for the first five volumes has strengthened the Physical Society's belief that these annual *Reports* satisfy a long-felt want. Despite the abnormal times, the sixth volume is now ready and is as comprehensive in scope as any of the preceding volumes. This volume includes articles on:

Production and Measurement of Short-Wave Radiations
Induced Radioactivity
Separation of Isotopes
Stellar Interiors and Evolution
Theory of Molecular Structure
Luminescence of Solids
Theory of Elasticity of Rubber
Ultra-Short Waves on Wires
Impedance Networks
Measurement of Capacitance
Dielectric Breakdown in Solids
Teaching of Physics in Technical Institutions
The Cyclotron
The Meson
Spectroscopy
X-Rays and Crystals
Reactions in Solids
Fluid Motion
Sound
Heat
Superconductivity
Liquid Helium

Volumes I, II and IV (1934, 1935 and 1937) are now out of print. Volumes III and V (1936 and 1938) are still available, $5.00 each post free.

Orders, with remittance, should be sent to

THE PHYSICAL SOCIETY, 1 Lowther Gardens, Exhibition Road, London, S.W.7

Write for
REVISED 44 PAGE ENGINEER'S DATA BOOK
also
• new enlarged vapor pressure-temperature chart.

HYDRON

METALLIC BELLOWS

HYDRON Metallic Bellows are used as control elements in temperature-and-pressure-control devices, and for liquid or gas seals of compressors and pumps. We are specialists in the design and production of complete thermostatic and pressure units for temperature and pressure controls. We are, therefore, prepared to extend the fullest co-operation to engineering departments of control manufacturers in the solution of design and engineering problems.

CLIFFORD MANUFACTURING CO.
564 E. FIRST STREET, BOSTON
BOSTON CHICAGO DETROIT LOS ANGELES
PRODUCERS OF BELLOWS EXCLUSIVELY
SERVING AUTOMATIC CONTROL MANUFACTURERS

ABSORPTION CELLS
With Optical Flats Fused On

Windows Flat Over Entire Area to Within 6 Wavelengths

* Parallelism of liquid-glass interfaces is ±0.01 mm. in high-precision cells and ±0.025 mm. in standard cells.
* Parallelism of the faces of each window is ±10 minutes.
* Actual mean length marked on each cell to nearest 0.001 mm.
* Actual mean length between faces of windows is ±1% or ±0.005 mm. of the nominal length.
* Cells matched to ±0.01 mm. are obtainable.
* Pyrex Bodies with Pyrex or Corex "D" Windows.
* Fused Quartz Bodies and Windows.

AMINCO

12 Styles
387 Standard Sizes

Write for Bulletin AP1170

AMERICAN INSTRUMENT CO.
8010 GEORGIA AVENUE · SILVER SPRING, MARYLAND

INDEX TO ADVERTISERS

The following firms have shown their interest in the advancement of physics through their support of the journals and other services of the American Institute of Physics and its Founder Societies. This should entitle them to consideration by physicists whenever possible.

Name	*Page*
AMERICAN INSTRUMENT COMPANY ..... Ion Type X-Ray Tube. Powder Spectrum Diffraction Cameras. Scientific Instruments and Supplies.	vi
BAKER & COMPANY, INC. ..... Platinum crucibles, dishes, triangles, filter cones, anodes, cathodes, electrodes, platinum tipped crucible tongs, fine wires and bismuth foil.	iv
JAMES G. BIDDLE COMPANY ..... "Jagabi" Rheostats; Adam Hilger and Kipp & Zonen Optical Instruments; "Pointolite" Lamps; Electrical Testing and Speed-measuring Instruments.	iv
CENTRAL SCIENTIFIC COMPANY ..... Manufacturers of Cenco Physical Apparatus and Instruments to meet all requirements of University, College and High School Physics Laboratories. Specializing in high vacuum pumps and development of instruments and apparatus for various sciences.	Cover 4
CLIFFORD MFG. COMPANY ..... Hydron metallic bellows for temperature and pressure control devices. Data for engineers.	vi
EASTMAN KODAK COMPANY ..... Purified Organic Chemicals for research purposes; Plates for Photography, Photomicrography, Spectroscopy, Photometry, Astronomy; Wratten Light Filters; Cameras and Films.	iii
THE EPPLEY LABORATORY, INC. ..... Standards of e.m.f. (standard cells). Precision electrical instruments; potentiometers, bridges, temperature bridges, volt boxes. Thermopiles and pyrheliometers.	v
GAERTNER SCIENTIFIC CORPORATION ..... Spectroscopes, Spectrometers, Spectrographs, Spectrophotometers, Heliostats, Measuring Microscopes, Comparators, Cathetometers, Reading Telescopes, Interferometers, Chronographs, Dividing Machines, etc.	ii
GENERAL RADIO COMPANY ..... Manufacturers of electronic measuring instruments; vacuum-tube voltmeters, amplifiers and oscillators; wave analyzers, noise meters and analyzers, stroboscopes; laboratory standards of capacitance, inductance and frequency; impedance bridges, decade resistors and condensers; air condensers and variable inductors; rheostats, Variacs, transformers; other laboratory accessories.	Cover 3
LEEDS & NORTHRUP COMPANY ..... Manufacturers of Galvanometers, Resistors, Bridges, Condensers, Inductances, Potentiometers, Testing Sets; Temperature Measuring, Recording and Controlling Apparatus; Instruments for Measuring and Controlling Conductivity of Electrolytes and Hydrogen Ion Concentrations.	i
THE LINDE AIR PRODUCTS CO. ..... Oxygen, Argon, Helium, Krypton, Neon, Xenon, Rare Gas Mixtures, Nitrogen, Hydrogen, Calcium Carbide, Acetylene, equipment for Oxy-Acetylene welding and cutting.	iv
MCGRAW-HILL BOOK COMPANY, INC.	iii
PHYSICAL SOCIETY (LONDON)	v
REINHOLD PUBLISHING CORPORATION	ii
RUBICON COMPANY ..... Galvanometers, electrometers, potentiometers, Wheatstone and Kelvin bridges, resistance boxes, hydrogen ion and conductivity apparatus.	iv

SITUATIONS OPEN

Writer and photographer wanted for regular part-time work
(1) articles on photography—new amateur gadgets, new devices amateurs can make themselves
(2) articles on homecraft
(3) articles on popular science
(4) articles on new instruments of any description
Address Box H3-14. Rm. 1502, 175 Fifth Ave., New York, N. Y.

THIS SWITCH was developed a number of years ago for use in vacuum-tube circuits where only very low capacitances could be tolerated. Due to its excellent design it has been widely adopted for hundreds of other uses requiring a switch with long life, good contacts and moderate price.

The Type 339 switch is operated by a 180 degree rotary motion. The blades are of nickel silver and the large contacts of pure silver. It is single hole mounting and can be used on panels up to 3/8 inch in thickness. It is insulated for 250-volt circuits and will carry up to 2 amperes. The construction is such that it can be used hundreds of thousands of times before the springs wear out.

Supplied in either 4-pole double-throw type (339–A . . $2.50) or 2-pole double-throw type (339–B . . $2.00), its springs can be bent easily so that practically any type of make or break arrangement possible with these number of contacts can be used for special switching.

The Type 339 Switch is typical of the wide variety of standardized parts made by G–R. These include a number of different plugs and jacks, binding posts, dials and dial plates, knobs, panel insulators, transformers, condensers, etc.

Write for Bulletin 618 for Complete Information

GENERAL RADIO COMPANY

CAMBRIDGE, MASSACHUSETTS

Branches in New York and Los Angeles

RCA CATHODE RAY OSCILLOGRAPH

At An All-Time Low Price While They Last

71546

A reliable instrument for the study of wave shapes, measurement of modulation, adjustment of radio receivers and transmitters, determination of peak voltages and other similar applications. By the addition of an acoustic pick-up, pulsations, such as heart beats, can be made visible on the screen of the cathode ray tube in their characteristic wave form. One of the most striking applications is the use of the oscillograph with No. 74720 Rectifier Demonstration Apparatus with which half wave and full wave rectification of alternating current is shown, as well as the smoothing out of the pulsating current by means of a condenser. Other experiments such as study of the discharge curve of a condenser, relaxation oscillations obtained with a neon glow lamp, and the wave form of the output of an induction coil, will suggest themselves to the teacher.

The oscillograph is enclosed in an attractive case with gray wrinkle finish and snap handle. Operation is through five radiotron tubes: a full wave rectifier; two amplifiers; timing axis oscillator; and a cathode ray tube with 1-inch screen.

71546 Oscillograph, 115 volts, 50–60 cycles..... $21.50

71546A Oscillograph, 115 volts, 25–60 cycles..... $23.50

CENTRAL SCIENTIFIC COMPANY

SCIENTIFIC INSTRUMENTS & LABORATORY APPARATUS

CHICAGO
1700 Irving Park Blvd.,
Lakeview Station

TRADE MARK CENCO REG. U.S. PAT. OFF.

BOSTON
79 Amherst St.,
Cambridge A Station

LANCASTER PRESS, INC., LANCASTER, PA.